[illegible] OF CHARGED PARTICLE MOTION IN A FREE VORTEX FLOWFIELD

R. A. Cuthrell

M. R. Welkoff

[illegible] Technical Report 812

Contract DA-31-124-ARO-D-245

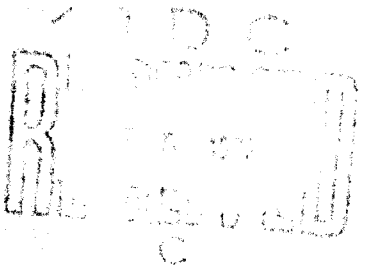

U. S. Army Research Office - Durham
Box CM, Duke Station
Durham, North Carolina 27706

July 1972

[illegible] State University Research Foundation
Columbus, Ohio 43212

DISCLAIMER

[illegible] in this report are not to be construed [illegible] Department of the Army position unless so [illegible] other authorized documents.

[illegible]

[illegible] of trade names and names of manufacturers [illegible] not to be construed as official Government [illegible] approval of commercial products or services

DISCLAIMER NOTICE

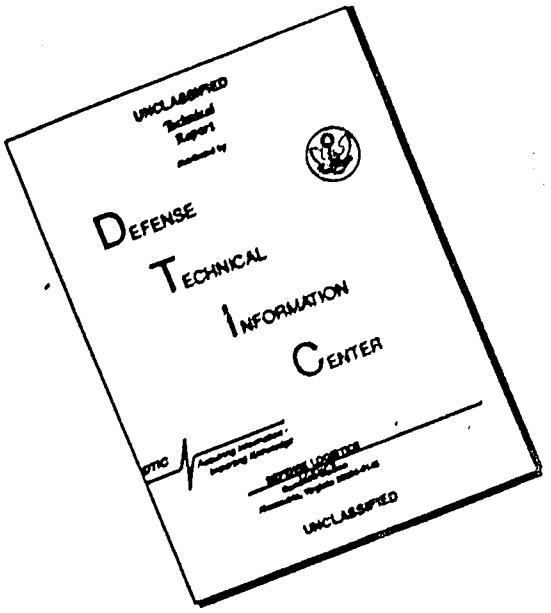

THIS DOCUMENT IS BEST QUALITY AVAILABLE. THE COPY FURNISHED TO DTIC CONTAINED A SIGNIFICANT NUMBER OF PAGES WHICH DO NOT REPRODUCE LEGIBLY.

UNCLASSIFIED

Security Classification

DOCUMENT CONTROL DATA - R & D

(Security classification of title, body of abstract and indexing annotation must be entered when the overall report is classified)

1 ORIGINATING ACTIVITY (Corporate author) The Ohio State University Research Foundation 1314 Kinnear Rd. Columbus, Ohio 43212	2a. REPORT SECURITY CLASSIFICATION Unclassified 2b. GROUP N/A

3 REPORT TITLE

A STUDY OF CHARGED PARTICLE MOTION IN A FREE VORTEX FLOWFIELD

4 DESCRIPTIVE NOTES (Type of report and inclusive dates)

Interim Technical

5 AUTHOR(S) (First name, middle initial, last name)

R. A. Cudnick H. R. Velkoff

6. REPORT DATE July 1972	7a. TOTAL NO. OF PAGES	7b. NO. OF REFS 49
8a. CONTRACT OR GRANT NO DA-31-124-ARO-D-246 b. PROJECT NO 20010501B700 c. 1D12140A142 d.	9a. ORIGINATOR'S REPORT NUMBER(S) Technical Report #12 9b. OTHER REPORT NO(S) (Any other numbers that may be assigned this report)	

10 DISTRIBUTION STATEMENT

11. SUPPLEMENTARY NOTES	12. SPONSORING MILITARY ACTIVITY U.S. Army Research Office - Durham Box CM, Duke Station Durham, North Carolina 27706

13. ABSTRACT

A study was made of charged particle motion in a free-vortex flow field to determine the parameters affecting particle motion and to determine the extent to which applied electric fields can influence the particle motion.

Four different cases were investigated. These included first, the analysis of the motion of an uncharged particle in a free-vortex; second, analysis of the motion of a charged particle in a viscous medium under the influence of an applied electrostatic field; third, analysis of charged particle motion in a free-vortex under the influence of the applied electrostatic field, assuming the particle is first positively and then negatively charged; and fourth, analysis of the motion of two charged particles in a free-vortex, accounting for field effects due to particle charge.

The results indicate that in all cases, as the particle diameter and ensity, and free-vortex flow velocity are increased, radial particle migration is increased. Radial particle migration is enhanced if the particle is assumed to be positively charged and under the influence of the electrostatic field due to a positively charged line source. If the particle is assumed to be negatively charged, the electrostatic force tends to balance the centrifugal force and allow the particle to maintain an equilibrium radius. Finally, the field effects due to the particle charges themselves are insufficient to affect particle motion in the two-particle system.

DD FORM 1 NOV 65 1473

Unclassified

Security Classification

14 KEY WORDS	LINK A		LINK B		LINK C	
	ROLE	WT	ROLE	WT	ROLE	WT
Electrofluidmechanics						
Electrohydrodynamics						
Electrogasdynamics						
Electrostatics						
Electrostatic Charging						
Tornadoes						
Dust Devils						
Charged Particle						
Vortex						
Fluid Mechanics						

A STUDY OF CHARGED PARTICLE MOTION IN A FREE VORTEX FLOWFIELD

R. A. Cudnick

H. R. Velkoff

Interim Technical Report #12

Contract DA-31-124-ARO-D-246

U. S. Army Research Office - Durham
Box CM, Duke Station
Durham, North Carolina 27706

July 1972

The Ohio State University Research Foundation
Columbus, Ohio 43212

FOREWORD

The work reported herein was sponsored in part by the United States Army Research Office, Durham, under Contract No. DA-31-124-ARO-D-246. The study presented herein was conducted by Mr. Ronald A. Cudnick in fulfilling the requirements for a thesis in his Master of Science program at The Ohio State University.

ABSTRACT

A study was made of charged particle motion in a free-vortex flow field to determine the parameters affecting particle motion and to determine the extent to which applied electric fields can influence the particle motion.

Four different cases were investigated. These included first, the analysis of the motion of an uncharged particle in a free-vortex; second, analysis of the motion of a charged particle in a viscous medium under the influence of an applied electrostatic field; third, analysis of charged particle motion in a free-vortex under the influence of the applied electrostatic field, assuming the particle is first positively and then negatively charged; and fourth, analysis of the motion of two charged particles in a free-vortex, accounting for field effects due to particle charge.

The results indicate that in all cases, as the particle diameter and density, and free-vortex flow velocity are increased, radial particle migration is increased. Radial particle migration is enhanced if the particle is assumed to be positively charged and under the influence of the electrostatic field due to a positively charged line source. If the particle is assumed to be negatively charged, the electrostatic force tends to balance the centrifugal force and allow the particle to maintain an equilibrium radius. Finally, the field effects due to the particle charges themselves are insufficient to affect particle motion in the two particle system.

TABLE OF CONTENTS

LIST OF FIGURES

Page

Page

Page

INTRODUCTION

The motion of charged and uncharged particles in a free-vortex flow field is of interest in a wide variety of areas. These areas range from particle separation and classification by centrifugal and electrostatic action, to possibly improved operation of electrostatic precipitators by addition of some device to impart swirling motion to the exhaust gases, to the extremely interesting area of the role of charged particles in the initiation and maintenance of two of nature's vortex systems -- the tornado and the dust devil.

When this thesis was first undertaken, it was with the goal of gaining some insight into determining the role played by the electrical activity associated with tornadoes and dust devils in the initiation and maintenance of these vortex systems. While it was soon realized that this was too complex a task to be undertaken for a thesis, the problem was still a fascinating one, and as a result a literature survey was made to determine the current theories on the significance of the electrical activity associated with tornadoes and dust devils. The information gained in the literature survey has been summarized and is discussed in the next section.

This survey of the literature also indicated that while work had been done in determining the motion of uncharged particles in a swirling flow by Hirschkron and Ehrich (Ref. 1), Kriebel (Ref. 2), Lapple and Shepherd (Ref. 3) and Uematu, et al., (Ref. 4), no work had been done in determining the motion of charged particles in a swirling flow under the influence of an applied electrostatic field.

It was then decided that the objective of this thesis would be to study the motion of a charged particle in a free-vortex under the influence of an applied electric field and to determine the parameters influencing the particle motion.

The significance of electrification on the dynamics of a particulate system has been extensively studied by Soo (Ref. 5, 6, 7, and 8). His work has shown that electrification of the solid particles in a gas-solid suspension affects the concentration distribution of the solid particles and would be expected to affect, for example, the friction, heat transfer, and settling of solid particles. However, his work has been primarily concerned with one-dimensional flow through pipes rather than swirling flow.

BACKGROUND OF THE ROLE OF ELECTRICAL ACTIVITY ASSOCIATED WITH VORTEX SYSTEMS, INCLUDING TORNADOES AND DUST DEVILS

Determining the role of electrical activity in vortex systems, in particular tornadoes and dust devils, is a complex problem which has puzzled man for many centuries. The idea that electrical activity may be a cause rather than a result of tornadoes is certainly not new, as evidenced by the works of Lucretius (60 B.C.) and Francis Bacon (1622) cited by Vonnegut (Ref. 9) in his discussion of the electrical theory of tornadoes. The various accounts of the electrical phenomena associated with tornadoes, dust devils, and confined vortex systems gives much credence to the belief that the electrical activity and the vortex motion are more than fortuitously interrelated. These accounts also serve as the basis for theories proposed to explain the role of electrical activity in vortex systems.

The accounts of electrical activity associated with vortex systems to be presented here are certainly not all that are available; it is hoped, however, that these accounts will give a representative sampling of the type of electrical behavior that has been observed in tornadoes, dust devils, and confined vortex systems.

Freier (Ref. 10) obtained measurements of the earth's electric field in the Minneapolis-St. Paul area while tornadoes were within a seventy-mile radius of the recording station. The measurements he obtained show a high frequency oscillation of the earth's electric field beginning nearly at the time of the first reported tornado

and continuing nearly an hour after the last tornadoes struck. The significant points noted from these measurements were first, that the high frequency oscillations of the earth's electric field present had not been observed at the recording station during any other thunderstorm activity during the previous year and second, the measurements were obtained when nowhere within the visible horizon was there an indication of a storm. Freier states that while it is difficult to draw any conclusions from the limited data, it is significant that the high frequency oscillations of the earth's electric field are observed only during the tornado activity.

Vonnegut and Weyer (Ref. 11) confirmed the existence of unusual electrical discharges in a tornado at Toledo, Ohio on April 11, 1965. They present a photograph showing two illuminated vertical pillars indicating the presence of some unusual luminous phenomena. From eyewitness reports and the paths of destruction, it appeared that there were two tornadoes following essentially the same path. Over a dozen eyewitness accounts were obtained, many of which indicated various kinds of luminosity. Many of the eyewitnesses reported a white or bluish-white light, definitely not lightning, but sufficiently bright to illuminate the surroundings and give the appearance of daylight. There were no observations of any significant lightning strokes. Several of the eyewitnesses observed bright balls of light, either orange or multicolored. These observations suggest the presence of ball lightning, a phenomenon of which very little is known.

In discussing the two columns of light appearing in the photograph, the authors suggest that the columns of light may be due to some kind of luminous electrical discharge or they may be tornado funnels illuminated by lightning or some other type of discharge within the vortex. While there are no other photographs of a luminous tornado funnel, there have been several other observations of an apparently similar phenomenon.

Brook (Ref. 12) reported a measurement of the perturbations in the magnetic field and the earth current taken in the vicinity of a tornado. The data were obtained by Boucher near Tulsa, Oklahoma on May 27, 1952. The significant feature of the measurements made is a large rapid deflection of the horizontal earth current. Coincident with this deflection was a large sudden shift in the horizontal component of the magnetic field, with smaller deflections in the declination and vertical component. The coincident, step-like deflections of all the parameters measured raise the possibility that a common source existed for all the disturbances. Brook believes that the source of the disturbance was the tornado that was seen touching down at the precise time at which the deflections occurred.

Vonnegut and Moore (Ref. 13) discuss electrical field measurements made by Gunn (Ref. 14) near a tornado on May 25, 1955 at Blackwell, Oklahoma and Udall, Kansas. In his work Gunn concluded that the measurements give little evidence that first, electrical effects near the tornado differ basically from ordinary thunderstorm

electrification and second, that the tornado is primarily an electrical phenomenon. Vonnegut and Moore postulate that although electrical effects are more severe in tornadoes than in ordinary thunderstorms, they are basically not different. Thus, they agree with Gunn's opinion that the electric field measurements made near the tornado are what would be expected in ordinary thunderstorms if an order of magnitude increase in the turbulent velocity occurred. Eyewitnesses to the tornado in Blackwell observed evidence of intense electrical activity similar to that reported by Vonnegut and Weyer in the Toledo tornado. According to the authors, the luminous discharges in a tornado suggest that large current densities and electric fields exist inside the funnel and on the ground directly beneath it.

Silberg (Ref. 15) reports that there have been repeated observations of a tornado burning, scorching, or dehydrating trees and vegetation in its path. In the past these heating effects were explained with the aid of a "hot wind" or a corona discharge. Silberg postulates that an intense ring current existing in the tornado cloud could be responsible for these heating effects and other phenomena associated with a tornado. The theory Silberg presents for this will be discussed in greater detail in another section of this summary.

Silberg (Ref. 16) also presents data obtained from passive electrical measurements from three tornadoes in Oklahoma during the spring of 1963. The tornado measurements, when compared with those of a local thunderstorm, show that the electrical discharges

within the tornadoes are much more intense than in the local thunderstorm, particularly in the frequency of occurrence.

Several observers have obtained measurements of the electric field of a dust devil. Freier (Ref. 17) obtained a record of the electric field of a dust devil in the Sahara Desert. The record shows that the electric field decreased from its average value of about 150 volts per meter before and after passage of the dust devil to -75 volts per meter, increased to approximately 200 volts per meter and then decreased again to -450 volts per meter before returning to its average value. Freier compares the experimental data to that predicted by a simple dipole model with negative charge above.

Crozier (Ref. 18) recorded the electric field for a fairly large dust devil passing within 1500 feet of the electric field recording instrument. The potential gradient record indicated that the gradient was lowered for approximately 10 minutes and the lowest value was approximately 100 volts per meter below the average value before and after passage of the dust devil. Crozier presents a simple model to explain the potential gradient record for the dust devil and also suggests mechanisms for obtaining the space charge densities necessary in his simple electrostatic model. Crozier attempts to compare the electrical properties of the dust devil he observed to those of the Sahara dust devil described by Freier (Ref. 17). Crozier suggests that the W-shape of the Sahara dust devil gradient record could be indicative of a rapid increase in electrical activity within

the dust devil. This model will be discussed in detail in a following section.

Bradley and Semonin (Ref. 19) conducted airborne electrical measurements in dust whirls in Illinois. Measurements were made of the vertical potential gradient and space charge concentration in the tops of three large dust whirls. In all cases the measurements showed the presence of a negative space charge with an increase in the potential gradient indicating an excess of negative charge below.

Silberg and Goshgarian (Ref. 20) described several experiments which demonstrate that rotary and vortical motion can be produced by initially electrostatic fields. A circular array of 16 electrodes was installed in a large lucite tube. Two adjacent electrodes, sufficiently separated to prevent complete breakdown, were connected to a 90 kilovolt power supply. A small smoke pot was placed on the tube axis three feet down from the electrode array and activated. When the power supply was turned on, rotary fluid motion was started and continued as long as the power was on.

Later work by Silberg, Goshgarian, and Johnson (Ref. 21) attempted to measure the electrostatically produced vortical motion. The equipment used was the same with the exception of a larger power supply (120 kilovolts). Air, bromine vapor, and smoke mixed with air were the fluids used. No vortical motion was observed at the power supply voltages used for air and for bromine vapor. Using smoke mixed with air, at 30 kv considerable turbulence was noted around the electrodes. Above 50 kv, the smoke particles at the top and bottom

assumed a regular rotary motion and in a short time the entire smoke column began rotating, increasing uniformly in velocity until a well defined vortex was formed. An attempt was made to measure the fluid motion using a Pitot-static tube with a minimum detectible velocity calibrated to be approximately 10 feet per second. When a traverse of the Pitot tube was made through the vortex about 4 inches above the mouth of the smoke pot where the smoke velocity appeared to be greatest, no velocity was measured. It appeared that if there was motion of the air caused either by the electrostatic field or by drag induced by the accelerated smoke particles, then this motion was below the minimum detectible threshold of the Pitot tube. Several conclusions were reached by the authors: first, the observed vortical motion existed primarily in the dielectric smoke; second, the vortical motion in the smoke was high, although immediately exterior to it no measurable air velocity was detectible; third, from the high potentials required to initiate vorticity, it was concluded that the dielectric particles to which the field initially couples were probably charged; and fourth, since the vortical motion did not extend to the boundary, no boundary effects were noted.

Lavan and Fejer (Ref. 22) observed a luminescent region near the axis of a cylindrical duct confining a supersonic swirling air flow at ambient temperature. This luminescence was identified as a glow discharge induced by a strong internal electric field produced by condensed water droplets impinging on the duct wall. It was found that the luminescence increased uniformly with swirl intensity and with the specific humidity of the ambient air, while it decreased

when the axial Mach number was increased or decreased. When the dielectric duct was replaced by one made of a conducting material, no luminescence was observed, suggesting that electrostatic charges on the surface of the dielectric wall were a likely cause of the phenomenon.

The various accounts presented here strongly suggest that an interrelationship does exist between electrical activity or phenomena and vortex systems. Several theories have been proposed to explain the role of electrical activity in the initiation and continuation of tornadoes. The two main theories here are the electrical heating theory and the electromagnetic or electrodynamic initiation theory. In these theories the electrical activity is the cause of tornadoes rather than a result of them. Other theories suggest that the electrical activity is the result of vortex motion. The various theories will be presented and briefly discussed here.

Vonnegut (Ref. 9) suggests that there is sufficient electrical energy in an intense thunderstorm to power a tornado and that the electrification could cause very intense winds by electrically heating air or by accelerating charged air in an electric field. Vonnegut notes that to obtain winds of the velocity that appear to exist in a tornado there must be temperature differences between air masses in the atmosphere probably of the order of several hundred degrees centigrade. He concludes it is doubtful that ordinary atmospheric processes could produce the large temperature differences required for winds of tornado speed. He notes that the quantities of heat sufficient to raise large volumes of air to a high temperature are

released by volcanic activity or large fires and that tornadoes or fire whirls have been observed under these conditions. His electrical theory of tornadoes uses as its bases observations of tornadoes which indicate the presence of sufficient electrical energy to account for their intensity, and the existence of mechanisms by which this electrical activity could produce the intense winds. The accounts of electrical activity in tornadoes presented previously will serve to verify its presence and Vonnegut estimates that roughly 10^8 kw of electrical power is available in a tornado producing storm. It thus appears that sufficient electrical energy probably exists in a violent thunderstorm to cause a tornado, if the energy is properly applied. Vonnegut next attempts to establish that this electrical energy can be transformed into the kinetic energy of rapidly moving air. Two mechanisms by which this can happen are presented. The first is that electrical energy could heat a volume of air to such a high temperature that very intense convection would take place. The second is that highly charged air could be accelerated to a high velocity in a strong electric field. Both processes are dependent on the transport of electric charge through a potential difference. Vonnegut considers three charge transport mechanisms that might operate in a storm.

The first mechanism is the lightning stroke, in which a narrow path through the air suddenly becomes highly ionized and conducting with the charge flowing in a fraction of a second. This is an intermittent process, however, in which the instantaneous current may reach many kiloamperes, although the average current is much less.

The second mechanism is a continuous arc or glow discharge in which current may flow and heat the air. Here the current flow is steady and does not reach the high instantaneous values of the lightning discharge.

The third mechanism is by the movement of charged particles such as ions or electrified cloud particles in an electric field. These conduction processes probably account for the largest part of the charge transport from the earth to the clouds in thunderstorms.

In all three processes a large portion of the electrical energy is released as heat. Vonnegut suggests that each of these three mechanisms can, under the right circumstances, cause intense winds by convection resulting from the hot air produced. The first two mechanisms are dependent on the efficiency of the conversion of energy released by lightning in the form of heat into kinetic energy of the wind. A simple calculation shows that an air mass could be continuously heated by more than 100°C under these conditions.

In the third mechanism, the flow of charge by conduction, transformation of electrical energy into kinetic energy can take place directly if the charge transport occurs by the movements of ions all having predominantly the same sign. The movement of these ions under the influence of an electric field will transfer momentum directly to the air and cause it to accelerate. The flow of current will cause it to move the air and heat it under the influence of electrical forces. The ratio of the fraction of the electrical energy transformed into heat to that transformed into mechanical work will be equal to the

ratio between the velocity of the ions relative to the air and the velocity of the air itself. The importance of the electrical acceleration of the air will be greatest when the wind velocity is high and the mobility of the charge carriers is low. The mobility will be smallest when the charge is carried predominantly on dust or cloud particles. Vonnegut presents a simple model showing that the electrical force acting on a charged water droplet in a typical thunderstorm electrical field is equivalent to that force which would result if the air were heated 20°C above its environment. Thus it would appear that the first two charging mechanisms would be primarily responsible for any vortex motion due to electrical heating. The third mechanism would contribute to the electrical heating effect, but its more important role may be that of accelerating the air due to the movement of ions under the influence of an electrical field.

Wilkins (Ref. 23) conducted laboratory model vortex experiments and theoretical investigations to determine whether the unusual electrical phenomena sometimes accompanying tornadoes might play an important role in the initiation or continuation of a tornado. Wilkins concluded that first, heat released by lightning may serve to initiate updrafts, but its effectiveness in tornado formation is difficult to evaluate due to the presence of the latent heat available in a convectively unstable atmosphere. Second, the electrodynamic accelerations of ions appear to be unimportant in either the formative or mature stages of a tornado.

Colgate (Ref. 24) postulates that the tornado vortex is driven by a line sink of electrically heated air extending at least

5 kilometers high. His argument for an electrical energy mechanism is that purely hydrodynamic motion cannot adequately account for the very high tornado wind speeds derivable from a maximum available adiabatic pressure difference of a tenth of an atmosphere from the ground to the base of the tropopause.

Theories proposed by Vonnegut (Ref. 9), Rathbun (Ref. 25), and Lewellen (Ref. 26) suggested that a tornado or a vortex could be electrodynamically or electromagnetically driven. The theory proposed by Vonnegut on the acceleration of air by the motions of ions under the influence of an electric field has already been discussed and Wilkins' (Ref. 23) objections to it have been stated. Rathbun (Ref. 25) proposed an electromagnetic basis for the initiation of a tornado. He suggests that the process leading to the formation of a tornado is the following:

(1) Electric charge accumulation in a cloud increases until the atmosphere is almost stressed to the point of breakdown.

(2) A leader stroke of lightning develops, but because of the energy available, it is not followed by a full lightning stroke. This threatening stroke is believed to exist for several seconds.

(3) A considerable volume of air is left in a highly charged state as a result of the above processes. This charged state will be maintained by the large potential gradient which energized the threatening stroke.

(4) The charged component of air will move in accordance with the laws governing electrostatic behavior. Positive ions will be attracted to a negatively charged region and vice versa. Ion-air molecule collisions will set uncharged air in motion.

(5) The air set in motion will have a tendency to move in a counterclockwise vortex due to the earth's magnetic field and the positive polarity of the ions.

(6) Vortex motion will develop until the aerodynamic factors assume control.

(7) The tornado will end when the local potential energy region of the storm has been dissipated or the vortex has reached a size of such proportions that the vortical motion is unstable.

Lewellen (Ref. 26) postulates that a magnetohydrodynamic body force can be used to drive a two-dimensional, axisymmetric, steady vortex in a viscous, conducting fluid. In order to drive such a vortex, Lewellen determines the field geometries which lead to an accelerating body force in the tangential direction. A force of this type results from either an axial electric field and radial magnetic field or an axial magnetic field and radial electric field.

The theories discussed thus far postulate that the electrical activity is a cause or a driving force rather than an effect of the interactions of charged particles and vortices. Several authors, including Freier (Ref. 17) and Crozier (Ref. 18), Silberg (Ref. 15),

and Loeb (Ref. 27) have postulated that the electrical activity associated with tornadoes, dust devils and other vortex systems may be the result of vortex motion rather than the cause of it.

Freier and Crozier, who both measured the electric field associated with dust devils, compared their experimental results to theoretical results based on a simple dipole theory. Both assumed a straight line passage of a simple vertical dipole at a known constant velocity. Crozier obtains good agreement between the experimental data and the theoretical curve. The simplest model of a vertical dipole having the apparent electric moment of the dust devil would be a uniform distribution of negative space charge density in an approximately cylindrical dust cloud. Crozier estimates that the space charge density of the cloud is about 1.6×10^6 elementary charges per cubic centimeter. Although this density may seem high in view of the atmospheric charge densities usually encountered, Crozier postulates that the dust particle density in such a cloud may be as high as several thousand particles per cubic centimeter. Since the dust has just been picked up from the ground by a relatively strong wind, the average particle size is probably quite large and the possibility exists that each particle can carry several hundred elementary charges per particle. Thus, the estimated space charge densities in the dust cloud are not unreasonable.

Crozier suggests that a principal feature of the charging mechanism is asymmetrical electrification of the dust particles at the ground surface, at the initial separation from the ground or on

subsequent impacts. Collisions between large and small particles within the cloud may also be a factor in the charging mechanism.

Crozier also attempts to explain the W-shape in the potential gradient record of the Sahara Desert dust devil reported by Freier (Ref. 17). He suggests first that it is possible for the electrical activity to increase rapidly due to rapid increases in dust density, for example. Freier pointed out that the W-shape of the curve could be explained by assuming that there was positive charge in the lower portion of the column and negative charge in the upper.

In his discussion of the dehydration and burning produced by a tornado, Silberg (Ref. 15) postulates that a pulsed oscillatory ring current or ring discharge could exist within a tornado cloud and possess a radiation field that could be responsible for these heating effects at close distances and the observed and measured tornado sferics at far distances. The ring current is defined as an electrodeless electrical discharge where the electric field within the gas forms closed curves. Silberg cites several accounts of tornado phenomena which could be very similar to the induced ring discharge. He also cites measurements of the radiation produced by the electrical discharges within a tornado known as sferics.

For simplicity, Silberg assumes the ring current is uniform and it is sufficient to deal with a single frequency. He then estimates the relatively low frequency radiation field at the ground plane by assuming the ring current behaves as a low frequency loop

antenna. Silberg concludes that by using realistic values for the ring current, it is possible to produce both the observed heating effects at short distances and the sferics measurements at larger distances without unreasonable electric field strengths or power densities.

Loeb (Ref. 27) postulates that the luminous phenomena occasionally seen in tornadoes and the electrical charging of dust devils can be explained by considering the charging mechanisms existing. He cites the work of Lavan and Fejer (Ref. 22) who observed that swirling jets of water or saturated air enclosed in transparent insulating walls produced extensive glow discharges. These discharges were shown to be caused by Lenard spray electrification. Larger drops of water were thrown to the insulating walls with the fine mist of negatively charged droplets in the interior of the tube as a result of centrifugal forces. The potential gradients existing were sufficient to set up a glow discharge in the moist air. The potentials measured were over 20 kilovolts and currents of 90 microamperes were recorded. Radio frequency radiations of from 10^4 to 10^7 cycles per second were also detected from the positive corona streamers. The luminosity arises from positive streamers coming from spray disintegrated drops in a high electric field.

Loeb states:

> "That such phenomena may occasionally appear in the tornado funnel is not surprising and depends on the amount of moisture present and entrained. The centrifugal forces in any case will hurl the larger solid masses, including positive water drops, toward the outside of the funnel, and the finer materials, including the negative water spray, will be interior. If, in addition, solid elastic impacts of water are needed, these would result from impact with larger debris particles. Whether a particular funnel is luminous or not depends on the water entrained--that is, on the character of the ground traversed."

He also suggests that highly electrically charged analogs of tornado funnels also exist even without water and cites the work of Crozier (Ref. 18). Loeb suggests that asymmetrical contact charging of dust with heavier particles is responsible for the static electrification of dust devils.

The theories presented thus far might lead one to believe that there is an absence of hydrodynamic theories for tornadoes and dust devils. This would, of course, be an erroneous conclusion; many hydrodynamic theories exist for tornadoes, dust devils, and other vortex systems.

Turner and Lilly (Ref. 28) describe a carbonated-water tornado vortex whose method of producing bouyancy by changes of phase in the fluid itself is closely analogous to the release of buoyancy by condensation in the atmosphere. When considering the implications of their experimental results to the atmosphere, they conclude that the most important condition appears to be the presence of a convectively overturning region above which is

consistent with observations of all tornadoes and most water-spouts and current theoretical descriptions of tornado vortices. Most current theoretical descriptions of tornadoes agree that the formation is related to the concentration of pre-existing angular momentum by convective processes. The presence of unstable air near the ground, and condensation in the vortex probably contribute to the persistence and intensity of the vortex but it is possible to form one without it. It is suggested that dust devils are the result of convection solely from an unstable region near the ground.

The authors conclude that the mechanism of tornado formation appears to be a concentration of the mean angular momentum by an inflow to the center of the vortex near the bottom boundary as a result of a decrease in pressure. This results in an increased velocity of circulation in the center and at the same time probably a decreased circulation in a region above the vigorous convection.

Turner (Ref. 29) in 1966 produced a laboratory model of a tornado which incorporates two features believed to be important to the understanding of the tornado. First, he showed that a vortex can be driven from above by a mechanism analagous to convection in a cloud, and that density differences within the funnel itself are not essential. Associated with this mechanism of formation is a vertical circulation, with upflow in the center surrounded by a compensating annular downflow. Second, he showed that the bottom boundary has a strong influence on the vortex,

since the horizontal and vertical flows are linked there by a rapid radial inflow in a thin boundary layer.

Turner also proposed an approximate theoretical description of the vortex.

Logan (Ref. 30) developed a simple analytical model for describing the velocity fields in a dust devil. The model has a viscous inner region or boundary layer composed of a Prandtl layer, a layer in which there is a transition from a viscous boundary layer to an inviscid outer region and an inviscid "outer" region which observations indicate can be approximated by a Rankine combined vortex. Logan's model cannot properly describe the core downdraft and does not deal explicitly with the thin, unstable, thermal boundary layer. He suggests that a more sophisticated model, including an energy equation and equation of state, would yield temperature and density fields.

Barcilon (Ref. 31) proposes a theoretical and experimental model for a dust devil. He considers the flow field found in a steady, axially symmetric, strong atmospheric vortex of the dust devil type. The plane containing the axis of the vortex is divided into an inviscid region where an unstratified free vortex flow exists, a plate boundary layer region, a corner region, and an axial boundary layer region. Each region is considered in turn and a solution to the overall flow field is found by matching the flow field at the interface between two adjacent regions. Using this model, Barcilon predicted some of the features found in the model

where the inviscid flow is stratified. He then discusses an experimental demonstration in which the fluid is given an unstable temperature stratification with height and a source of angular momentum. Under certain conditions a vortex of the dust devil type formed.

Battan (Ref. 32) notes that a dust devil, unlike a tornado, forms in the absence of clouds and as a consequence derives none of its energy from latent heat. Calculations have been made by him to determine the total amount of energy (internal and potential) available for conversion into kinetic energy, and the amount of kinetic energy in a dust devil. He concludes that his calculations reaffirm the fact that the kinetic energy of a dust devil results from a reduction of the internal and potential energy of the air involved.

Dergarabedian and Fendell (Ref. 33) discuss the parameters governing the generation of free vortices. They propose an expansion of the Navier-Stokes equations which provides a new basis for free vortex equations. The description of vortex generation leads to two main parameters: the first is the Ekman number, $E = \nu/\Gamma_\infty$, where ν is the kinematic viscosity and Γ_∞ is the ambient circulation; the second indicates that unless the product of the area of the updraft and the average vertical gradient of the vertical velocity greatly exceeds the kinematic viscosity coefficient, no localized vortical flow develops. The model is for the most part axially invariant, but the lines of constant

pressure described by the model are shown to have a funnel-cloud-like shape. The authors propose that the analysis may describe the competition between the convective influx to concentrate the ambient circulation about the axis of the updraft and the efforts of the viscous forces to smooth out the circulation distribution.

Donaldson and Sullivan (Ref. 34) made a study of the complete class of solutions of the Navier-Stokes equations in which the radial, tangential and axial velocities in cylindrical coordinates are of the form $u = u(r)$, $v = v(r)$, and $\bar{w} = zw(r)$. These solutions were found to represent a large class of three dimensional viscous vortex motions. The solutions obtained show that vortex motions are possible which have more than one cell. That is, the flow may not simply spiral in toward an axis and out along it as in a one-celled configuration but may have nested regions of successively reversed axial flow. The flow streamlines and velocity profiles for vortices having one and two cells are shown in Figure 1. The behavior of the solutions in passing from single to multiple celled configurations is discussed and the solution for the case of a two-celled analogue to Burgers' unconstrained vortex (Ref. 35) reported by Sullivan (Ref. 36) is given. A solution of the type reported by Sullivan is of considerable practical importance because many laboratory vortex chambers exhibit a two-celled flow and many large vortex phenomena such as hurricanes and tornadoes also exhibit this two-celled character.

The discussion now turns to look at some of the related electrical phenomena, such as discharge stabilization and charging

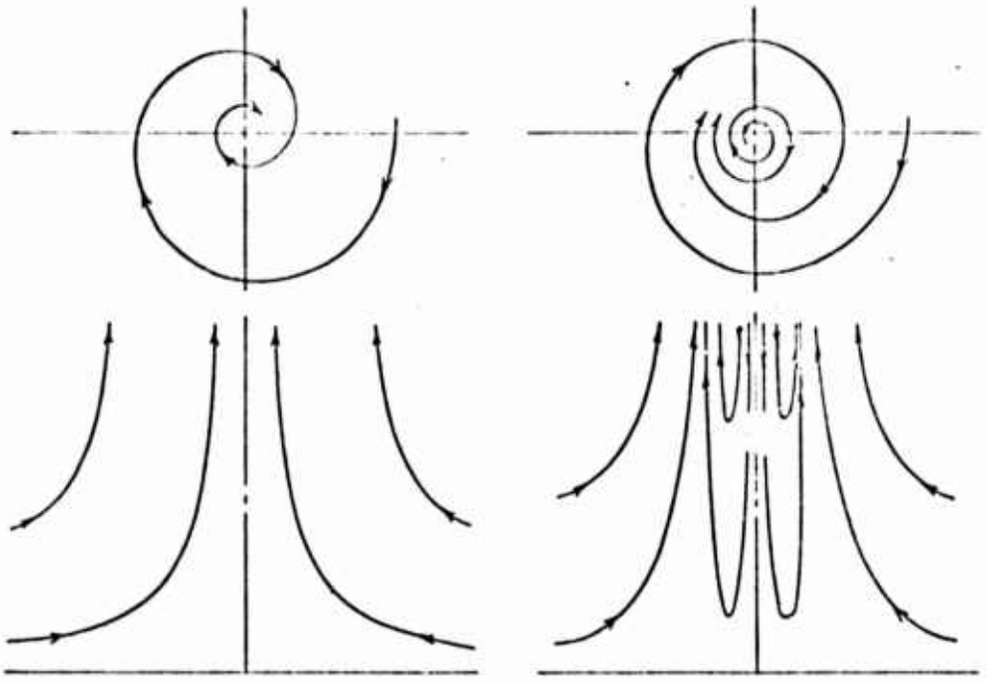

Flow Streamlines

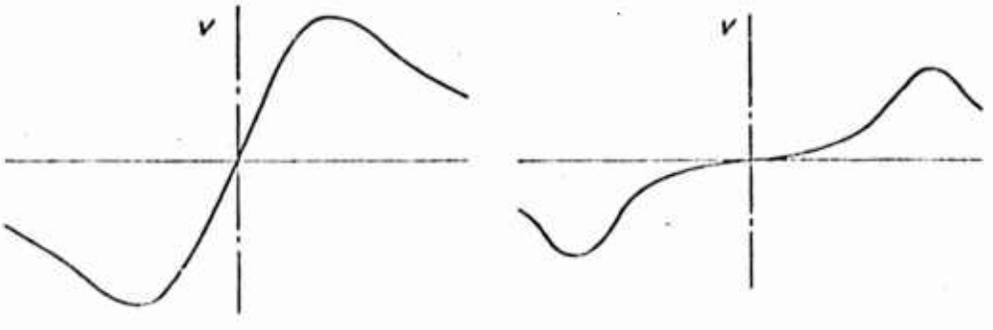

Tangential Velocity Profiles

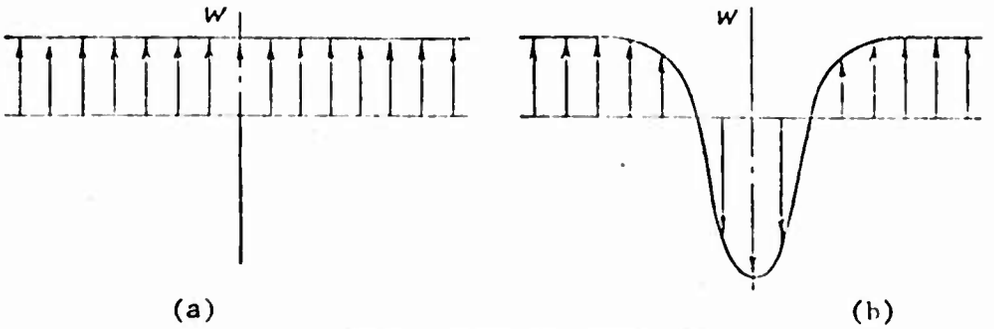

(a) (b)

Axial Velocity Profiles

FIGURE 1. Comparison of Burgers' One Cell Vortex (a) and Sullivan's Two Cell Vortex (b)

mechanisms, which should give better insight into the problem of determining the role of electrical activity in vortex systems.

Vonnegut, Moore, and Harris (Ref. 37) conducted simple laboratory experiments to determine what effects, if any, a vortex would have on a continuous high voltage discharge. They found that the vortex produced the following effects on the high-voltage discharge:

1) it makes the discharge more stable;
2) it causes the character of the discharge to change from successive sparks to a continuous glow;
3) it increases the distance over which the discharge can be maintained;
4) it decreases the electrical resistance of the discharge;
5) it decreases the noise of the discharge;
6) it decreases the production of the electromagnetic radiation in the discharge band;
7) it causes the discharge to center itself along the axis of rotation.

The authors believe that the effects produced by the vortex on the discharge can be explained in terms of the centrifugal force it exerts. A radial pressure gradient which is zero at the axis and increases with the distance away from it is produced by the rotation of the air in the tube. In a pressure gradient like this, bouyant forces cause the hot gas in the discharge to move toward the region of lowest pressure at the axis. The centrifugal action automatically confines the discharge at the center of the vortex. This stabilizes the vortex by forcing the hot ionized gases together

at the axis and by preventing them from mixing with the cool surrounding air.

The authors also concluded that the results suggest that the tornado funnel might serve as a preferred path for lightning and that the vortex may stabilize and modify lightning discharges.

Wilkins and McConnell (Ref. 38) in 1968 attempted to determine experimentally the threshold conditions for vortex-stabilized discharges in the atmosphere and whether or not a vortex core is an improved conductor for arc discharges. They concluded that if point discharging is a factor in the prevention of lightning as indicated by the laboratory analogy, then, since high velocity flow tends to speed up point discharging, a tornado funnel is not a favored region in this respect for cloud to ground lightning. The core region is however, more favorable than the region just outside it, and if the air above the tornado were stressed to the breakdown point, it is possible for a ground stroke to occur along the vortex axis.

The experiments show that the threshold power required to maintain a steady discharge decreases as vortex velocity increases, but this effect is not very pronounced and one would not conclude from it that a tornado axis would provide a highly favored environment for continuous cloud-to-ground discharging. The power for the initial lightning discharge would somehow have to be maintained for periods of several seconds, and there is no reason to suppose this is possible. The experiments indicate that the discharge will flame out between

lightning strokes because the centrifuge action of the vortex in confining and concentrating the plasma is not sufficient to appreciably lengthen the restrike time. In view of these considerations the authors suggest that a tornado funnel is not a highly favored region for multistroke lightning discharges unless the tornado thunderstorm is a considerably more efficient charging system than other thunderstorms.

Dunham (Ref. 39) made measurements of the charge produced by snow striking various surfaces at high speed. He concluded that electrostatic charging by friction and fragmentation of snow particles is dependent on the substance the snow is striking and the charging rate increases with a decrease in temperature from 0°C to -7°C. Charging rate per gram varies as the square of the speed.

Latham (Ref. 40) made an analysis of the available observations on the electrical properties of natural and artificial snowstorms. These electrical effects are in qualitative agreement with the theory of charge transfer associated with temperature gradients in ice, which has been shown to provide a tenable theory of thunderstorm electrification. The electrical effects associated with natural and artificial sandstorms have a marked resemblance to the snowstorm electrification phenomena and appear to be explainable in terms of a similar temperature gradient effect.

Kunkel (Ref. 41) conducted an extensive study on the static electrification of dust particles on dispersion into a cloud under

a variety of conditions ranging from blowing with a minimum of turbulence to violent and maximum impact with various types of surfaces. He concluded that there appears to be no doubt that the act of separating a mass of solid particles in contact with each other into a cloud of particles of assorted sizes yields in all cases a cloud which as a whole is neutral, but in which practically all the particles are charged. The number of particles of similar size but with opposite charges was about equal. The magnitude of the charges did not increase as rapidly as the surface of the particle. No correlation was observed between particle size and sign of charge. There appears to be strong evidence that charging occurs on separation of the contacts between particles in the dispersion of the cloud. Charging did not appear to be affected by humidity. Heterogeneous systems making contact with solid walls of different composition from the powder gave consistent asymmetry of charge of varying degrees depending on the proportion of particles striking the surfaces relative to those just separated.

Much work has been done in the area of raindrop electrification and raindrop charge and thunderstorm electrification by Gunn (Ref. 42, 43, 44, 45, 46). His work is significant to this study in that the droplet charging mechanisms he presents and discusses are possibly the mechanisms causing the initial electrification of droplets in a thunderstorm and buildup of the potential gradients in thunderstorms.

It is hoped that the accounts of electrical activity in vortex systems, the electrical and hydrodynamic theories for tornadoes,

dust devils, and vortex systems, and the charging mechanisms related to other electrical phenomena presented here will permit some substantial conclusions to be drawn concerning the role of electrical activity in vortex systems.

The first area to be discussed is the role of electrical activity in tornadoes. It appears that three choices are available here: 1) tornadoes are caused by electrical activity; 2) electrical activity is caused by tornadoes; 3) any association between the two is fortuitous. Each of these choices will be examined in greater detail. If tornadoes are caused by electrical activity, than the electrical heating theories of Vonnegut (Ref. 9) and Colgate (Ref. 24), the electromagnetic theory of Rathbun (Ref. 25), the idea of electrodynamic acceleration of ions proposed by Vonnegut (Ref. 9), or the magnetohydrodynamically driven vortex theory of Lewellen (Ref. 26) could be used to explain the relationship. The electrical heating theory does not appear feasible because it requires long, sustained lightning strokes or some totally unknown phenomenon to heat the air sufficiently to provide the intense winds found in a tornado. A tornado funnel may be a preferred path for a lightning stroke, but it is doubtful that even this could lead to a very large heating of air. This theory is certainly not sufficient to account for the intense updrafts and high angular momentum associated with funnel clouds.

Rathbun's (Ref. 25) electromagnetic theory suffers because there is no known physical process that could cause the ion concentration

in the air to remain as large as the theory assumes it is for as long a period of time as the theory assumes also. The idea of electrodynamic acceleration of ions or a magnetohydrodynamically driven vortex are both dependent on the development of a tangential body force within the air to accelerate it. Lewellen (Ref. 26) has shown that this requires an axial electric field and a radial magnetic field or conversely, a radial electric field and an axial magnetic field. The first combination can be eliminated because as Wilkins (Ref. 23) has pointed out, there is no way for a radial magnetic field to exist. The second combination is physically possible, but it is felt that the axial electric field required to maintain the ion concentration will probably overshadow any radial electric field.

With the theories available at present, it appears unlikely that tornadoes are definitely and directly caused by electrical activity. It may be possible that electrical forces help to maintain a tornado, but it is difficult to conclude this based on present day knowledge or thinking.

The third hypothesis: any association between tornadoes and electrical activity is fortuitous, will be discussed next. The various accounts of electrical activity in tornadoes make it difficult to conclude that this activity happens by chance. Present knowledge in the field of thunderstorm electrification, raindrop electrification and other atmospheric electrical phenomena as evidenced by the work of Gunn (Ref. 46), for example, quickly dispel

any notions that the electrical activity is fortuitous. The relationship may be a complex one with many interacting variables, but there is no doubt that a relationship does exist.

The second hypothesis: the tornado or vortex motion causes electrical activity, appears to be most plausible at this time. The remarks by Loeb (Ref. 27), the work of Lavan and Fejer (Ref. 22), the measurements by Freier (Ref. 17), Crozier (Ref. 18), and Bradley and Semonin (Ref. 19) all serve to bolster the belief that this is the correct relationship between the two phenomena. The measurements of Freier (Ref. 17), Crozier (Ref. 18), and Bradley and Semonin (Ref. 19) on the electric fields associated with dust devils all indicated that this vortex system had a large region of negative charge above it. Loeb (Ref. 27) credits this to asymmetrical contact charging of dust with heavier particles. The centrifugal action of the vortex and gravitational attraction would cause the lighter, negatively charged dust to be at the top of the dust devil. The work of Lavan and Fejer (Ref. 22) on swirling flows in ducts showed that swirling jets of saturated air or water enclosed in insulating walls produced glow discharges. Here the centrifugal action of the vortex served as a charge separator by causing the larger, positive water drops to go to the wall with a fine mist of light negative charges remaining in the center of the tube. A glow discharge in the tube was set up by the more than adequate potential gradients that developed.

This survey has served to illustrate that the determination of the role of electrical activity in vortex systems such as the tornado or the dust devil is a very complex problem, requiring research in many

different areas. This study of charged particle motion in a free-vortex flow field is intended to determine if particle motion in a free vortex can be influenced by the interaction between the particle charge and an applied electrostatic field.

DISCUSSION AND DESCRIPTION OF PARTICLE-FLOW SYSTEMS AND THEORY

In order to simplify the analysis of the motion of a charged particle in a free-vortex under the influence of an applied electrostatic field, several assumptions were made. First, rather than attempting to analyze the motion of a large number of particles having some size distribution and charge distribution, this analysis is concerned with the motion of a single charged particle. The analysis of the general motion of a gas-solid system with some size distribution of solid particles and including interactions among particles may be treated using the methods discussed by Soo (Ref. 47). Second, the particle is assumed to be charged prior to its introduction into the free-vortex flow field. No explanation of how the particle became charged will be advanced, other than to indicate that electrification of solid particles does occur when contact and separation are made between the particles and a dissimilar material, or a similar material under different surface conditions. Kunkel (Ref. 41) has made an extensive study on the static electrification of dust particles on dispersion in a cloud in which he concludes that electrification occurs when contact and separation are made between the particles. Third, the assumption is made that the flow field is an axisymmetric free-vortex, that is, the tangential flow is inversely proportional to the radius. To avoid the problem of the infinite velocity at the origin, the particle is assumed to be initially at some finite radius and its predominant motion is away

from the origin. Fourth, the assumption is made that the drag force on the particle is proportional to its relative velocity and that the drag coefficient can be represented using Stokes' law. This assumption is valid at low Reynolds number when streamline or viscous flow exists around the particle. The drag force is given by:

$$\bar{F}_D = C_D \rho \frac{(\bar{u} - \bar{v}_p)^2}{2} \frac{\pi D_p^2}{4} \quad ,$$

and the drag coefficient is given by:

$$C_D = \frac{24\mu}{\rho |\bar{u} - \bar{v}_p| D_p} \quad .$$

Therefore, the drag force can be expressed as:

$$\bar{F}_D = 3\pi\mu D_p (\bar{u} - \bar{v}_p) \quad .$$

Fifth, it was assumed that the applied electrostatic field was the result of a line source of positively charged particles located at the axis of the free-vortex. The electrostatic field due to the charged line source is given by $E = \lambda / 2\pi\epsilon_o r$ (Ref. 48).

In order to analyze the motion of a charged particle in a free-vortex under the influence of an applied electric field and determine the parameters affecting the particle motion, four different particle-flow systems were considered. The first case analyzed the motion of an uncharged particle in a free-vortex. This system was analyzed to provide a baseline for determining the effects of the drag force and

centrifugal force on particle motion. The analysis of this system is referred to as Case I in the following discussions. The second system considered consisted of a positively charged particle free to move in a viscous medium under the influence of an applied electrostatic field due to a line source of positively charged particles. The analysis of this system indicated the effects of the electrostatic body force on particle motion. The analysis of this system will be referred to as Case II. The third system investigated consisted of a positively charged particle moving in a free-vortex under the influence of an applied electrostatic field. In effect, this system is created by superimposing the first two systems considered on each other. The analysis of this system is referred to as Case III. A variation to this system, in which the particle is assumed to be negatively charged, will be referred to as Case III A. Finally the fourth particle-flow system consisted of two charged particles moving in a free-vortex under the influence of the electrostatic field due to the charge on each of the particles. The analysis of this system is referred to as Case IV.

The determination of the equations governing the particle motion for each of the four systems considered will now be presented. The nomenclature used here is defined in Appendix A.

Case 1

The prediction of the motion of uncharged particles in a free-vortex system follows the analysis of Hirschkron and Ehrich, (Ref. 1), who studied the trajectories of uncharged particles entrained in a swirling flow. The following assumptions were made in their analysis:

1) The flow field is an axisymmetric free-vortex with a constant axial velocity;

2) The particle mass flow is small compared to the carrier-fluid mass flow;

3) The particles do not interact with each other, nor do they affect the flow field;

4) The particles are not charged;

5) The drag force is given by the Stokes relation:

$$F_D = 3\pi\mu D_p(\bar{u} - \bar{V}_p).$$

The equation of motion of a particle is then given by:

$$F = m_p \frac{d\bar{V}_p}{dt} = 3\pi\mu D_p(\bar{u} - \bar{V}_p) + \bar{B}, \qquad (1)$$

where $\bar{B}$ is the body force.

The particle coordinates, particle velocity components, and the flow field components in the (r,θ) plane and the (r,z) plane are shown in Figures 2 and 3.

In (r,θ,z) coordinates, Equation (1) can be expanded to,

$$m_p\left(V_r \frac{dV_r}{dr} - \frac{V_\theta^2}{r}\right) = 3\pi\mu D_p(u_r - V_r), \qquad (2)$$

$$m_p\left(V_r \frac{dV_\theta}{dr} + \frac{V_r V_\theta}{r}\right) = 3\pi\mu D_p(u_\theta - V_\theta), \qquad (3)$$

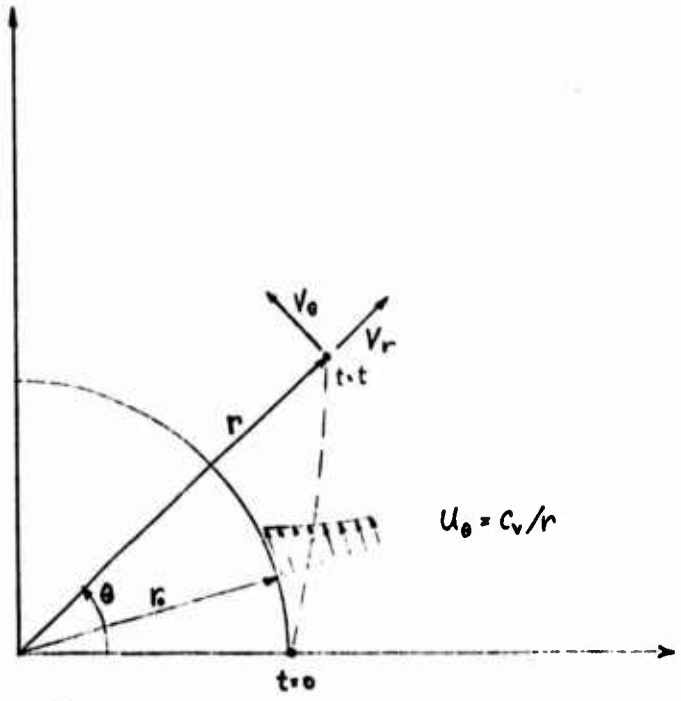

FIGURE 2

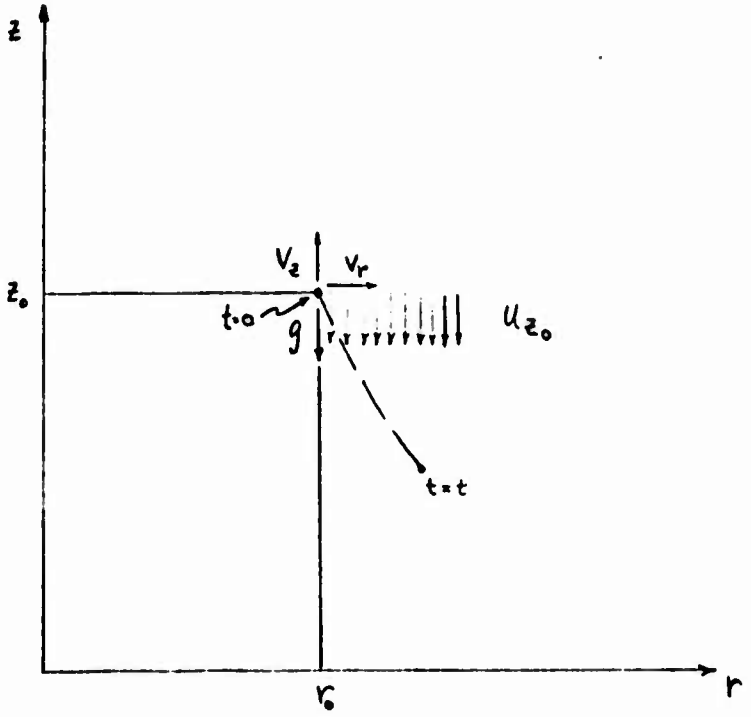

FIGURE 3

$$m_p\left(V_z \frac{dV_z}{dz}\right) = 3\pi\mu D_p (u_z - V_z) - m_p g. \tag{4}$$

Assume that the flow field is an axisymmetric free-vortex. Therefore,

$$u_r = 0, \tag{5a}$$

$$u_\theta = C_v/r, \tag{5b}$$

$$u_z = u_{z_o}, \quad \text{constant}. \tag{5c}$$

Define $$C = 3\pi\mu D_p/m_p. \tag{6}$$

Applying 5a, 5b, 5c, and 6 to Equations 2, 3, and 4 reduce the latter to the following form:

$$V_r \frac{dV_r}{dr} - \frac{V_\theta^2}{r} = -C V_r, \tag{7}$$

$$V_r \frac{dV_\theta}{dr} + \frac{V_r V_\theta}{r} = C(C_v/r - V_\theta), \tag{8}$$

$$V_z \frac{dV_z}{dz} = C(u_{z_o} - V_z) - g. \tag{9}$$

Setting $$X_\theta = V_\theta - C_v/r, \tag{10}$$

and substituting for v_θ in Equation (8), the following result is obtained:

$$V_r \frac{dX_\theta}{dr} + \frac{V_r X_\theta}{r} = -C X_\theta, \tag{11}$$

or, $$\frac{V_r}{r} \frac{d}{dr}(r X_\theta) = -C X_\theta. \tag{12}$$

The variable (rx_θ) can now be separated such that

$$\frac{d(rX_\theta)}{(rX_\theta)} = -C\frac{dr}{V_r}. \tag{13}$$

Along the particle trajectory, $V_r = \frac{dr}{dt}$. (14)

Therefore, $\frac{d(rX_\theta)}{(rX_\theta)} = -C\,dt$. (15)

Integrating Equation (15) from t = 0 to t = t,

$$(rX_\theta) = (rX_\theta)_o e^{-Ct}, \tag{16}$$

where $(rX_\theta)_o = r_o(V_{\theta_o} - C_v/r_o)$. (17)

Since $V_\theta = X_\theta + C_v/r$,

$$V_\theta = \left[r_o(V_{\theta_o} - C_v/r_o)e^{-Ct} + C_v\right]/r. \tag{18}$$

Substituting for v_θ in Equation (7), and applying Equation (14),

$$\frac{d^2r}{dt^2} - \left[\frac{r_o(V_{\theta_o} - C_v/r_o)e^{-Ct} + C_v}{r^2}\right]^2 = -C\frac{dr}{dt}. \tag{19}$$

Along a particle trajectory, $V_\theta = r\frac{d\theta}{dt}$. (20)

Therefore, $\frac{d\theta}{dt} = \frac{r_o(V_{\theta_o} - C_v/r_o)e^{-Ct} + C_v}{r^2}$. (21)

Define $v_z = dz/dt$ and substitute for v_z in Equation (4).

$$\frac{d^2z}{dt^2} = C(u_{z_o} - \frac{dz}{dt}) - g. \tag{22}$$

Equations 19, 21, and 22 describe the particle motion within the free-vortex system. The case where the initial particle injection velocity, v_{θ_o}, is zero will be examined in some detail.

Using $v_{\theta_o} = 0$, the equations describing the particle motion are:

$$\frac{d^2r}{dt^2} + C\frac{dr}{dt} - \frac{\left[C_v(1-e^{-Ct})\right]^2}{r^3} = 0, \tag{23}$$

$$\frac{d\theta}{dt} - \frac{C_v(1-e^{-Ct})}{r^2} = 0, \tag{24}$$

$$\frac{d^2z}{dt^2} + C\frac{dz}{dt} - Cu_{z_o} + g = 0. \tag{25}$$

These equations can be nondimensionalized through the use of nondimensional parameters $R = r/r_o$, $Z = z/z_o$, and $T = Ct$.

$$\frac{d^2R}{dT^2} + \frac{dR}{dT} - \left(\frac{C_v}{Cr_o^2}\right)^2\frac{(1-e^{-T})^2}{R^3} = 0, \tag{26}$$

$$\frac{d\theta}{dT} - \left(\frac{C_v}{Cr_o^2}\right)\frac{(1-e^{-T})}{R^2} = 0, \tag{27}$$

$$\frac{d^2z}{dT^2} + \frac{dz}{dT} - \frac{u_{z_o}}{Cz_o} + \frac{g}{C^2z_o} = 0. \tag{28}$$

Assume the following boundary conditions:

At $t = 0$,

$r = r_o$, $V_r = \frac{dr}{dt} = 0$,

$\theta = 0$,

$z = z_o$, $V_z = \frac{dz}{dt} = 0$.

In nondimensional form, the boundary conditions are:

At $T = 0$,

$R = 1$, $\frac{dR}{dT} = 0$,

$\theta = 0$,

$z = 1$, $\frac{dz}{dT} = 0$.

Equations 26 and 27 cannot be explicitly solved for the particle trajectories; however, they can be integrated relatively easily using

a numerical procedure. A fourth-order Runge-Kutta scheme was programmed for a digital computer to obtain the solutions to these equations. The computerized equations and the Runge-Kutta scheme will be described in greater detail in the chapter on the computer programs.

Equation (28) can be integrated directly, subject to its associated boundary conditions.

$$\frac{d^2Z}{dT^2} + \frac{dZ}{dT} - \frac{U_{z_0}}{CZ_0} + \frac{g}{C^2 z_0} = 0 \tag{29}$$

Boundary Conditions:

$$At \quad T = 0, \quad Z = 1, \quad \frac{dZ}{dT} = 0.$$

The solution to this differential equation, subject to its boundary conditions, is given by:

$$Z = 1 + \left(\frac{Cu_{z_0} - g}{C^2 z_0}\right)\left(T + e^{-T} - 1\right). \tag{30}$$

In dimensional form, the axial particle trajectory is given by

$$z = z_0 + (Cu_{z_0} - g)(t/C + e^{-Ct}/C - 1/C). \tag{31}$$

Case II

The second case analyzed considered the motion of a charged particle due to the presence of a line source some distance r_o away from the charged particle. Viscous drag in the gas is to be accounted for through the use of the Stokes relation. This analysis is similar to that conducted by Soo (Ref. 6). Figure 4 indicates that the line source of strength λ coincides with the Z-axis and the particle having charge-to-mass ratio (q/m) is initially a distance r_o away from the line source.

The following assumptions were made in this analysis:

1) No flow field is acting;

2) The particle is charged;

3) The applied electrostatic field due to a line source affects the particle motion;

4) The drag force is given by the Stokes relation:

$$\bar{F}_D = 3\pi\mu D_p (\bar{u} - \bar{v}_p).$$

The equation of motion of the particle is then given by:

$$m_p \frac{d\bar{v}_p}{dt} = 3\pi\mu D_p (\bar{u} - \bar{v}_p) + q_p \bar{E}. \qquad (32)$$

Since the applied electrostatic field due to the charged line source acts in the radial direction only, and since the initial particle velocities in the tangential and axial directions are zero, the equation of motion reduces to:

$$m m_p v_r \frac{dv_r}{dr} = -3\pi\mu D_p v_r + q_p \cdot E_r \qquad (33)$$

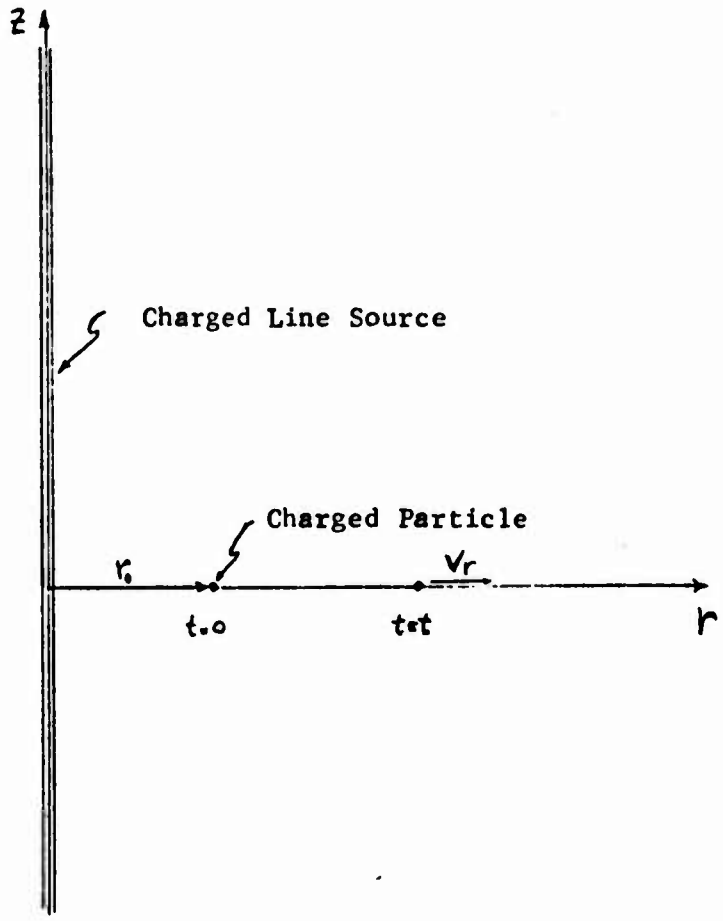

FIGURE 4

For a line source, E_r is given by (Ref. 48):

$$E_r = \lambda q_e / 2\pi\epsilon_o r \tag{34}$$

Defining $$V_r = \frac{dr}{dt}, \tag{6}$$

$$C = 3\pi\mu D_p / m_p, \tag{14}$$

$$D = q_p \lambda q_e / 2\pi\epsilon_o m_p, \tag{35}$$

and substituting Equations (6), (14), (34), and (35) into Equation (33), the following equation results:

$$\frac{d^2r}{dt^2} + C\frac{dr}{dt} - \frac{D}{r} = 0. \tag{36}$$

Assume the following boundary conditions:

$$\text{At} \quad t = 0, \quad r = r_o, \quad \frac{dr}{dt} = 0.$$

This differential equation and its associated boundary conditions can be nondimensionalized through the use of the nondimensional parameters $R = r/r_o$, and $T = Ct$.

$$\frac{d^2R}{dT^2} + \frac{dR}{dT} - \frac{D}{C^2R} = 0. \tag{37}$$

The boundary conditions are:

$$\text{At} \quad T = 0, \quad R = 1, \quad \frac{dR}{dT} = 0.$$

Equation (37) can be integrated using the numerical procedure mentioned in Case I.

Case III

The third case studied involved a charged particle moving in a free-vortex flow field, under the influence of an applied electrostatic field due to an axial line source of charges. The forces on the particle under consideration are the drag force, a body force due to the applied electrostatic field, and the gravitational force.

The following assumptions were made in this case:

1) The flow field is an axisymmetric free-vortex with a constant axial velocity;

2) The particle mass flow is small compared to the carrier fluid mass flow;

3) The particle is charged;

4) The applied electrostatic field due to the line source affects the particle motion;

5) The drag force is given by the Stokes relation, $\bar{F}_D = 3\pi\mu D_p\ (\bar{u} - \bar{v}_p)$.

Figures 5 and 6 indicate the particle coordinates, particle velocity components, and fluid velocity components in the (r,θ) and (r,z) planes. Also indicated in Figures 5 and 6 are the initial particle positions and the location of the charged line source on the Z-axis.

The equation of motion of the particle is then given by:

$$m_p \frac{dv_p}{dt} = 3\pi\mu D_p (\bar{u} - \bar{v}_p) + \bar{B} \tag{38}$$

where $\bar{B}$ is the body force.

Equation (38) can be expanded in (r,θ,z) coordinates to

$$m_p\left(v_r \frac{dv_r}{dr} - \frac{v_\theta^2}{r}\right) = 3\pi\mu D_p (u_r - v_r) + B_r \tag{39}$$

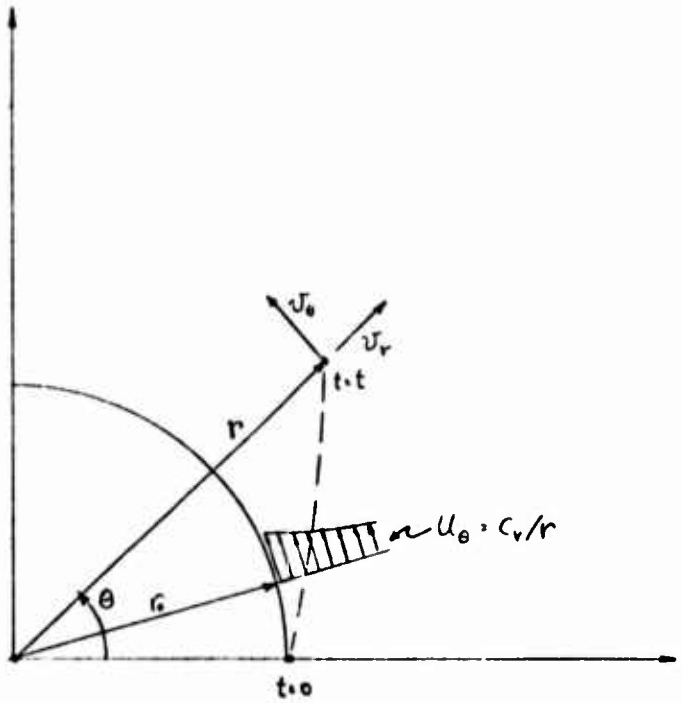

FIGURE 5

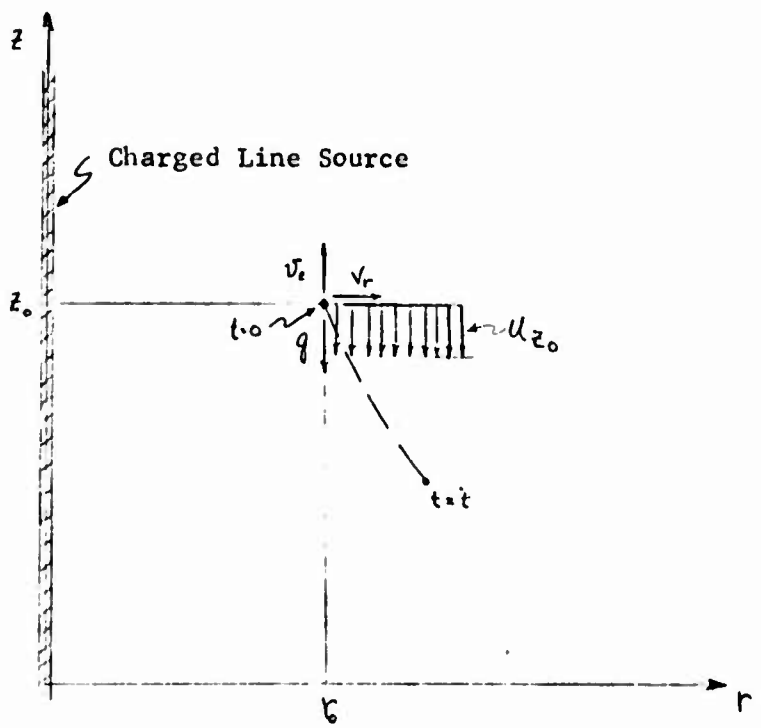

FIGURE 6

$$m_p\left(V_r \frac{dV_\theta}{dr} + \frac{V_r V_\theta}{r}\right) = 3\pi\mu D_p (u_\theta - V_\theta) + B_\theta, \tag{40}$$

$$m_p\left(V_z \frac{dV_z}{dz}\right) = 3\pi\mu D_p (u_z - V_z) + B_z. \tag{41}$$

In the radial direction, $B_r = \lambda q_p g_c / 2\pi\epsilon_o r$; in the tangential direction, $B_\theta = 0$; and in the axial direction, $B_z = -m_p g$.

Assuming that the flow field is an axisymmetric free-vortex,

$$u_r = 0, \tag{5a}$$

$$u_\theta = C_v / r, \tag{5b}$$

$$u_z = u_{z_c} \qquad \text{constant}. \tag{5c}$$

Substituting into Equations 39, 40, and 41 for B_r, B_θ, B_z, and U_r, U_θ, U_z, the following equations result:

$$V_r \frac{dV_r}{dr} - \frac{V_\theta^2}{r} = C(-V_r) + \frac{D}{r}, \tag{42}$$

$$V_r \frac{dV_\theta}{dr} + \frac{V_r V_\theta}{r} = C\left(\frac{C_v}{r} - V_\theta\right), \tag{43}$$

$$V_z \frac{dV_z}{dz} = C(u_{z_o} - V_z) - g. \tag{44}$$

where $C = 3\pi\mu D_p / m_p$ and $D = \lambda g_c q_p / 2\pi\epsilon_o m_p$. Let $X_\theta = v_\theta - C_v / r$, and substitute for v_θ in Equation 43.

$$V_r \frac{dX_\theta}{dr} + \frac{V_r X_\theta}{r} = -C X_\theta. \tag{45}$$

Equation (45) can be rewritten as:

$$\frac{V_r}{r} \frac{d}{dr}(r X_\theta) = -C X_\theta. \tag{46}$$

The variable rX_θ can now be separated such that:

$$\frac{d(rX_\theta)}{(rX_\theta)} = -C\frac{dr}{V_r}. \tag{47}$$

Using $v_r = dr/dt$,

$$\frac{d(rX_\theta)}{(rX_\theta)} = -C\,dt. \tag{48}$$

Integrating Equation (48) from t = 0 to t,

$$rX_\theta = r_o X_{\theta_o} e^{-Ct}, \tag{49}$$

where $$r_o X_{\theta_o} = r_o(V_{\theta_o} - C_v/r_o).$$

Since $$V_\theta = X_\theta + C_v/r,$$

$$V_\theta = \frac{r_o(V_{\theta_o} - C_v/r_o)e^{-Ct}}{r} + \frac{C_v}{r}. \tag{50}$$

Substituting for v_θ in Equation (42), using $v_r = dr/dt$, the equation for the radial trajectory becomes:

$$\frac{d^2r}{dt^2} - \frac{\left[r_o(V_{\theta_o} - C_v/r_o)e^{-Ct} + C_v\right]^2}{r^3} + C\frac{dr}{dt} - \frac{D}{r} = 0. \tag{51}$$

Along the particle trajectory $v_\theta = r\,d\theta/dt$. The equation for the tangential particle trajectory becomes:

$$r\frac{d\theta}{dt} = \frac{\left[r_o(V_{\theta_o} - C_v/r_o)e^{-Ct} + C_v\right]}{r}, \quad \text{or,} \tag{52}$$

$$\frac{d\theta}{dt} - \frac{\left[r_o(V_{\theta_o} - C_v/r_o)e^{-Ct} + C_v\right]}{r^2} = 0. \tag{53}$$

Define $v_z = dz/dt$ and substitute for v_z in Equation (44)

$$\frac{d^2z}{dt^2} + C\frac{dz}{dt} - CV_{z_o} + g = 0. \tag{54}$$

Equations 51, 53, and 54 describe the motion of a charged particle in a free-vortex system under the influence of an applied electrostatic field. Once again the initial particle velocity in the tangential direction, v_{θ_o}, will be assumed zero. This case will be examined in some detail.

Using $v_{\theta_o} = 0$, the equations of motion are:

$$\frac{d^2r}{dt^2} + C\frac{dr}{dt} - \frac{\left[C_v(1-e^{-Ct})\right]^2}{r^3} - \frac{D}{r} = 0, \tag{55}$$

$$\frac{d\theta}{dt} - \frac{C_v(1-e^{-Ct})}{r^2} = 0, \tag{56}$$

$$\frac{d^2z}{dt^2} + C\frac{dz}{dt} - Cv_{z_o} + g = 0. \tag{57}$$

The nondimensional form of these equations, using $R = r/r_o$, $T = Ct$, and $Z = z/z_o$, is given by:

$$\frac{d^2R}{dT^2} + \frac{dR}{dT} - \left(\frac{C_v}{Cr_o^2}\right)^2 \frac{(1-e^{-T})^2}{R^3} - \frac{D}{(Cr_o)^2}\,\frac{1}{R} = 0. \tag{58}$$

$$\frac{d\theta}{dT} - \left(\frac{C_v}{Cr_o^2}\right)\frac{1-e^{-T}}{R} = 0 \tag{59}$$

$$\frac{d^2z}{dT^2} + \frac{dz}{dT} - \frac{v_{z_o}}{Cz_o} + \frac{g}{C^2z_o} = 0 \tag{60}$$

Assume the following boundary conditions:

At $t = 0$,
$r = r_o$, $v_r = dr/dt = 0$,
$\theta = 0$,
$z = z_o$, $v_z = dz/dt = 0$.

In nondimensional form, the boundary conditions are:

At $T = 0$,
$R = 1$, $dR/dT = 0$,
$\theta = 0$,
$Z = 1$, $dZ/dT = 0$.

Equations (58) and (59), describing the radial and tangential particle trajectories, can be integrated using the numerical procedure mentioned previously in Case I. The computerized form of these equations will be described in the chapter on the computer programs. Equation (60), the axial particle trajectory, is identical to Equation (28) which describes the axial particle trajectory in Case I. This is expected, because the axial flow velocity is independent of radial or tangential position and also because the force due to the electrostatic field does not have an axial component.

Case IV

The fourth case analyzed considered the motion of two charged particles in a free-vortex flow field. Viscous drag in the fluid was accounted for through the Stokes relation, and the particles were assumed to influence the motion of each other due to the electrostatic body forces arising from the electric charge on each particle. The following assumptions were made in this analysis:

1) The velocity distribution of the flow field is known;
2) The particle mass flow is small compared to the carrier fluid mass flow;
3) The particles are charged;
4) The drag force is given by the Stokes relation;
5) There is no fluid or particle motion in the axial direction.

The equation of motion of the first particle is given by:

$$m_{P_1} \frac{d\bar{V}_{P_1}}{dt} = 3\pi\mu D_1 (\bar{u}_1 - \bar{V}_{P_1}) + q_{P_1} \bar{E}_1 \quad (61)$$

and that of the second particle is

$$m_{P_2} \frac{d\bar{V}_{P_2}}{dt} = 3\pi\mu D_2 (\bar{u}_2 - \bar{V}_{P_2}) + q_{P_2} \bar{E}_2 \quad (62)$$

where $\bar{E}_1$ and $\bar{E}_2$ are the electric fields at points 1 and 2 respectively, as shown in Figure 7. Expanding these equations in (r,θ) coordinates, the following equations result:

$$V_{r_1} \frac{dV_{r_1}}{dr_1} - \frac{V_{\theta_1}^2}{r_1} = \frac{3\pi\mu D_1}{m_1}(u_{r_1} - V_{r_1}) + \frac{q_1 E_{r_1}}{m_1} \quad (63)$$

$$V_{r_1} \frac{dV_{\theta_1}}{dr_1} + \frac{V_{r_1} V_{\theta_1}}{r_1} = \frac{3\pi\mu D_1}{m_1}(u_{\theta_1} - V_{\theta_1}) + \frac{q_1 E_{\theta_1}}{m_1} \quad (64)$$

$$V_{r_2}\frac{dV_{r_2}}{dr_2} - \frac{V_{\theta_2}^2}{r_2} = \frac{3\pi\mu D_2}{m_2}\left(u_{r_2} - V_{r_2}\right) + \frac{q_2 E_{r_2}}{m_2}, \tag{65}$$

$$V_{r_2}\frac{dV_{\theta_2}}{dr_2} + \frac{V_{r_2}V_{\theta_2}}{r_2} = \frac{3\pi\mu D_2}{m_2}\left(u_{\theta_2} - V_{\theta_2}\right) + \frac{q_2 E_{\theta_2}}{m_2}. \tag{66}$$

where E_{r_1}, E_{θ_1} are the radial and tangential components of the electric field at a point (r_1,θ_1) due to the charged particle q_2, and E_{r_2}, E_{θ_2} are the radial and tangential components of the electric field at a point (r_2,θ_2) due to the charged particle q_1.

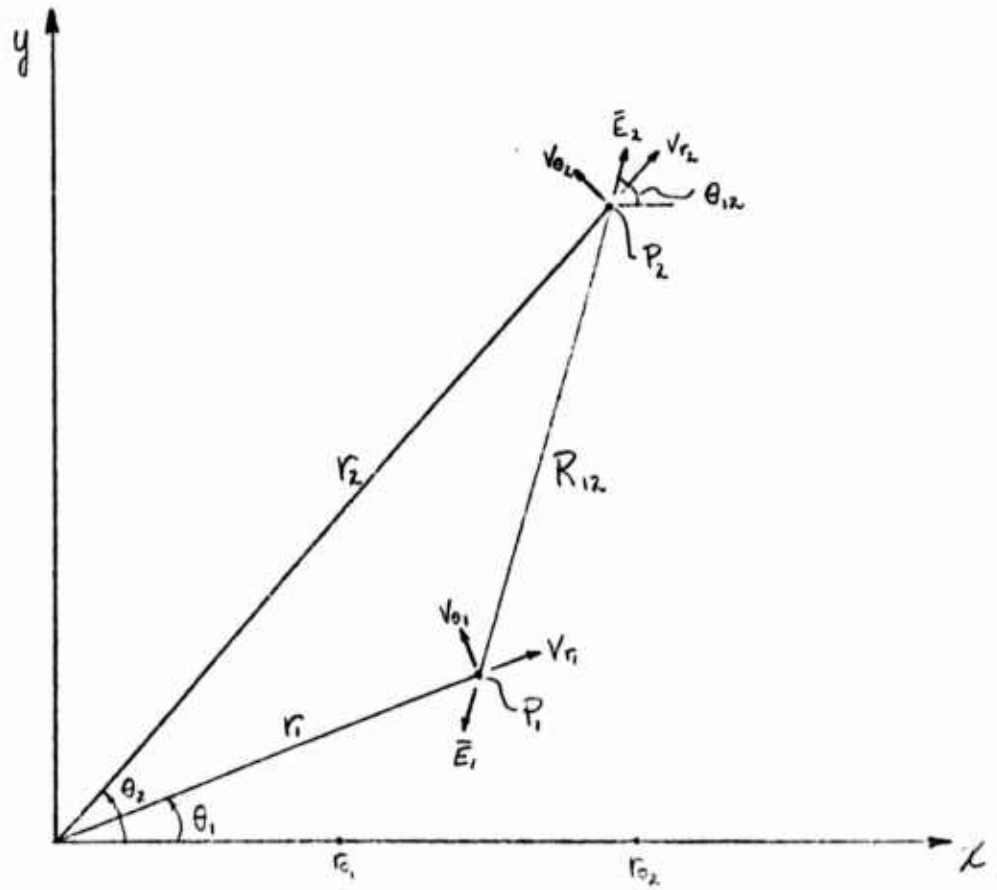

FIGURE 7

Referring of Figure 7, Point P_1 has coordinates (r_1,θ_1), and P_2 has coordinates (r_2,θ_2).

The electric field at P_1 due to a charge q_2 at Point P_2 is given by

$$\bar{E}_{P_1} = \frac{q_2}{4\pi\epsilon_0 R_{12}^2}\left(-\cos\theta_{12}\,\hat{\imath} - \sin\theta_{12}\,\hat{\jmath}\right). \tag{67}$$

Therefore

$$E_{r_1} = \frac{-q_2}{4\pi\epsilon_0 R_{12}^2}\left(\cos\theta_{12}\cos\theta_1 + \sin\theta_{12}\sin\theta_1\right). \tag{68a}$$

$$E_{\theta_1} = \frac{-q_2}{4\pi\epsilon_0 R_{12}^2}\left(-\cos\theta_{12}\sin\theta_1 + \sin\theta_{12}\cos\theta_1\right). \tag{68b}$$

or

$$E_{r_1} = \frac{-q_2}{4\pi\epsilon_0 R_{12}^2}\cos(\theta_{12} - \theta_1), \tag{69a}$$

$$E_{\theta_1} = \frac{-q_2}{4\pi\epsilon_0 R_{12}^2}\sin(\theta_{12} - \theta_1). \tag{69b}$$

The electric field at P_2 due to a charge q_1 at Point P_1 is given by

$$\bar{E}_{P_2} = \frac{q_1}{4\pi\epsilon_0 R_{12}^2}\left(\cos\theta_{12}\,\hat{\imath} + \sin\theta_{12}\,\hat{\jmath}\right). \tag{70}$$

Therefore

$$E_{r_2} = \frac{q_1}{4\pi\epsilon_0 R_{12}^2}\left(\cos\theta_{12}\cos\theta_2 + \sin\theta_{12}\cos(\pi/2 - \theta_2)\right), \tag{71a}$$

$$E_{\theta_2} = \frac{q_1}{4\pi\epsilon_0 R_{12}^2}\left(-\cos\theta_{12}\sin\theta_2 + \sin\theta_{12}\sin(\pi/2 - \theta_2)\right), \tag{71b}$$

or

$$E_{r_2} = \frac{q_1}{4\pi\epsilon_0 R_{12}^2}\cos(\theta_{12} - \theta_2), \tag{72a}$$

$$E_{\theta_2} = \frac{q_1}{4\pi\epsilon_0 R_{12}^2}\sin(\theta_{12} - \theta_2), \tag{72b}$$

where

$$R_{12}^2 = (r_2\cos\theta_2 - r_1\cos\theta_1)^2 + (r_2\sin\theta_2 - r_1\sin\theta_1)^2. \tag{73}$$

$$\tan\theta_{12} = \frac{r_2\sin\theta_2 - r_1\sin\theta_1}{r_2\cos\theta_2 - r_1\cos\theta_1} \tag{74}$$

or

$$\theta_{12} = \tan^{-1}\left(\frac{r_2\sin\theta_2 - r_1\sin\theta_1}{r_2\cos\theta_2 - r_1\cos\theta_1}\right). \tag{75}$$

Therefore E_{r_1}, E_{θ_1}, E_{r_2}, and E_{θ_2} can be expressed entirely in terms of r_1, θ_1, r_2, and θ_2.

Assume that the flow field is an axisymmetric free vortex. Therefore,

$$u_{r_1} = 0, \quad u_{r_2} = 0, \tag{76}$$

$$u_{\theta_1} = C_v/r_1, \quad u_{\theta_2} = C_v/r_2. \tag{77}$$

Along the particle trajectories,

$$V_{r_1} = \frac{dr_1}{dt}, \quad V_{\theta_1} = r_1 \frac{d\theta_1}{dt}, \tag{78}$$

$$V_{r_2} = \frac{dr_2}{dt}, \quad V_{\theta_2} = r_2 \frac{d\theta_2}{dt}. \tag{79}$$

Substituting into Equations (63) through (66), the following equations result:

$$\frac{d^2r_1}{dt^2} - r_1\left(\frac{d\theta_1}{dt}\right)^2 = -C_1 \frac{dr_1}{dt} - \frac{q_1 q_2 q_c}{m_1 4\pi\epsilon_0} \frac{\cos(\theta_{12} - \theta_1)}{R_{12}^2} \tag{80}$$

$$r_1 \frac{d^2\theta_1}{dt^2} + 2\frac{dr_1}{dt}\frac{d\theta_1}{dt} = C_1\left(\frac{C_v}{r_1} - r_1 \frac{d\theta_1}{dt}\right) - \frac{q_1 q_2 q_c}{m_1 4\pi\epsilon_0} \frac{\sin(\theta_{12} - \theta_1)}{R_{12}^2} \tag{81}$$

$$\frac{d^2r_2}{dt^2} - r_2\left(\frac{d\theta_2}{dt}\right)^2 = -C_2 \frac{dr_2}{dt} - \frac{q_1 q_2 q_c}{m_2 4\pi\epsilon_0} \frac{\cos(\theta_{12} - \theta_2)}{R_{12}^2} \tag{82}$$

$$r_2 \frac{d^2\theta_2}{dt^2} + 2\frac{dr_2}{dt}\frac{d\theta_2}{dt} = C_2\left(\frac{C_v}{r_2} - r_2 \frac{d\theta_2}{dt}\right) - \frac{q_1 q_2 q_c}{m_2 4\pi\epsilon_0} \frac{\sin(\theta_{12} - \theta_2)}{R_{12}^2} \tag{83}$$

where $C_1 = 3\pi\mu D_1/m_1$ and $C_2 = 3\pi\mu D_2/m_2$.

These equations can be nondimensionalized through the use of the following parameters:

$$R_1 = r_1/r_0$$

$$R_2 = r_2/r_0$$

$$T = C_1 t$$

$$r_0 C_1^2 \frac{d^2R_1}{dT^2} - r_0 C_1^2 R_1 \left(\frac{d\theta_1}{dT}\right)^2 = -C_1^2 r_0 \frac{dR_1}{dT} - \frac{q_1 q_2 q_0}{4\pi\epsilon_0 r_0^2 m_1} \frac{\cos(\theta^* - \theta_1)}{R^{*2}} \tag{84}$$

$$r_0 C_1^2 R_1 \frac{d^2\theta_1}{dT^2} + 2 r_0 C_1^2 \frac{dR_1}{dT}\frac{d\theta_1}{dT} = C_1\left(\frac{C_v}{r_0 R_1} - r_0 C_1 R_1 \frac{d\theta_1}{dT}\right) - \frac{q_1 q_2 q_0}{4\pi\epsilon_0 r_0^2 m_1} \frac{\sin(\theta^* - \theta_1)}{R^{*2}} \tag{85}$$

$$r_0 C_1^2 \frac{d^2R_2}{dT^2} - r_0 C_1^2 R_2 \left(\frac{d\theta_2}{dT}\right)^2 = -C_2 C_1 r_0 \frac{dR_2}{dT} + \frac{q_1 q_2 q_0}{4\pi\epsilon_0 r_0^2 m_2} \frac{\cos(\theta^* - \theta_2)}{R^{*2}} \tag{86}$$

$$r_0 C_1^2 R_2 \frac{d^2\theta_2}{dT^2} + 2 r_0 C_1^2 \frac{dR_2}{dT}\frac{d\theta_2}{dT} = C_2\left(\frac{C_v}{r_0 P_2} - r_0 C_1 R_2 \frac{d\theta_2}{dT}\right) + \frac{q_1 q_2 q_0}{4\pi\epsilon_0 r_0^2 m_2} \frac{\sin(\theta^* - \theta_2)}{R^{*2}} \tag{87}$$

$$\frac{d^2R_1}{dT^2} - R_1\left(\frac{d\theta_1}{dT}\right)^2 + \frac{dR_1}{dT} + A_1 A_2 \frac{\cos(\theta^* - \theta_1)}{R^{*2}} = 0 \tag{88}$$

$$R_1 \frac{d^2\theta_1}{dT^2} + \frac{d\theta_1}{dT}\left(2\frac{dR_1}{dT} + R_1\right) - \frac{A_2}{r_1} + A_1 A_2 \frac{\sin(\theta^* - \theta_1)}{R^{*2}} = 0 \tag{89}$$

$$\frac{d^2R_2}{dT^2} - R_2\left(\frac{d\theta_2}{dT}\right)^2 + A_4 \frac{dR_2}{dT} - A_1 A_3 \frac{\cos(\theta^* - \theta_2)}{R^{*2}} = 0 \tag{90}$$

$$R_2 \frac{d^2\theta_2}{dT^2} + \frac{d\theta_2}{dT}\left(2\frac{dR_2}{dT} + A_4 R_2\right) - \frac{A_3 A_4}{R_2} - A_1 A_5 \frac{\sin(\theta^* - \theta_2)}{R^{*2}} = 0 \qquad (91)$$

where $A_1 = q_c/4\pi\epsilon_0 r^3$, $A_2 = q_1 q_2/m_1 C_1^2$,

$A_3 = C_v/r_0^2 C_1$, $A_4 = C_2/C_1$, $A_5 = q_1 q_2/m_2 C_1^2$,

and $\theta^* = \tan^{-1}\left(\frac{R_2 \sin\theta_2 - R_1 \sin\theta_1}{R_2 \cos\theta_2 - R_1 \cos\theta_1}\right)$

and $R^{*2} = (R_2 \sin\theta_2 - R_1 \sin\theta_1)^2 + (R_2 \cos\theta_2 - R_1 \cos\theta_1)^2$

Assume the following boundary conditions:

at $T = 0$, $R_1 = 1$, $\frac{dR_1}{dT} = 0$, $\theta_1 = 0$, $\frac{d\theta_1}{dT} = 0$,

$R_2 = 2$, $\frac{dR_2}{dT} = 0$, $\theta_2 = 0$, $\frac{d\theta_2}{dT} = 0$.

Equations (88) through (91), subject to the boundary conditions above, can be solved using the numerical procedure mentioned previously. The computerized equations are given in the chapter on the computer programs.

NUMERICAL PROCEDURE AND COMPUTER PROGRAMS

The numerical procedure used to solve the equations governing the particle trajectories in the radial and tangential directions is the Runge-Kutta method with Gill's coefficients. Initial-value problems of the type encountered in this analysis can be easily solved using this method.

For a first order differential equation,

$$y' = f(y, t),$$

with initial conditions y_o and t_o, the basic formula in the Runge-Kutta method with Gill's coefficients is given by:

$$y_{m+1} = y_m + \Delta y_m$$

where

$$\Delta y_m = \frac{\Delta t}{6}\left[z_0 + (2-\sqrt{2})\, z_1 + (2+\sqrt{2})\, z_2 + z_3 \right],$$

and

$$z_0 = f(y_m, t_m)$$

$$z_1 = f(y_m + z_0/2,\ t_m + \Delta t/2)$$

$$z_2 = f\left(y_m + \left(-\tfrac{1}{2} + \tfrac{1}{\sqrt{2}}\right) z_0 + \left(1 - \tfrac{1}{\sqrt{2}}\right) z_1,\ t_m + \Delta t/2\right)$$

$$z_3 = f\left(y_m - \tfrac{1}{\sqrt{2}}\, z_1 + \left(1 + \tfrac{1}{\sqrt{2}}\right) z_2,\ t_m + \Delta t\right)$$

The derivation of this method is quite straightforward and is presented in Reference 49.

The following equations and their associated boundary conditions were to be solved using the Runge-Kutta-Gill method.

Case I

$$C_1 = 3\pi\mu D/m, \quad C_2 = C_v/r_0^2$$

$$\frac{d^2R}{dT^2} + \frac{dR}{dT} - \left(\frac{C_2}{C_1}\right)^2 \frac{(1-e^{-T})^2}{R^3} = 0$$

$$\frac{d\theta}{dT} - \frac{C_2}{C_1}\frac{(1-e^{-T})}{R^2} = 0.$$

Boundary conditions: T = 0, R = 1, dR/dT = 0, θ = 0.

Case II

$$C_3 = q_c/2\pi\epsilon_0, \quad C_4 = \lambda/r_0^2, \quad C_5 = q/m.$$

$$\frac{d^2R}{dT^2} + \frac{dR}{dT} - \frac{C_3 \cdot C_4 \cdot C_5}{C_1^2}\frac{1}{R} = 0$$

Boundary conditions: T = 0, R = 1, dR/dT = 0.

Case III

$$\frac{d^2R}{dT^2} + \frac{dR}{dT} - \left(\frac{C_2}{C_1}\right)^2 \frac{(1-e^{-T})^2}{R^3} - \frac{C_3 \cdot C_4 \cdot C_5}{C_1^2}\frac{1}{R} = 0$$

$$\frac{d\theta}{dT} - \left(\frac{C_2}{C_1}\right)\frac{(1-e^{-T})}{R^2} = 0$$

Boundary conditions: T = 0, R = 1, dR/dT = 0, θ = 0.

It is obvious that these three cases could be solved by one general computer program through the proper choice of the constants C_1, C_2, C_3, C_4, and C_5.

A general program was then written to solve the following equations:

$$\frac{d^2R}{dT^2} + \frac{dR}{dT} - \left(\frac{C_2}{C_1}\right)^2 \frac{(1-e^{-T})^2}{R^3} - \frac{C_3 \cdot C_4 \cdot C_5}{C_1^2}\frac{1}{R} = 0$$

$$\frac{d\theta}{dT} - \left(\frac{C_2}{C_1}\right)\frac{1-e^{-T}}{R^2} = 0$$

Subject to the boundary conditions: T = 0, R = 1, dR/dT = 0, θ = 0.

In Case I, $C_3 = C_4 = C_5 = 0$. In Case II, $C_2 = 0$.

These equations were reduced to a set of first order equations which can be solved simultaneously using the Runge-Kutta-Gill method. The following transformations were used:

$$Y_2 = R, \quad Y_3 = \frac{dR}{dT} = \frac{dY_2}{dT}, \quad Y_4 = \Theta.$$

The three first order, differential equations are:

$$\frac{dY_2}{dT} = Y_3$$

$$\frac{dY_3}{dT} = -Y_3 + \left(\frac{C_2}{C_1}\right)^2 \frac{(1-e^{-T})^2}{Y_2^3} + \frac{C_3 C_4 C_5}{C_1^2} \frac{1}{Y_2} = 0$$

$$\frac{dY_4}{dT} = \left(\frac{C_2}{C_1}\right) \frac{1-e^{-T}}{Y_2^2}$$

A separate computer program was written for Case IV. The following equations and their associated boundary conditions were solved using the Runge-Kutta-Gill method.

$$\frac{d^2R_1}{dT^2} - R_1\left(\frac{d\Theta_1}{dT}\right)^2 + \frac{dR_1}{dT} + \frac{A_1 A_2 \cos(\Theta^* - \Theta_1)}{R^{*2}} = 0$$

$$R_1 \frac{d^2\Theta_1}{dT^2} + \frac{d\Theta_1}{dT}\left(2\frac{dR_1}{dT} + R_1\right) - \frac{A_3}{R_1} + \frac{A_1 A_2 \sin(\Theta^* - \Theta_1)}{R^{*2}} = 0$$

$$\frac{d^2R_2}{dT^2} - R_2\left(\frac{d\Theta_2}{dT}\right)^2 + A_4 \frac{dR_2}{dT} - A_1 A_5 \frac{\cos(\Theta^* - \Theta_2)}{R^{*2}} = 0$$

$$R_2 \frac{d^2\Theta_2}{dT^2} + \frac{d\Theta_2}{dT}\left(2\frac{dR_2}{dT} + A_4 R_2\right) - \frac{A_3 A_4}{R_2} - A_1 A_5 \frac{\sin(\Theta^* - \Theta_2)}{R^{*2}} = 0$$

where

$$A_1 = q_c / \pi C_0 r_0^3, \quad A_2 = q_1 q_2 / m_1 C_1^2, \quad A_3 = C_1 / C_1 r_0^2,$$

$$A_4 = C_2 / C_1, \quad A_5 = q_1 q_2 / m_2 C_1^2,$$

$$\epsilon^* = \tan^{-1}\left(\frac{R_2 \sin\theta_2 - R_1 \sin\theta_1}{R_2 \cos\theta_2 - R_1 \cos\theta_1}\right)$$

and $$R^{*2} = (R_2 \sin\theta_2 - R_1 \sin\theta_1)^2 + (R_2 \cos\theta_2 - R_1 \cos\theta_1)^2$$

The following boundary conditions apply:

at $$T = 0, \quad R_1 = 1, \quad \frac{dR_1}{dT} = 0, \quad \theta_1 = 0, \quad \frac{d\theta_1}{dT} = 0,$$

$$R_2 = 2, \quad \frac{dR_2}{dT} = 0, \quad \theta_2 = 0, \quad \frac{d\theta_2}{dT} = 0.$$

The following transformations were used to obtain the first order, differential equations:

$$Y_2 = R_1$$
$$Y_3 = \frac{dR_1}{dT} = \frac{dY_2}{dT}$$
$$Y_4 = \theta_1$$
$$Y_5 = \frac{d\theta_1}{dT} = \frac{dY_4}{dT}$$
$$Y_6 = R_2$$
$$Y_7 = \frac{dR_2}{dT} = \frac{dY_6}{dT}$$
$$Y_8 = \theta_2$$
$$Y_9 = \frac{d\theta_2}{dT} = \frac{dY_8}{dT}$$

The first order equations which were then programmed are:

$$\frac{dY_2}{dT} = Y_3$$

$$\frac{dY_3}{dT} = Y_2 Y_5^2 - Y_3 - A_1 A_2 \cos(\theta - Y_4)/R^2$$

$$\frac{dY_4}{dT} = Y_5$$

$$\frac{dY_5}{dT} = -Y_5(2Y_3/Y_1 + 1) + A_2/Y_2^2 - A_1 A_2 \sin(\theta - Y_4)/R^2 Y_2$$

$$\frac{dY_5}{dT} = Y_7$$

$$\frac{dY_7}{dT} = Y_6/Y_5^2 - A_4/Y_7 + A_1 A_5 \cos(\theta - Y_8)/R^2$$

$$\frac{dY_6}{dT} = Y_9$$

$$\frac{dY_9}{dT} = -Y_9(2Y_7/Y_6 + A_4) + A_3 A_4/Y_6^2 + A_1 A_5 \sin(\theta - Y_8)/R^2 Y_6$$

where $$\theta = \tan^{-1}\left(\frac{Y_6 \sin Y_8 - Y_2 \sin Y_4}{Y_6 \cos Y_8 - Y_2 \cos Y_4}\right)$$

and $$R^2 = (Y_6 \sin Y_8 - Y_2 \sin Y_4)^2 + (Y_6 \cos Y_8 - Y_2 \cos Y_4)^2.$$

The two computer programs used to determine the particle trajectories for each of the five cases considered are listed here. The computer program PARVOR was used in the determination of particle trajectories for the first three cases. The computer program TWOPAR was used to analyze the motion of the two charged particles in Case IV.

```
      PROGRAM PARVCR(INPUT,OUTPUT)
      DIMENSION Y(7),YP(7),ABC(20),C1(20),C2(20),C4(20),C5(20),X(7)
      READ 1,N1,N2,N4,N5
    1 FORMAT(10X,7I10)
      READ 1,N,KPR
      READ 2,C3,DELT,IMAX
    2 FORMAT(10X,7E10.0)
      READ 2,(C1(K),K=1,N1)
      READ 2,(C2(K),K=1,N2)
      READ 2,(C4(K),K=1,N4)
      READ 2,(C5(K),K=1,N5)
      NN=N+1
      NNN=NN+3
      READ 2,(Y(I),I=1,NN)
      DO 13 I=1,NN
   13 X(I)=Y(I)
      DO 11 L1=1,N1
      DO 11 L2=1,N2
      DO 11 L4=1,N4
      DO 11 L5=1,N5
      CON=C2(L2)/C1(L1)
      CON1=C3*C4(L4)*C5(L5)/C1(L1)**2
      PRINT 3,N,KPR,C1(L1),C2(L2),C3,C4(L4),C5(L5),CON,CON1,DELT,IMAX
    3 FORMAT(1X,*N=*,I5,10X,*KPR=*,I5/12X,*C1=*,1PE13.5,4X,*C2=*,E13.5,
     C4X,*C3=*,E13.5,4X,*C4=*,E13.5,4X,*C5=*,E13.5/12X,*CON =*,E13.5,2X,
     C*CON1=*,E13.5/12X,*DELT=*,E13.5,2X,*IMAX=*,E13.5)
      KOUNT=0
      TIME=0.
      YP(1)=1.
      YP(2)=Y(3)
      YP(3)=CON**2*(1.-EXP(-Y(1)))**2/Y(2)**3-CON1/Y(2)-Y(1)
      YP(4)=CON*(1.-EXP(-Y(1)))/Y(2)**2
      AVEL=Y(2)*YP(4)
      ANG=Y(4)*180./3.14159
      PRINT 4
    4 FORMAT(/15X,*TIME*,9X,*RADIUS*,5X,*RADIAL VEL*,2X,*ANGLE (RAD)*,2X
     C,*ANGULAR VEL*,2X,*ANGLE (DEG)*)
      PRINT 5,(Y(I),I=1,NN),AVEL,ANG
    5 FORMAT(10X,1P6E13.5)
      DO 6 I=1,NN
    6 ABC(I)=0.
      ABC(NN+1)=.5
      ABC(NN+2)=.292893218814
      ABC(NN+3)=1.70710678118
      ABC(NN+4)=.166666666667
      ABC(NN+5)=2.
      ABC(NN+6)=1.
      ABC(NN+7)=1.
      ABC(NN+8)=2.
      ABC(NN+9)=.5
      ABC(NN+10)=.292893218814
      ABC(NN+11)=1.70710678118
      ABC(NN+12)=.5
    7 DO 9 J=NN,NNN
      DO 8 I=1,NN
      TEMP=ABC(J+1)*(YP(I)-ABC(J+5)*ABC(I))
```

```
      Y(I)=Y(I)+DEL(I)*TEMP
    8 ABC(I)=ABC(I)+1.*TEMP*ABC(J+9)*YP(I)
      YP(1)=1.
      YP(2)=Y(3)
      YP(3)=CON**2*(1.-EXP(-Y(1)))**2/Y(2)**3*CON1/Y(2)-Y(3)
    9 YP(4)=CON*(1.-EXP(-Y(1)))/Y(2)**2
      AVEL=Y(2)*Y(4)
      ANG=Y(4)*180./3.14159
      TMA=TMA+DELT
      KOUNT=KOUNT+1
      IF(KOUNT.NE.KPR)GO TO 10
      PRINT 5,(Y(I),I=1,ND),AVEL,ANG
      KOUNT=
   10 IF(TMA+1.E-5.LT.TMAX)GO TO 7
      DO 14 I=1,ND
   14 Y(I)=X(I)
   11 PRINT 12
   12 FORMAT(1H1)
      CALL EXIT
      END
```

```
      PROGRAM TROPAR(INPUT,OUTPUT)
      DIMENSION Y(8),YP(8),ABC(22)
      READ 1,N[illegible]
    1 FORMAT(I[illegible]X,7[illegible])
      READ 2,A1,A2,A3,A4,A5,DELT,TMAX
    2 FORMAT(1[illegible]X,7E1[illegible].5)
      PRINT 3,A1,A2,A3,A4,A5,DELT,TMAX
    3 FORMAT(12X,*A1=*,E13.5,4X,*A2=*,E13.5,4X,*A3=*,E13.5,4X,*A4=*,
     CE13.5,4X,*A5=*,E13.5/12X,*DELT=*,E13.5,2X,*TMAX=*,E13.5)
      NS=[illegible]
      NP=[illegible]
      READ 2,(Y(I),I=1,[illegible])
      KOUNT=[illegible]
      T[illegible]A= .
      YP(1)=1.
      YP(2)=Y(3)
      XCOMP=Y(6)*COS(Y(8))-Y(2)*COS(Y(4))
      YCOMP=Y(6)*SIN(Y(8))-Y(2)*SIN(Y(4))
      THETA=ATAN(YCOMP/XCOMP)
      RST=XCOMP*XCOMP+YCOMP*YCOMP
      YP(3)=Y(2)*Y(5)*Y(5)-Y(3)-A1*A2*COS(THETA-Y(4))/(RST*RST)
      YP(4)=Y(5)
      YP(5)=-Y(5)*(2.*Y(3)/Y(2)+1.)+A3/(Y(2)*Y(2))-A1*A2*SIN(THETA-
     -Y(4))/(RST*RST*Y(2))
      YP(6)=Y(7)
      YP(7)=Y(6)*Y(9)*Y(9)-A4*Y(7)+A1*A5*COS(THETA-Y(8))/(RST*RST)
      YP(8)=Y(9)
      YP(9)=-Y(9)*(2.*Y(7)/Y(6)+A4)+A3*A4/(Y(6)*Y(6))+A1*A5*SIN(THETA-
     -Y(8))/(RST*RST*Y(6))
      ANG1=57.295[illegible]*Y(4)
      ANG2=57.295[illegible]*Y(8)
      AVEL1=Y(2)*Y(5)
      AVEL2=Y(6)*Y(9)
      PRINT 4
    4 FORMAT(/[illegible]X,*T[illegible]*,[illegible]X,*RAD 1*,[illegible]X,*VEL R1*,4X,*ANG1 (DEG)*,6X,
     C*AVEL1*,[illegible]X,*RAD 2*,[illegible]X,*VEL R2*,4X,*ANG2 (DEG)*,6X,*AVEL2*)
      PRINT 5,T,Y(1),Y(2),Y(3),ANG1,AVEL1,Y(6),Y(7),ANG2,AVEL2
    5 FORMAT(1[illegible]X,1[illegible]E13.5)
      DO 6 I=1,[illegible]
    6 ABC(I)= .
      ABC([illegible]+1)=.5
      ABC([illegible]+2)=.2928932188[illegible]4
      ABC([illegible]+3)=1.7071067811[illegible]
      ABC([illegible]+4)=.1666666666667
      ABC([illegible]+5)=2.
      ABC([illegible]+6)=1.
      ABC([illegible]+7)=1.
      ABC([illegible]+[illegible])=2.
      ABC([illegible]+[illegible])=.
      ABC([illegible]+1[illegible])=.2928932188[illegible]4
      ABC([illegible]+11)=1.7071067811[illegible]
      ABC([illegible]+12)=.5
    7 DO 9 J=1,[illegible]
      DO 8 I=1,[illegible]
      TEMP=ABC(J+1)*(YP(I)-ABC(J+5)*ABC(I))
      Y(I)=Y(I)+DELT*TEMP
```

```
      A=C(I)=ABC(I)+1.*(EXP-ABC(J+9)*YP(I)
        YP(1)=1.
        YP(2)=Y(3)
        XCOMP=Y(6)*COS(Y(8))-Y(2)*COS(Y(4))
        YCOMP=Y(6)*SIN(Y(8))-Y(2)*SIN(Y(4))
        THETA=ATAN(YCOMP/XCOMP)
        RSI=XCOMP*XCOMP+YCOMP*YCOMP
        YP(3)=Y(2)*Y(5)*Y(5)-Y(3)-A1*A2*COS(THETA-Y(4))/(RSI*RSI)
        YP(4)=Y(5)
        YP(5)=-Y(5)*(2.*Y(3)/Y(2)+1.)+A3/(Y(2)*Y(2))-A1*A2*SIN(THETA-
       -Y(4))/(RSI*RSI*Y(2))
        YP(6)=Y(7)
        YP(7)=Y(6)*Y(9)*Y(9)-A4*Y(7)+A1*A5*COS(THETA-Y(8))/(RSI*RSI)
        YP(8)=Y(9)
      9 YP(9)=-Y(9)*(2.*Y(7)/Y(6)+A4)+A3*A4/(Y(6)*Y(6))+A1*A5*SIN(THETA-
       -Y(8))/(RSI*RSI*Y(6))
        ANG1=57.295*Y(4)
        ANG2=57.295*Y(8)
        AVEL1=Y(2)*Y(5)
        AVEL2=Y(6)*Y(9)
        TMA=TMA+DELT
        KOUNT=KOUNT+1
        IF(KOUNT.NE.KPR)GO TO 10
        PRINT 5,Y(1),Y(2),Y(3),ANG1,AVEL1,Y(6),Y(7),ANG2,AVEL2
        KOUNT=1
     10 IF(TMA+.5E-5.LT.TMAX)GO TO 7
        CALL EXIT
        END
```

RESULTS AND DISCUSSION OF RESULTS

The results presented and discussed here are based on the data presented in Appendix B. The numerical procedure and computer programs discussed in the previous section were used to calculate these results.

For the case of an uncharged particle moving in a free-vortex flow field, Case I, particle trajectories have been determined for various values of particle density and diameter, and various values of free-vortex flow velocity. Figures 8 through 13 describe the particle trajectories in the $(r/r_o,\theta)$ plane and the radial migration as a function of dimensionless time. The axial particle trajectory as a function of dimensionless time is plotted in Figure 14.

Figures 8 through 11 indicate that as the particle density and diameter increase at constant free-vortex velocity, the entrainment of the particle in the free-vortex is decreased. Figures 12 and 13 indicate the radial migration of the particle tends to increase as the free-vortex flow velocity increases while the particle density and diameter are held constant.

These results can be explained by examining the parameter (C_v/Cr_o^2), which represents the ratio of the centrifugal or inertial force per unit mass on a particle moving with a velocity equal to the tangential velocity of the flow field to the drag force per unit mass on the particle. As such, the parameter is indicative of the relative importance of the centrifugal or inertial force compared with the drag force for a given particle. As the particle density

or diameter increases, the parameter (C_v/Cr_o^2) increases, indicating that the centrifugal force tends to dominate, resulting in an increase in the radial migration and conversely, reducing the particle entrainment. As the free vortex flow velocity, represented by the parameter C_v, increases, the centrifugal force once again tends to dominate, increasing the radial migration.

The results also indicate that the angular displacement of the particle is strongly dependent on the free-vortex velocity. Examination of Figure 13 indicates that as the free-vortex flow velocity is increased, radial particle migration increases, and the angular displacement of the particle increases also. However, at constant free-vortex velocity, as the radial particle migration increases, the angular displacement of the particle decreases. Figures 9 and 11 illustrate this behavior. These results can be explained by examining the differential equation governing the angular displacement in Case I:

$$\frac{d\theta}{dt} = C_v(1 - e^{-Ct})/r^2 \quad .$$

The angular displacement is seen to be directly proportional to the free vortex flow velocity parameter, C_v, and inversely proportional to the square of the radial position of the particle.

Examination of the equation governing particle motion in the axial direction indicates that it is completely decoupled from the equations of motion in the radial and tangential directions. This will be true if the axial flow field is assumed to be independent of the radial and tangential coordinates of the particle. This is, of course, the assumption made in these analyses. Figure 14 indicates

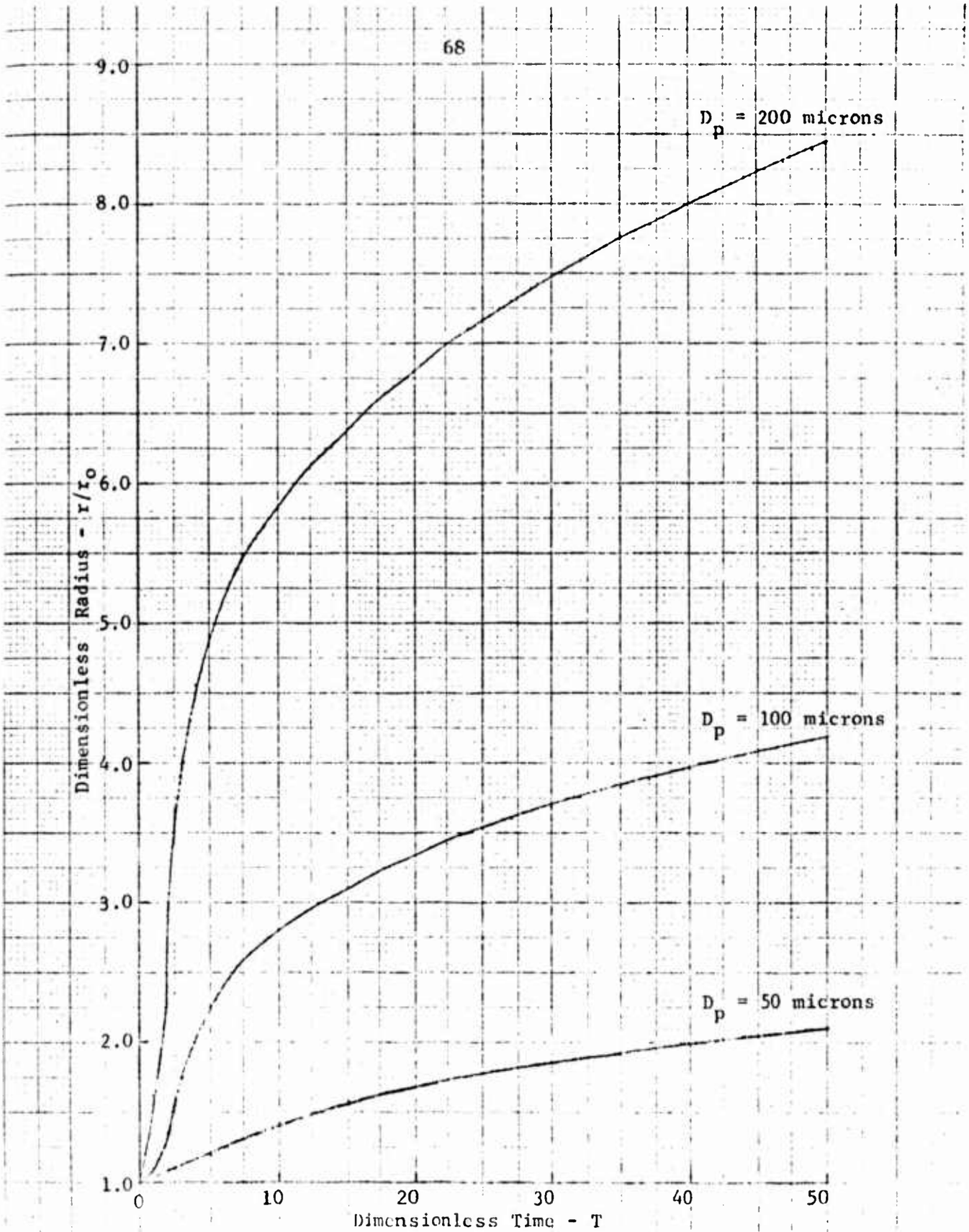

FIGURE 8. Radial Particle Migration as a Function of Particle Diameter - Case I

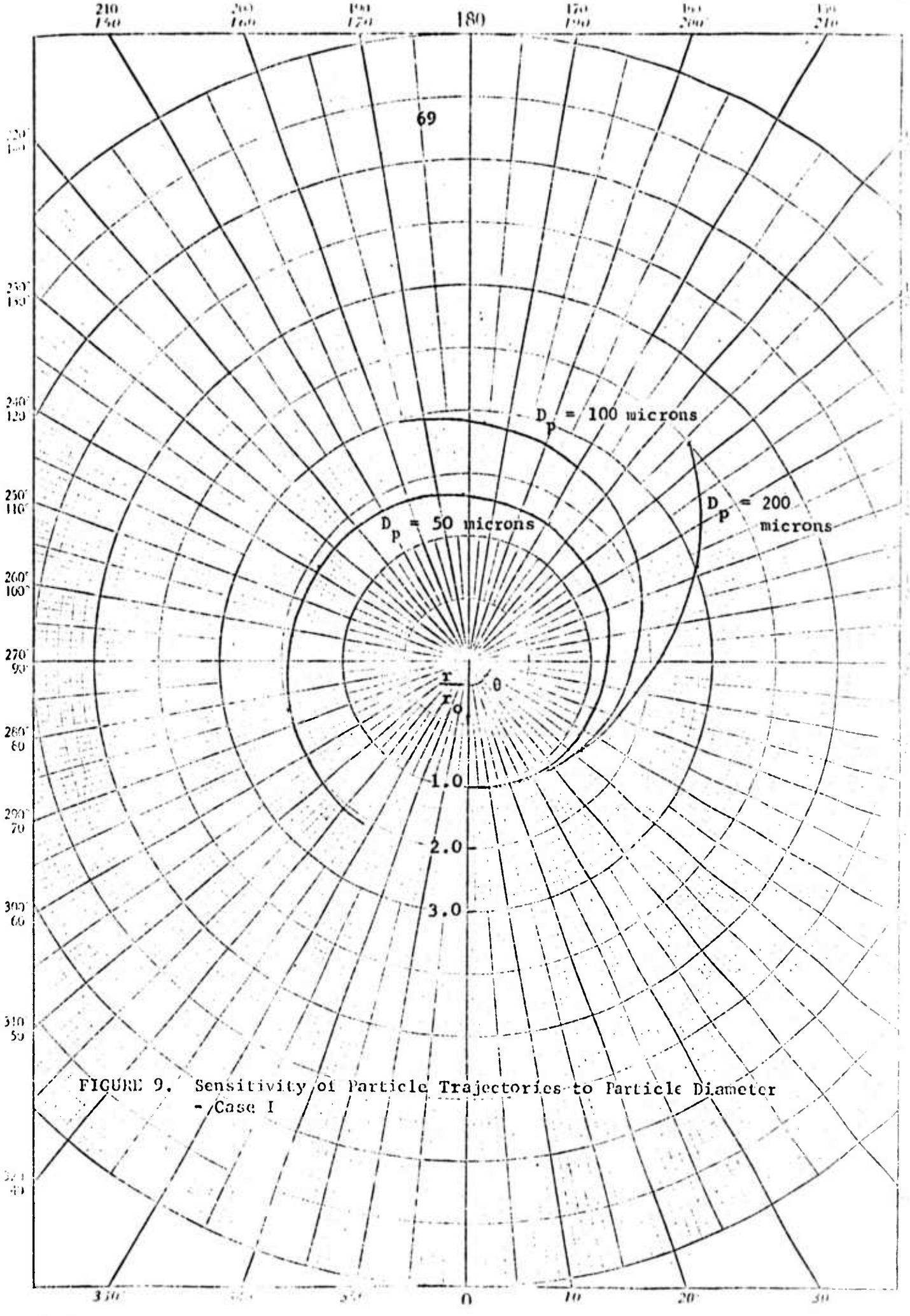

FIGURE 9. Sensitivity of Particle Trajectories to Particle Diameter - Case I

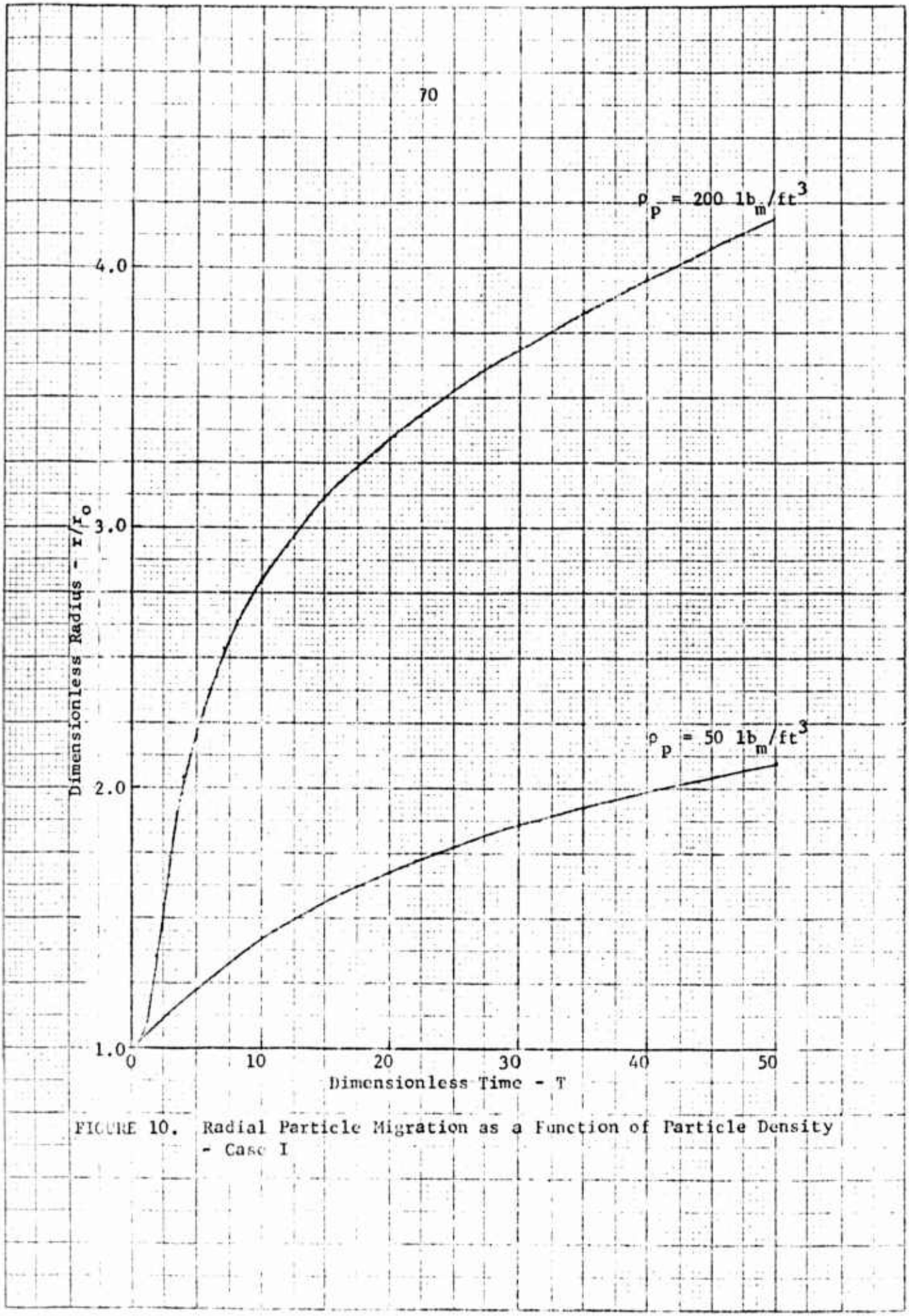

FIGURE 10. Radial Particle Migration as a Function of Particle Density - Case I

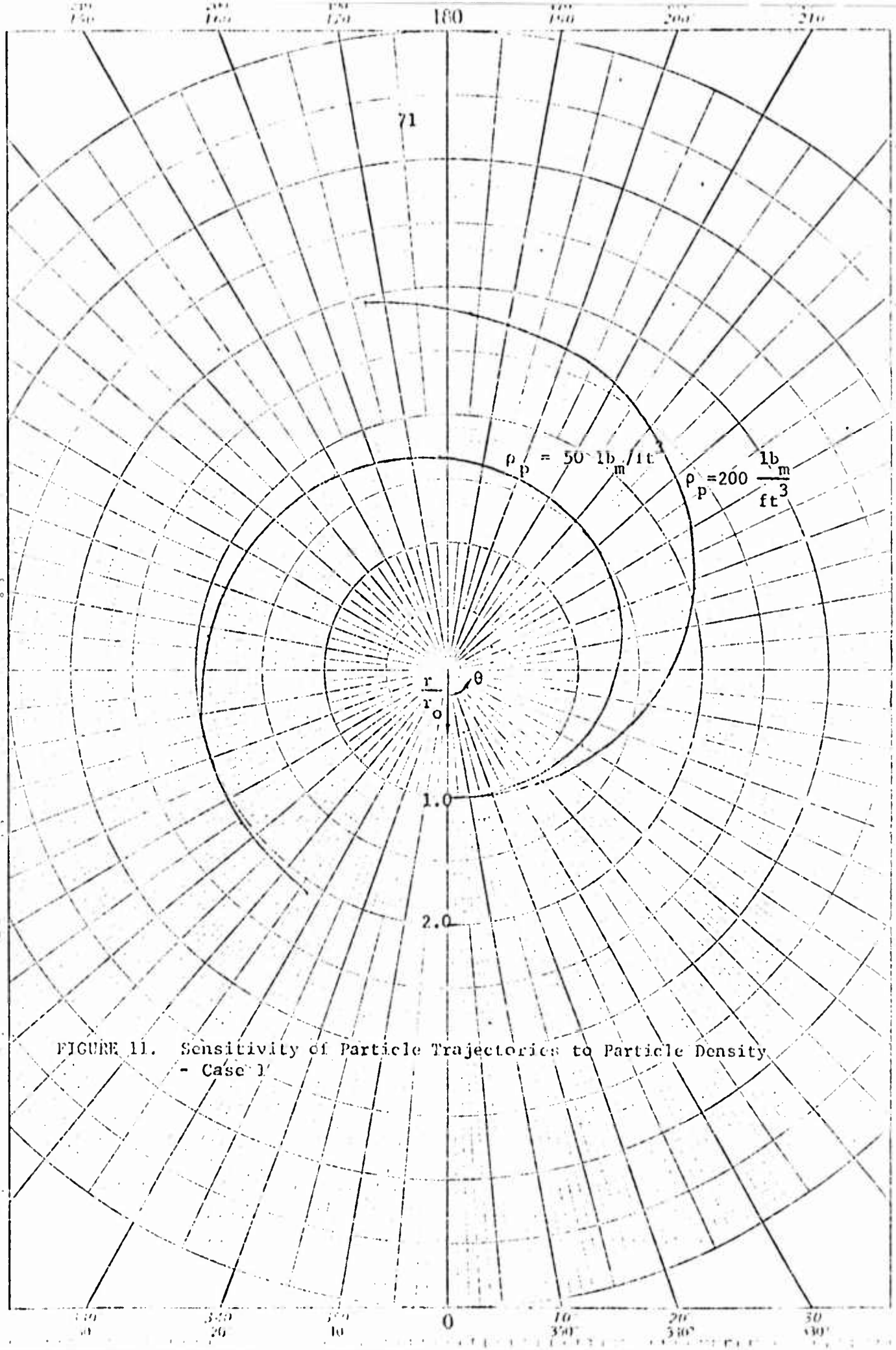

FIGURE 11. Sensitivity of Particle Trajectories to Particle Density - Case 1

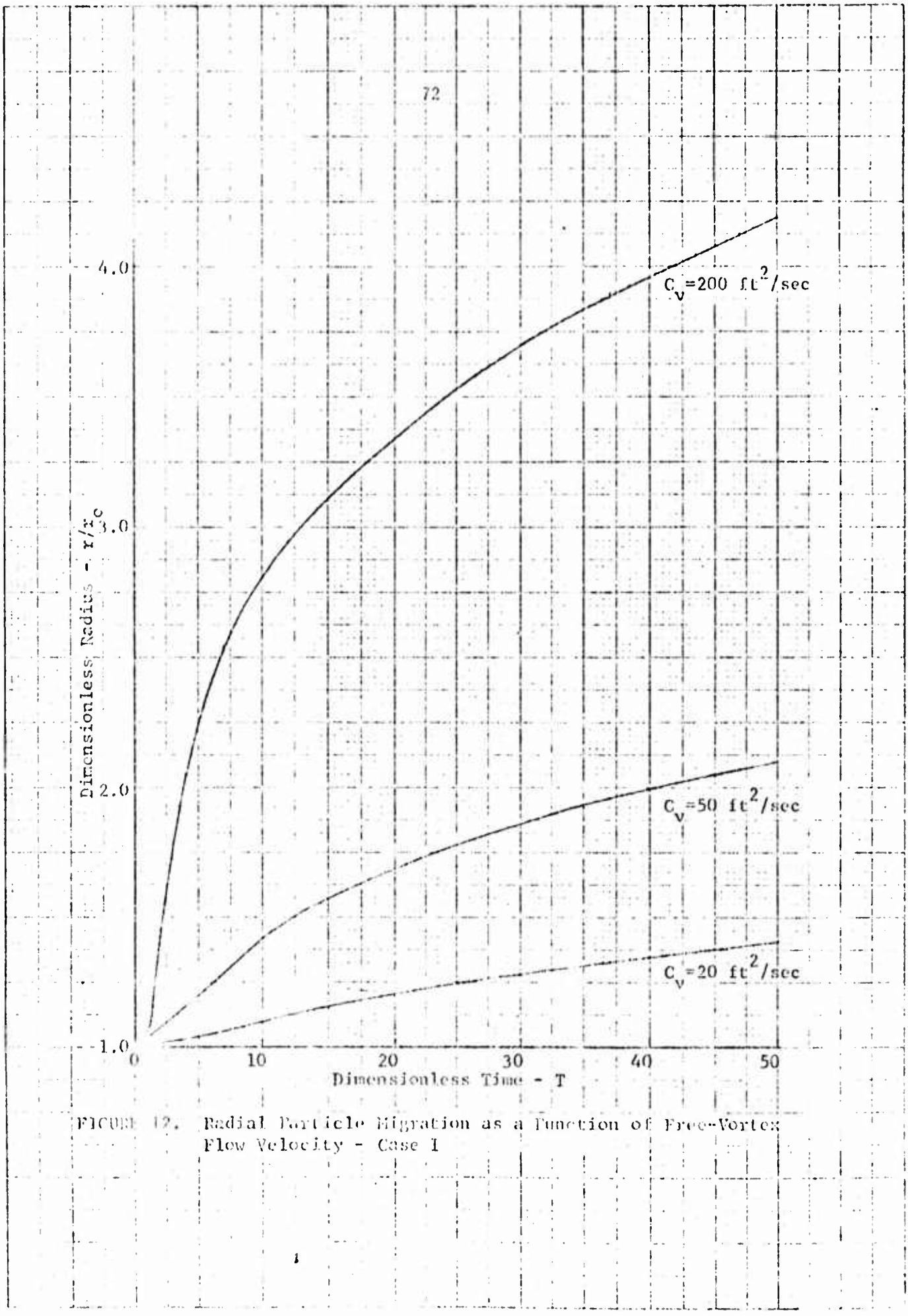

FIGURE 12. Radial Particle Migration as a Function of Free-Vortex Flow Velocity - Case I

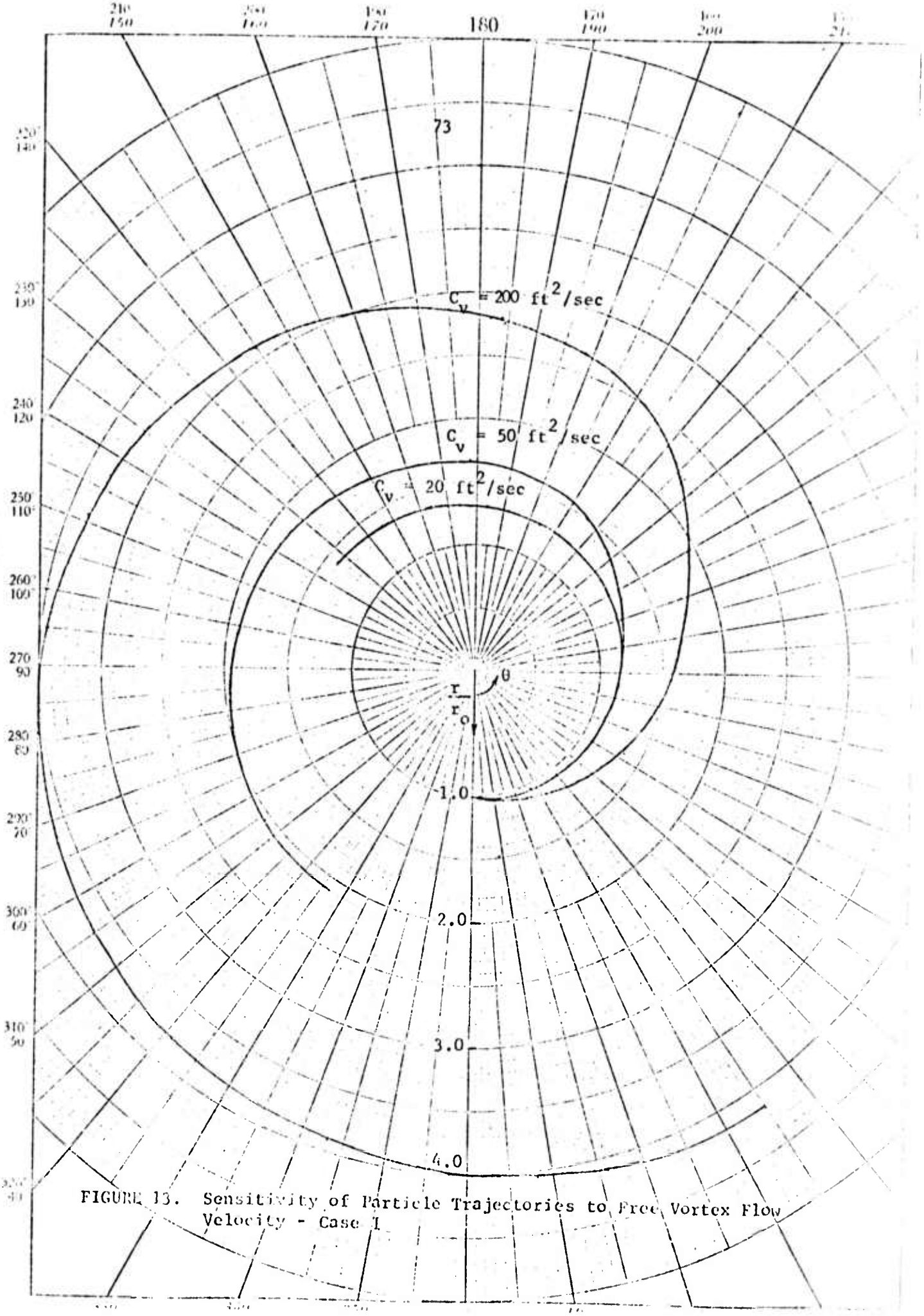

FIGURE 13. Sensitivity of Particle Trajectories to Free Vortex Flow Velocity - Case I

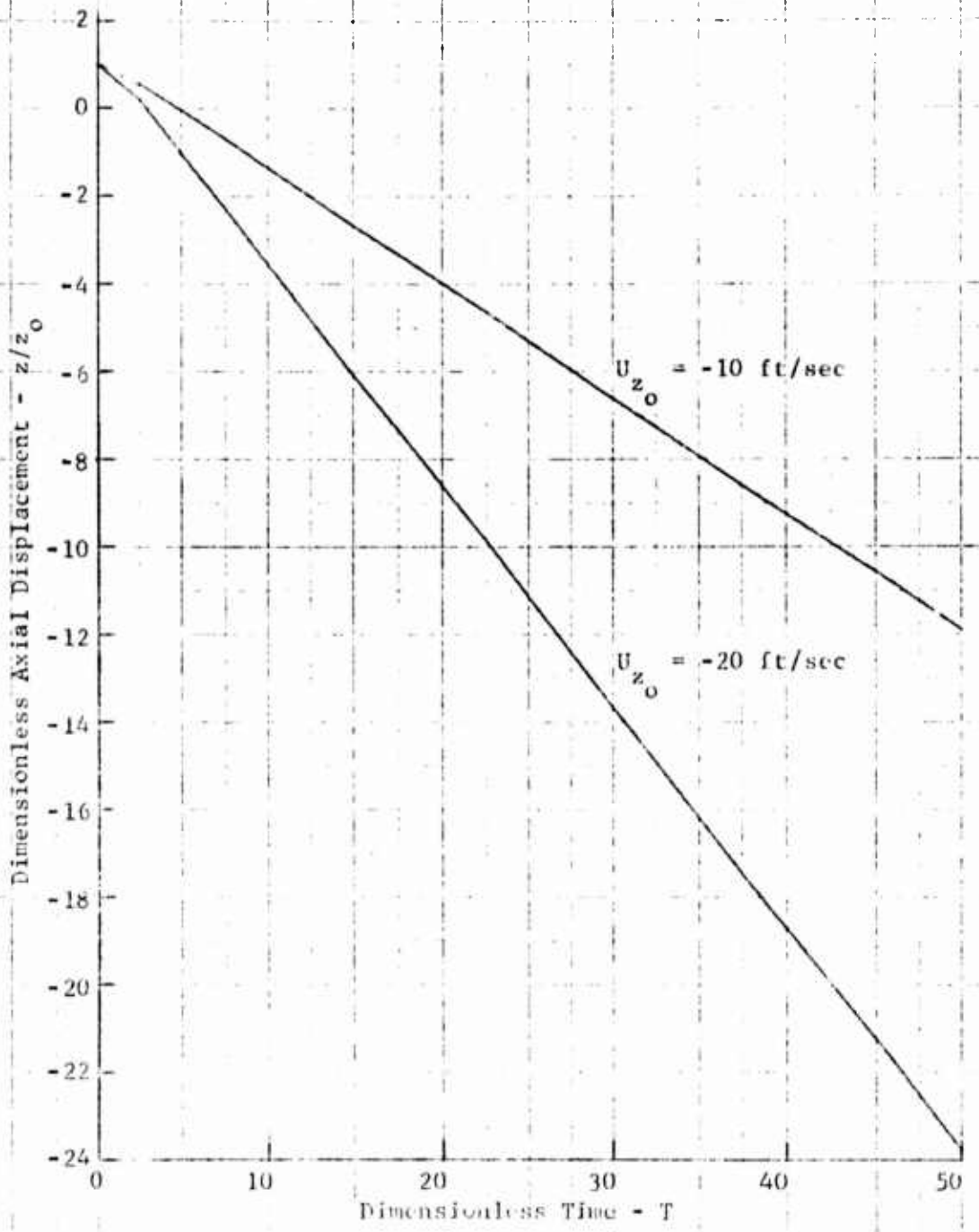

FIGURE 14. Axial Particle Trajectory as a Function of Axial Fluid Velocity

that as the axial fluid velocity becomes more negative, the particle is displaced a larger axial distance, and the terminal velocity of the particle becomes larger, as expected. The axial fluid velocity in effect controls the settling rate of the particle, and as such would be an important parameter in a centrifugal separator, since it would be desirable to obtain separation of particles prior to their settling out of the system.

The second case considered was that of a positively charged particle moving in a viscous medium under the influence of an applied electric field due to a positively charged line source. Radial particle trajectories as a function of dimensionless time are shown in Figures 15 through 18 for various values of particle density and diameter, line source strength, and particle charge-to-mass ratio. Figures 15 and 16 indicate that as the particle density and diameter increase at constant charge-to-mass ratio and line source strength, the radial migration increases. Figures 17 and 18 indicate that as the particle charge-to-mass ratio increases, or the line source strength increases while particle density and diameter are held constant, radial particle migration also increases. As the particle density and diameter increase, the drag force per unit mass is decreased, permitting an increase in the radial particle migration. As the line source strength or particle charge-to-mass ratio is increased, the repulsive force between the charged particle and the line source is increased, since both are assumed to be positively

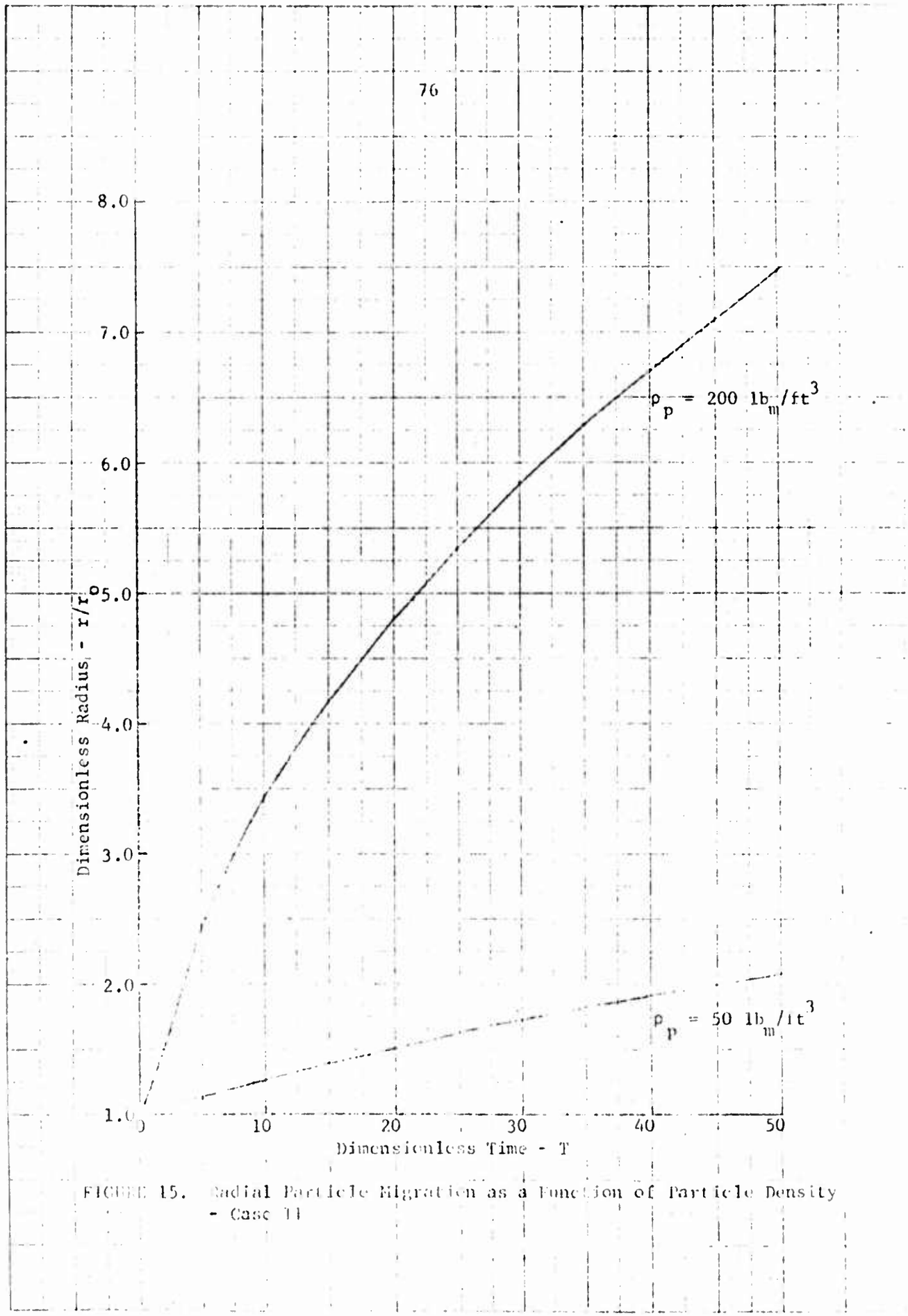

FIGURE 15. Radial Particle Migration as a Function of Particle Density - Case II

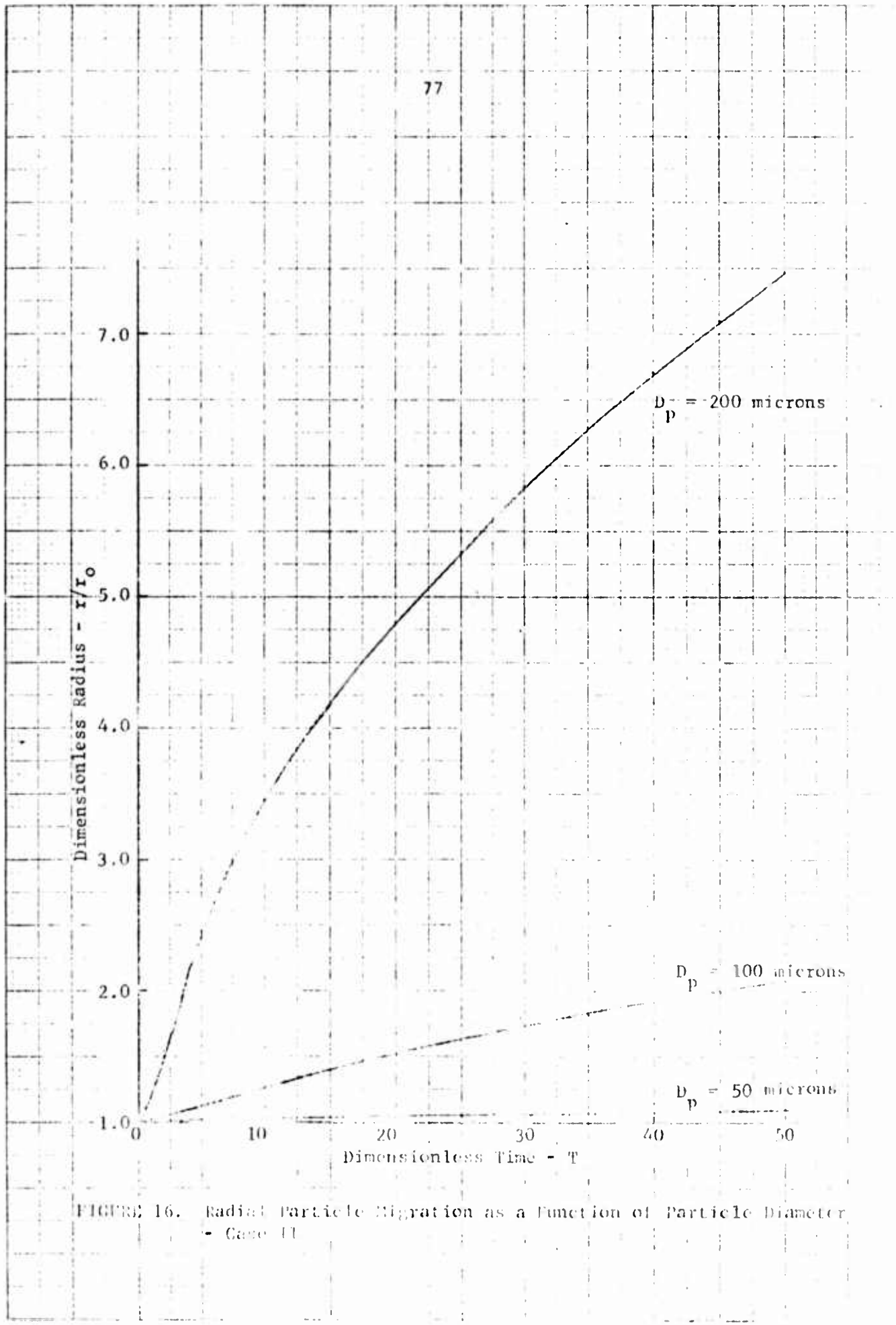

FIGURE 16. Radial Particle Migration as a Function of Particle Diameter - Case II

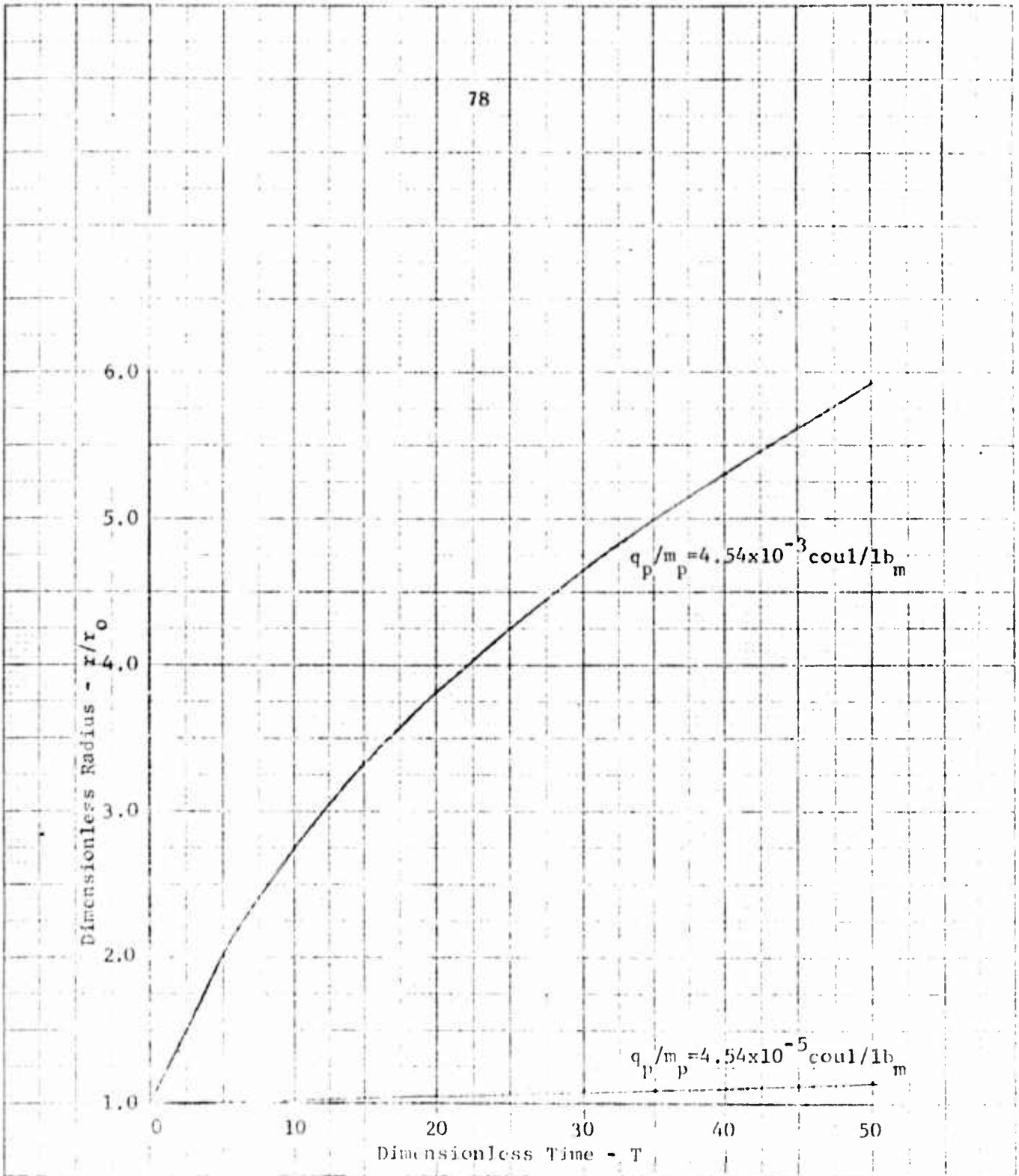

FIGURE 17. Radial Particle Migration as a Function of Particle Charge-to-Mass Ratio - Case II

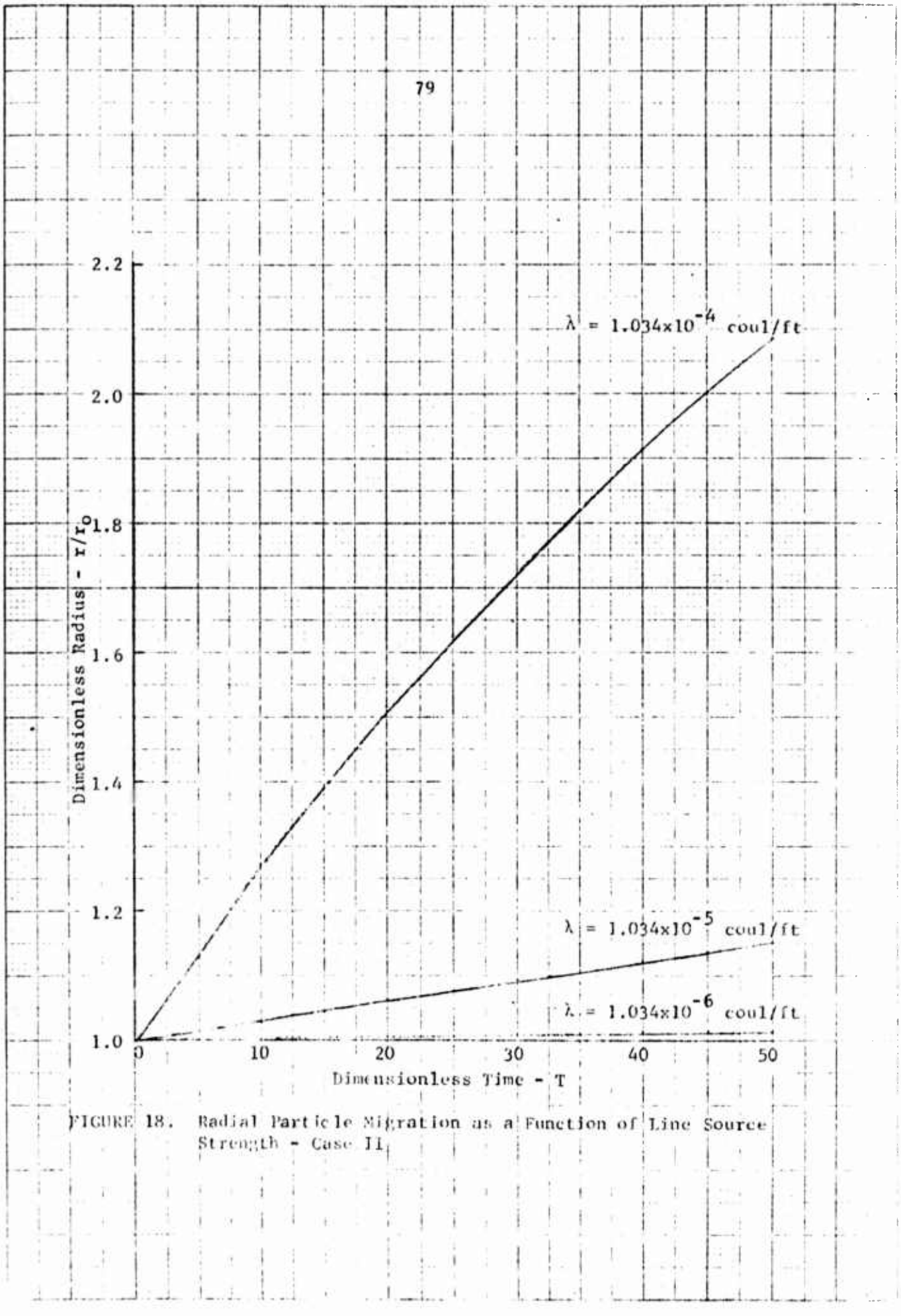

FIGURE 18. Radial Particle Migration as a Function of Line Source Strength - Case II

charged. The result is an increase in the radial particle migration also.

The third case analyzed the trajectories of a positively charged particle in a free-vortex flow field, subject to an applied electric field due to a positively charged line source. This case in essence combined the forces acting on the particle which were considered in the two previous cases. Figures 19 through 28 illustrate the particle trajectories and radial particle migration as a function of dimensionless time for various values of particle density and diameter, free-vortex flow velocity, line source strength, and particle charge-to-mass ratio. The trends in radial particle migration as a function of these parameters which were observed in Cases I and II were observed here also.

In order to assess the relative effects of each of the forces involved, centrifugal, drag, and electrostatic, this analysis was repeated assuming the particle was negatively charged. This assumption results in the electrostatic force and the centrifugal force opposing each other, rather than reinforcing each other as in Case III. Figures 29 through 38 give the particle trajectories and the radial particle migration as a function of dimensionless time for Case III A. Figures 29 through 32 indicate that at constant particle charge-to-mass ratio, line source strength, and free-vortex velocity, as the particle density and diameter increase, radial migration reaches a limiting radius at which the particle becomes entrained in the free-vortex. The attractive electrostatic force between the positively

charged line source and the negatively charged particle and the drag force in effect tend to balance the centrifugal or inertial force, allowing the particle to reach an equilibrium position. Figures 33 and 34 indicate that as the free-vortex flow velocity is increased with all other parameters held constant, radial particle migration is increased. This indicates that the centrifugal force becomes dominant as the free-vortex flow velocity is increased. Examination of Figures 35 and 36 indicates that as the line source strength is increased with all other parameters held constant, particle entrainment is increased. Thus the attractive electrostatic force between the positively charged line source and the negatively charged particle tends to balance the centrifugal force on the particle. This same trend is noted as the particle charge to mass ratio becomes more negative, as evidenced by the results shown in Figures 37 and 38.

Examination of the radial particle trajectories shown in Figure 29 indicates that at times shortly after the particle is released, its motion is inward toward the center of the free-vortex. This can be explained as follows: since initially the particle is motionless, some time is required for it to achieve a tangential velocity of sufficient magnitude such that the centrifugal force is larger than the electrostatic force. Until this occurs, the net motion of the particle will be inward. It is also evident that the particle having the greatest inward penetration will achieve an equilibrium radius earliest.

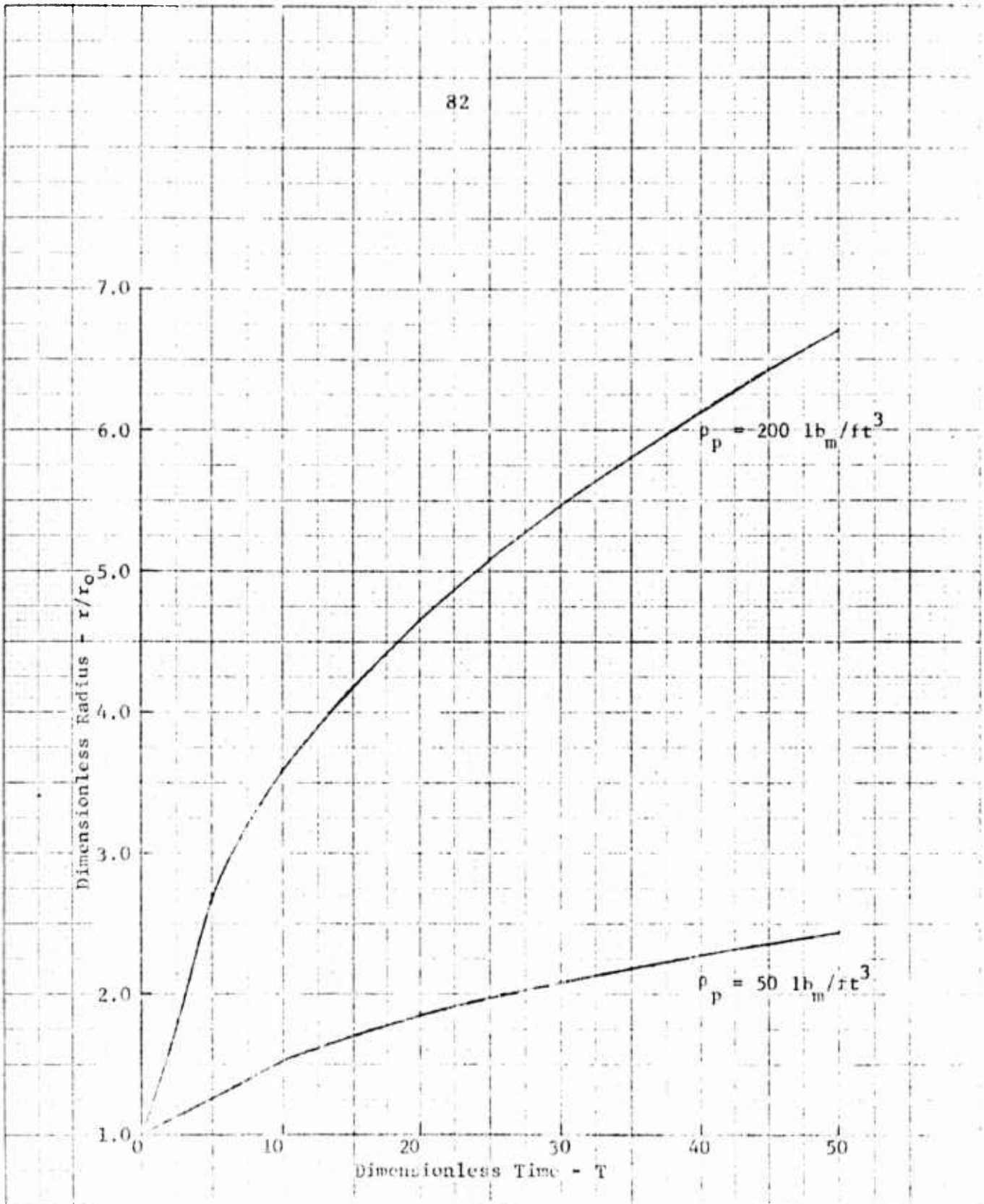

FIGURE 19. Radial Particle Migration as a Function of Particle Density - Case III

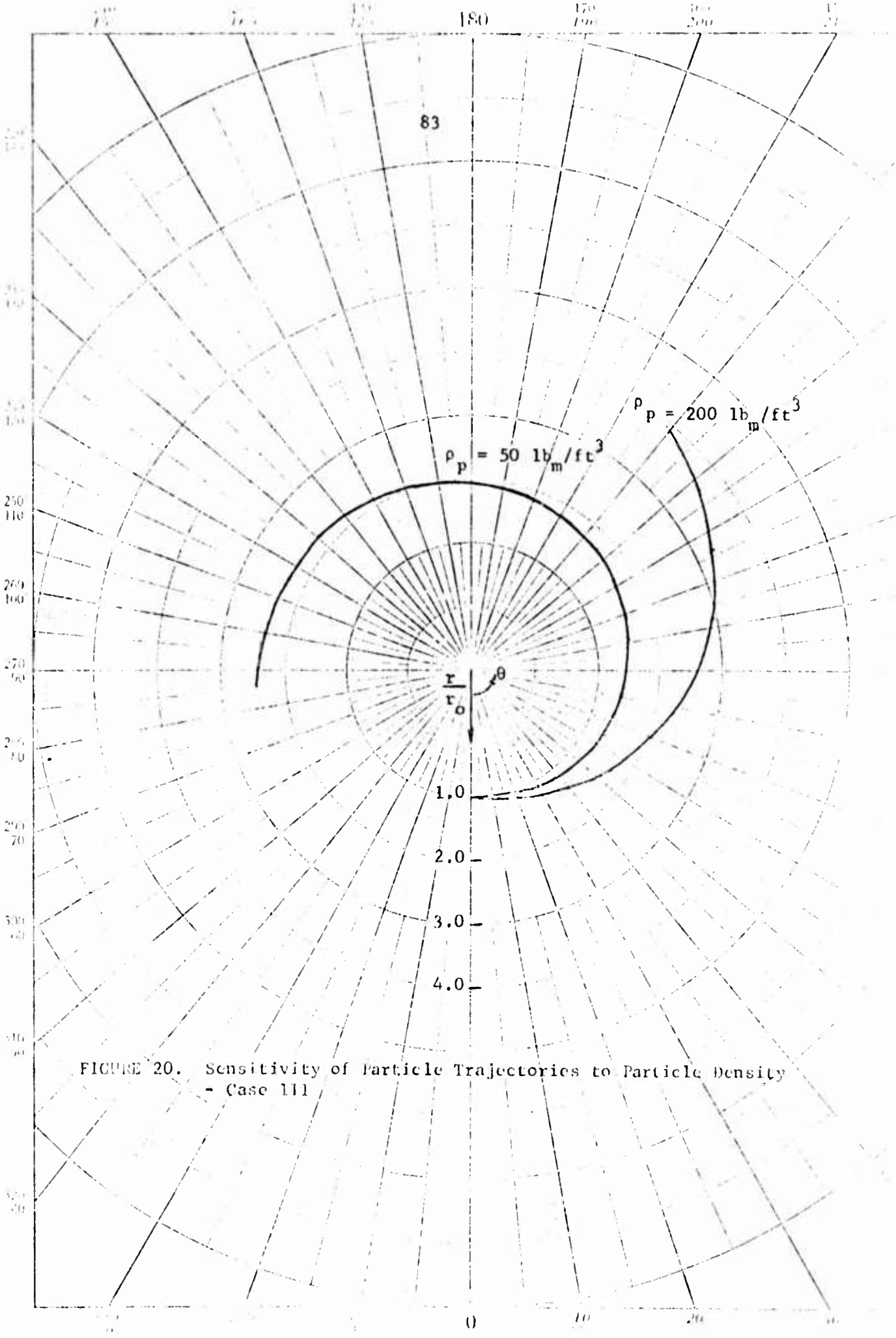

FIGURE 20. Sensitivity of Particle Trajectories to Particle Density - Case 111

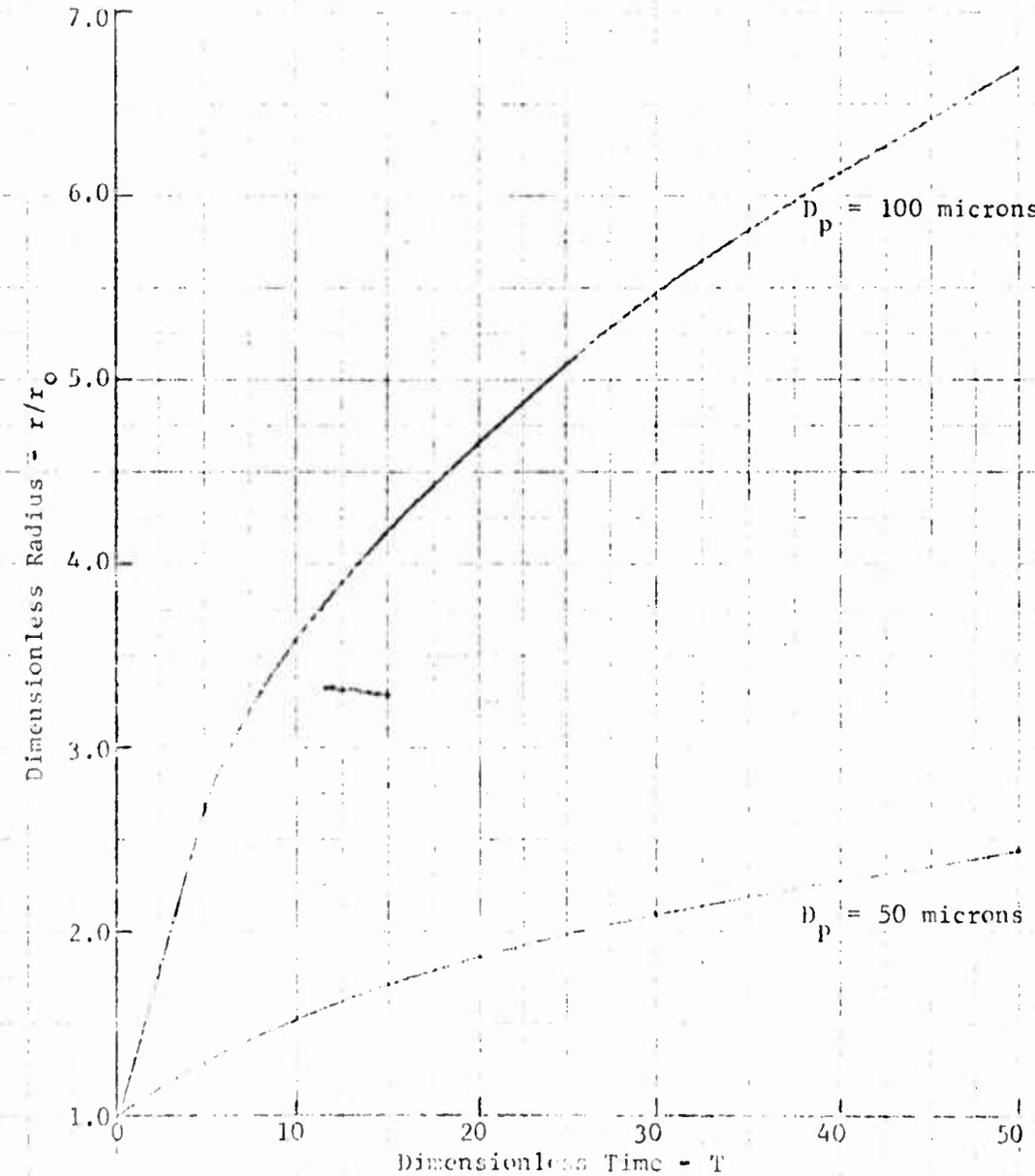

FIGURE 21. Radial Particle Migration as a Function of Particle Diameter - Case III

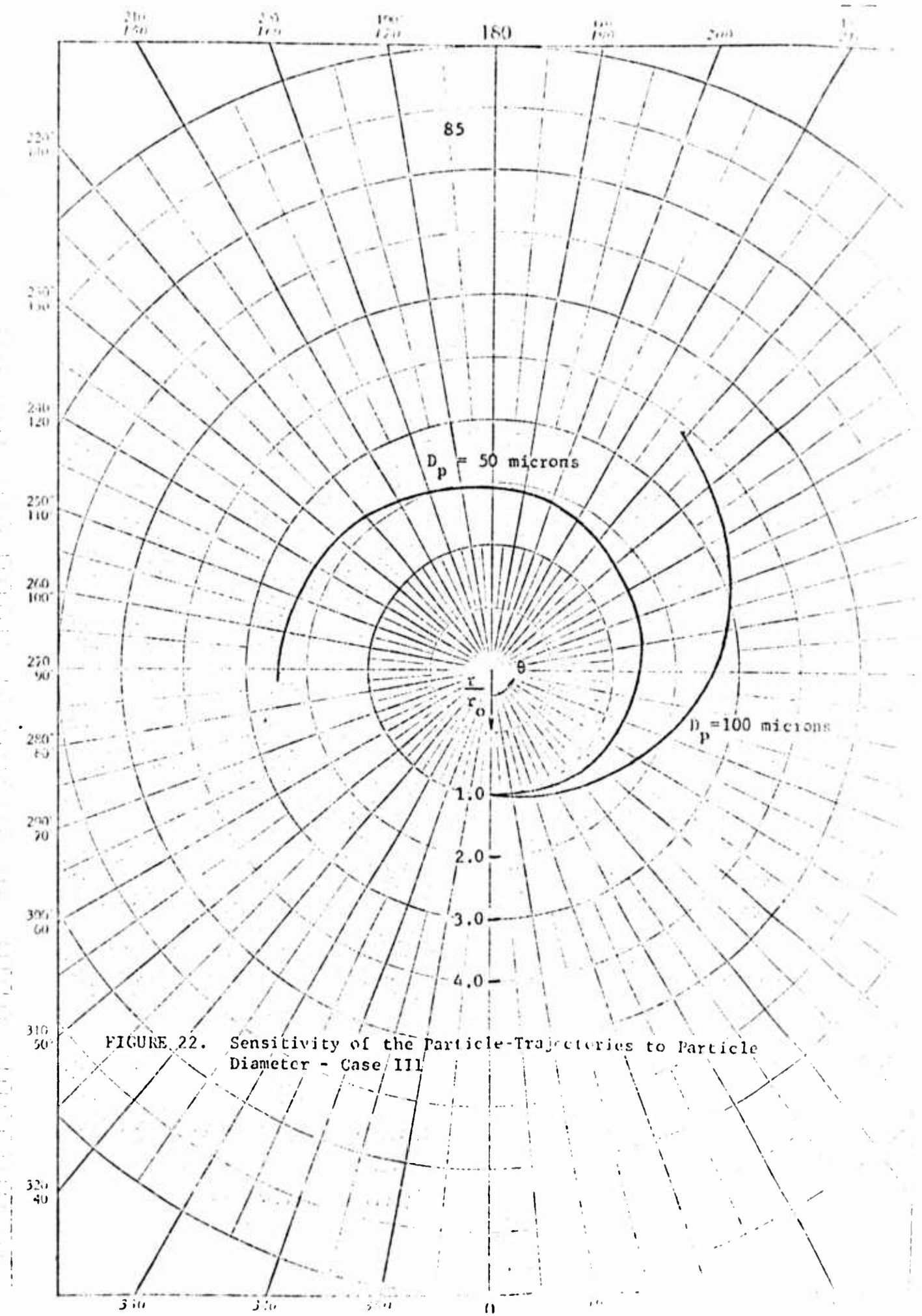

FIGURE 22. Sensitivity of the Particle-Trajectories to Particle Diameter - Case III

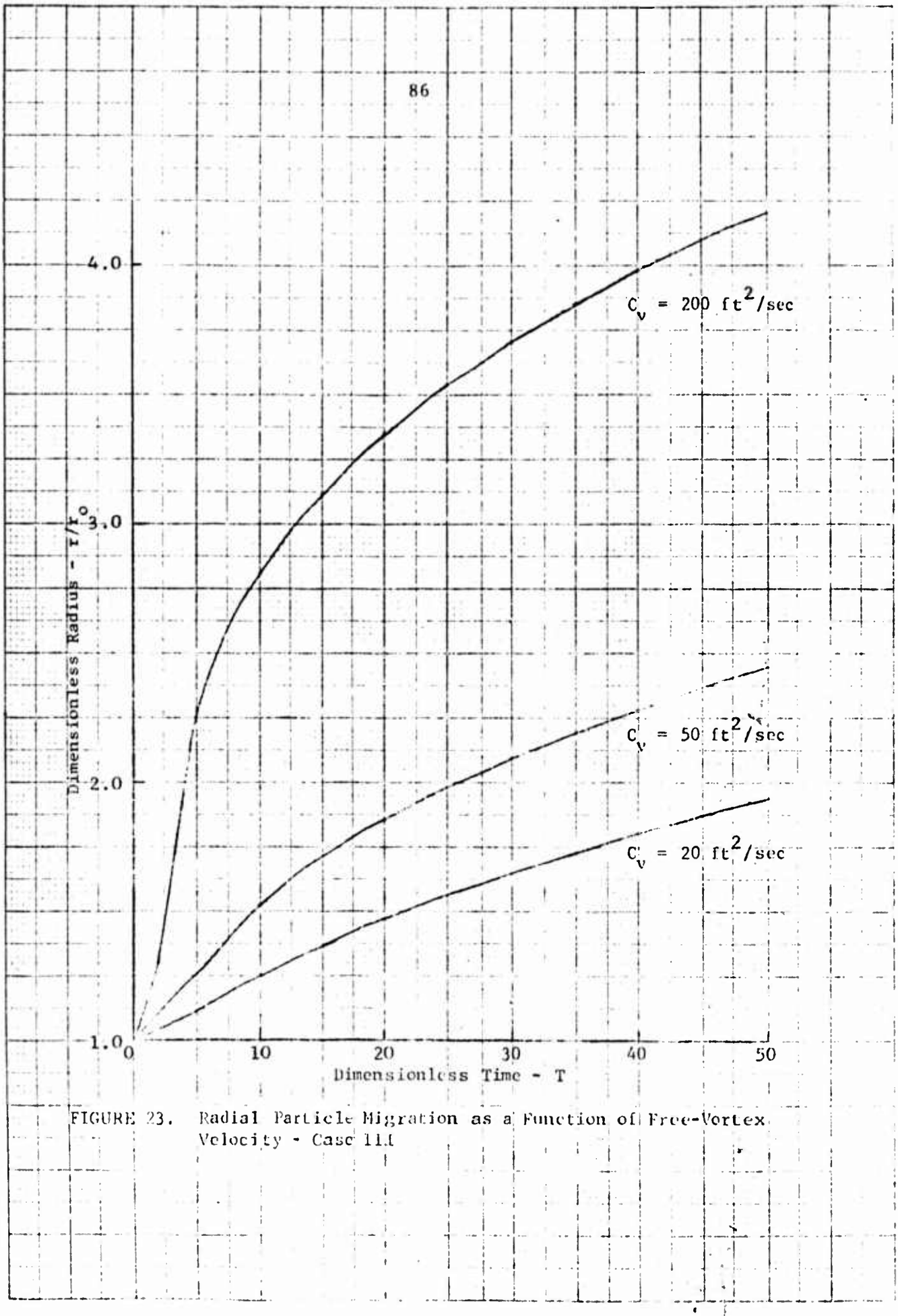

FIGURE 23. Radial Particle Migration as a Function of Free-Vortex Velocity - Case III

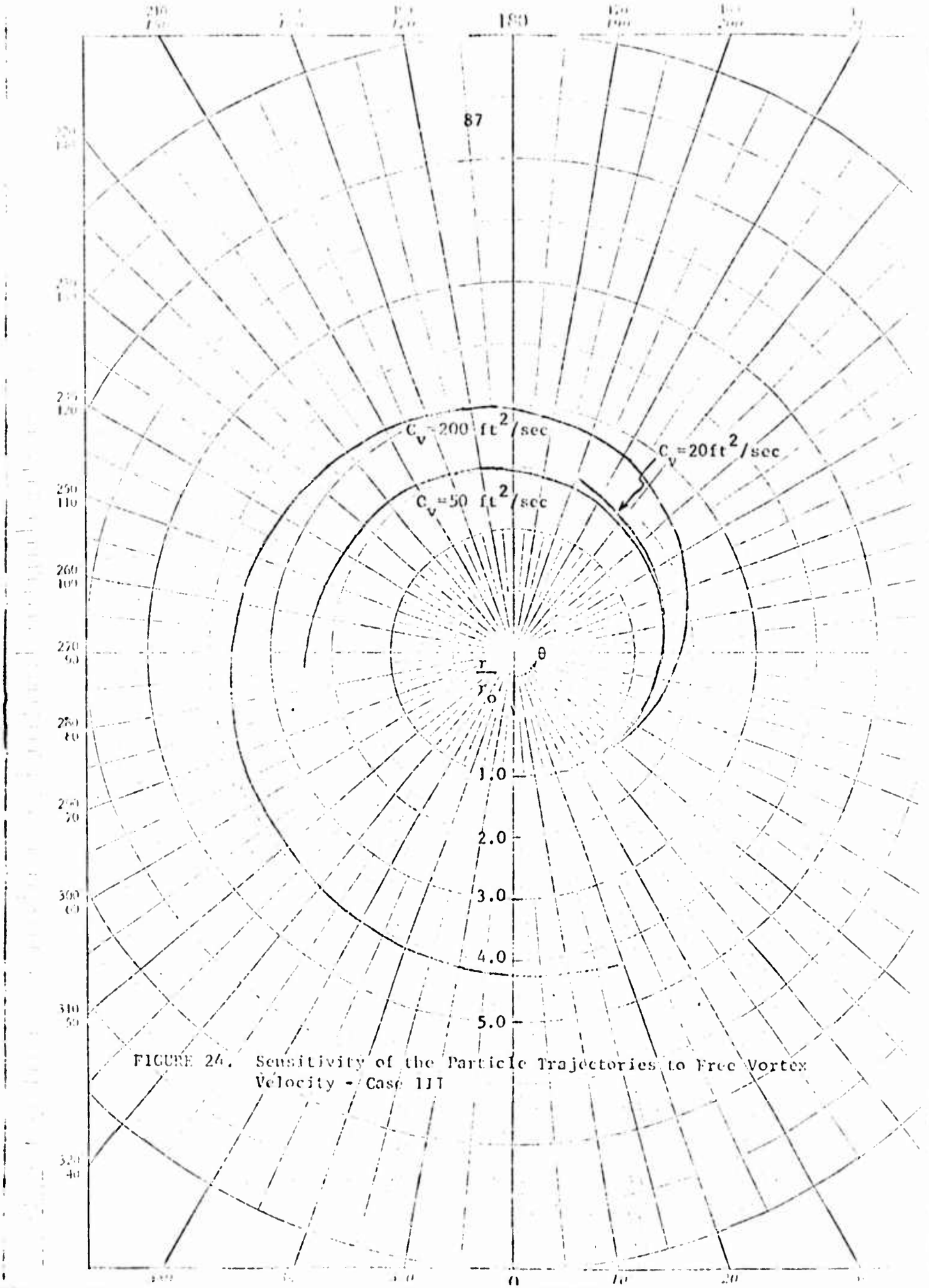

FIGURE 24. Sensitivity of the Particle Trajectories to Free Vortex Velocity - Case III

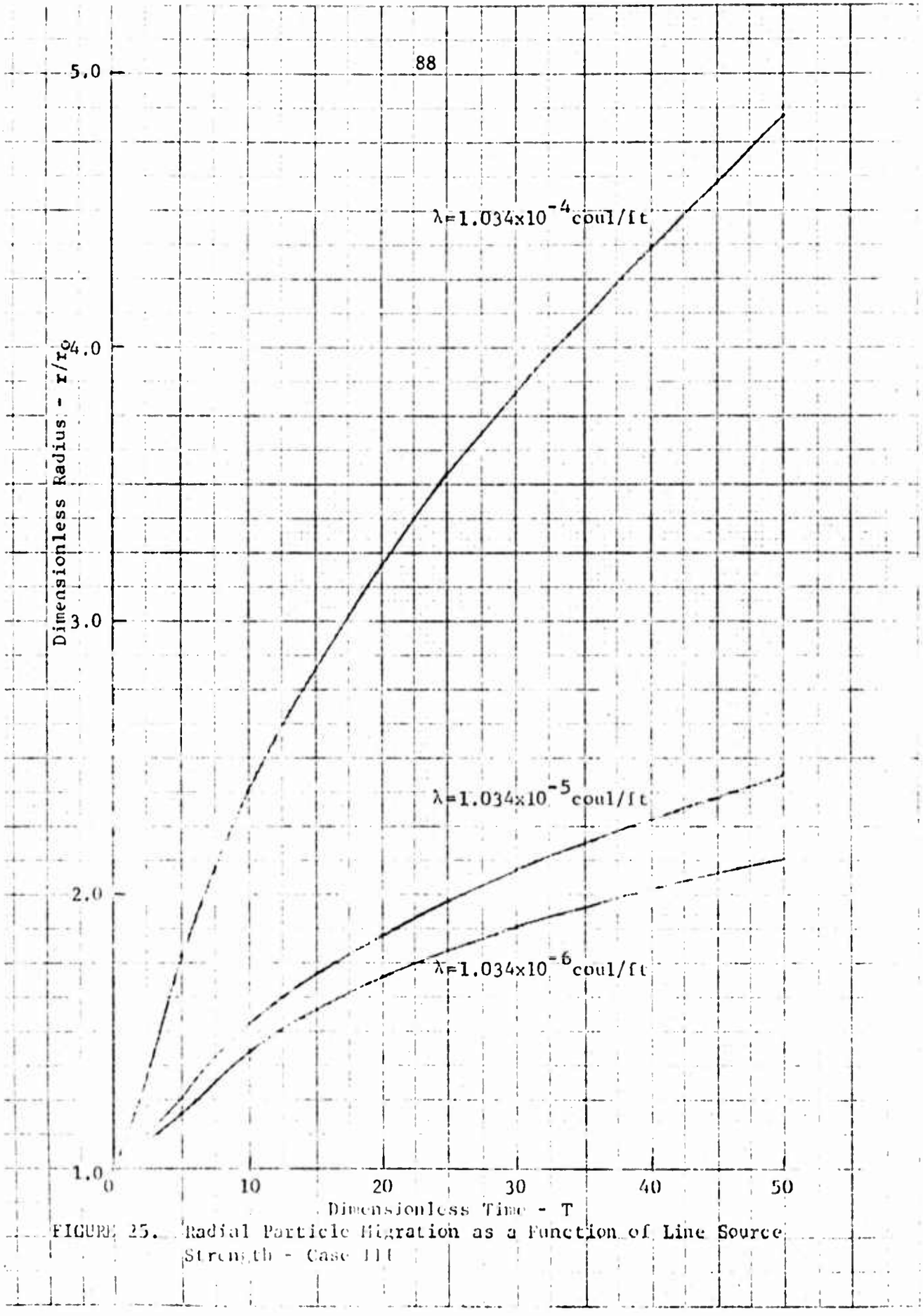

FIGURE 25. Radial Particle Migration as a Function of Line Source Strength - Case III

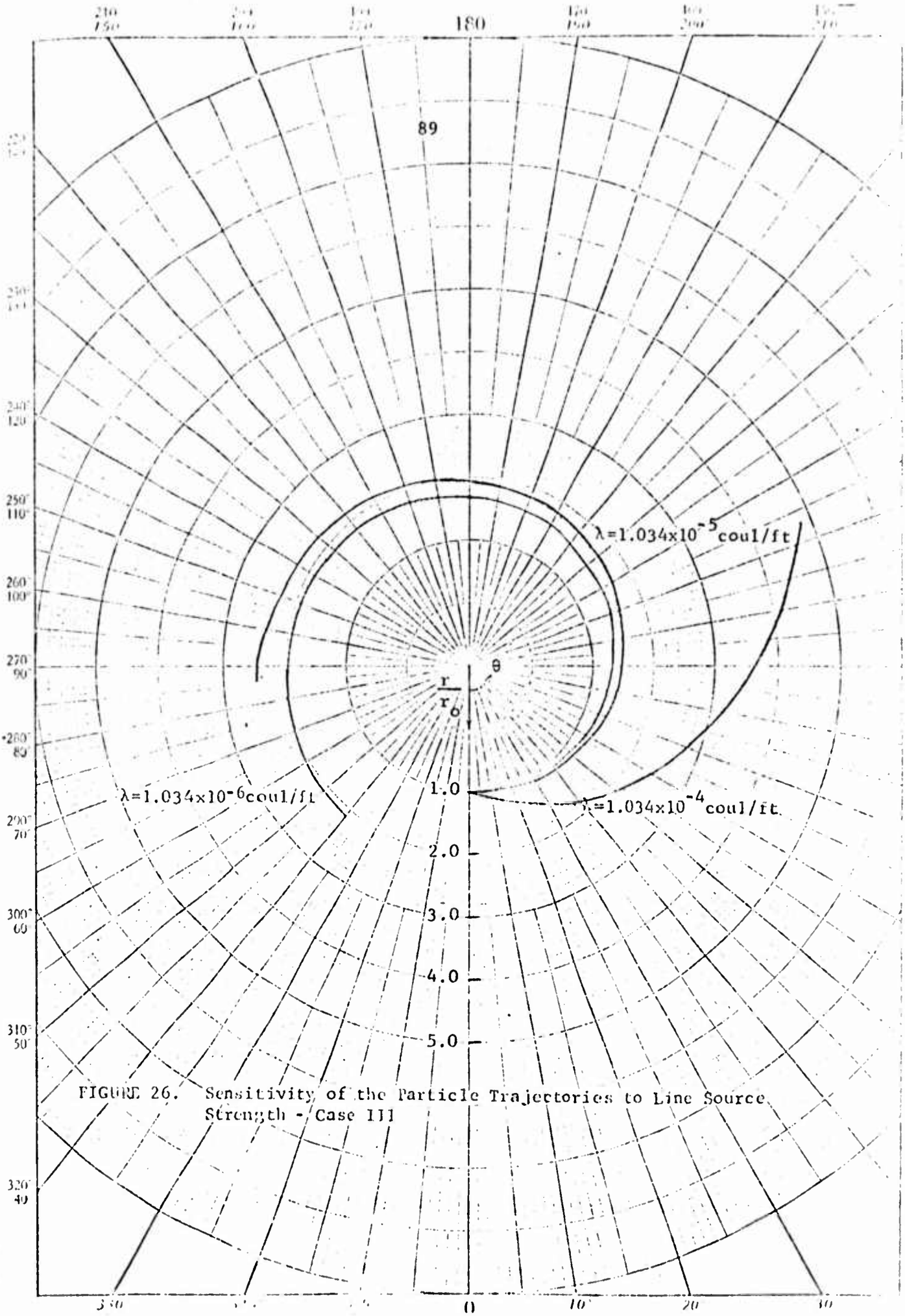

FIGURE 26. Sensitivity of the Particle Trajectories to Line Source Strength - Case III

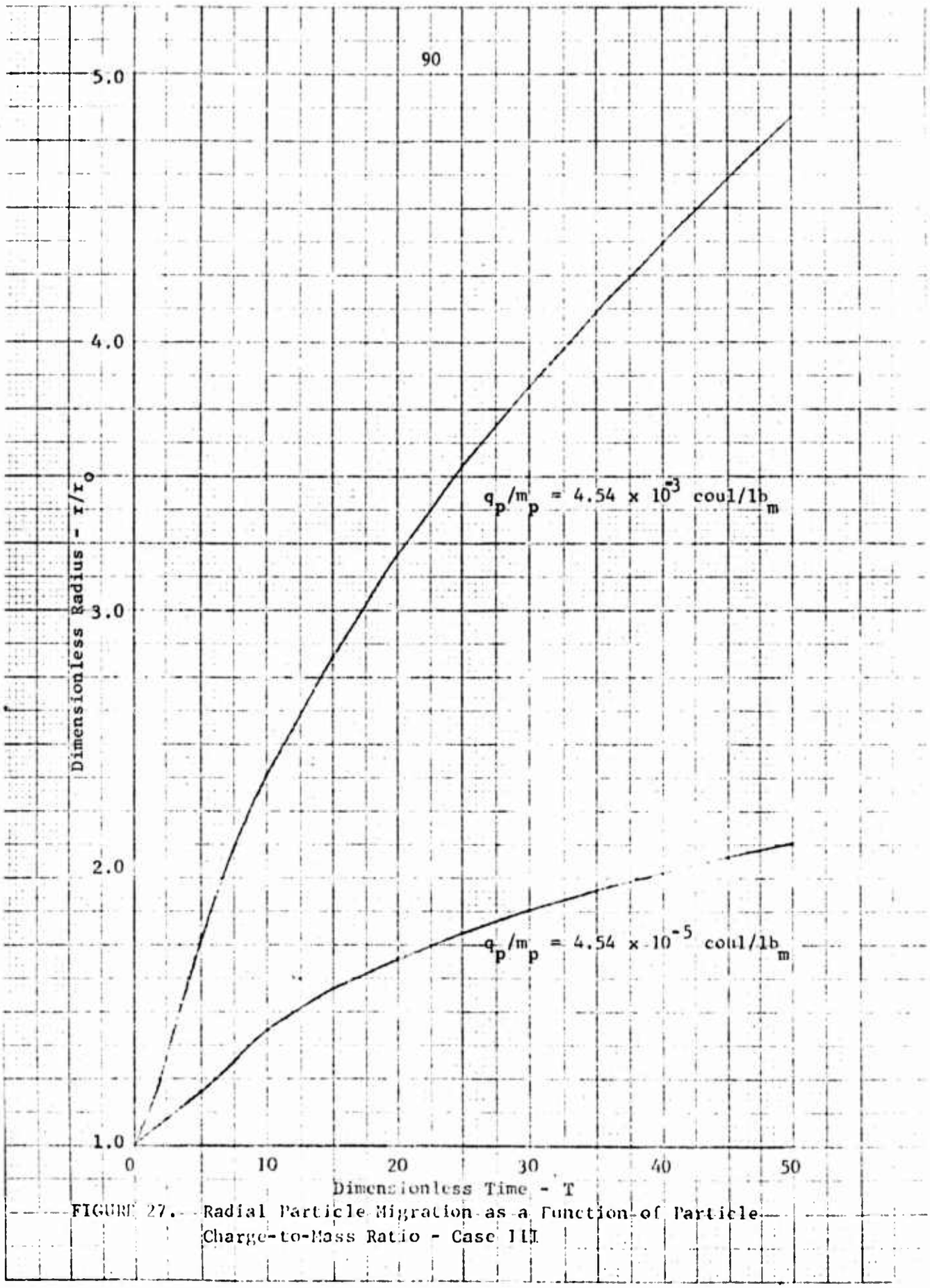

FIGURE 27. Radial Particle Migration as a Function of Particle Charge-to-Mass Ratio - Case III

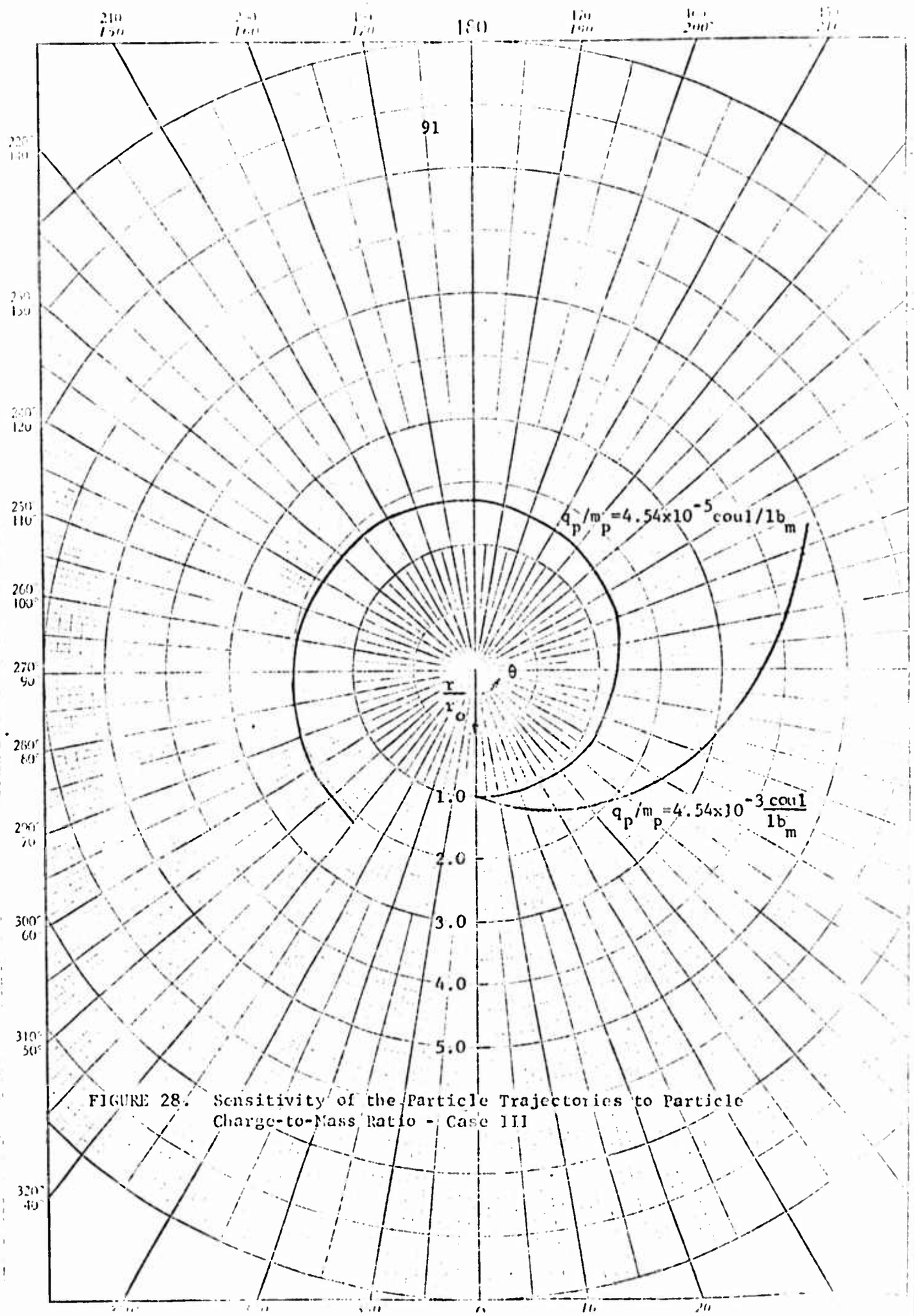

FIGURE 28. Sensitivity of the Particle Trajectories to Particle Charge-to-Mass Ratio - Case III

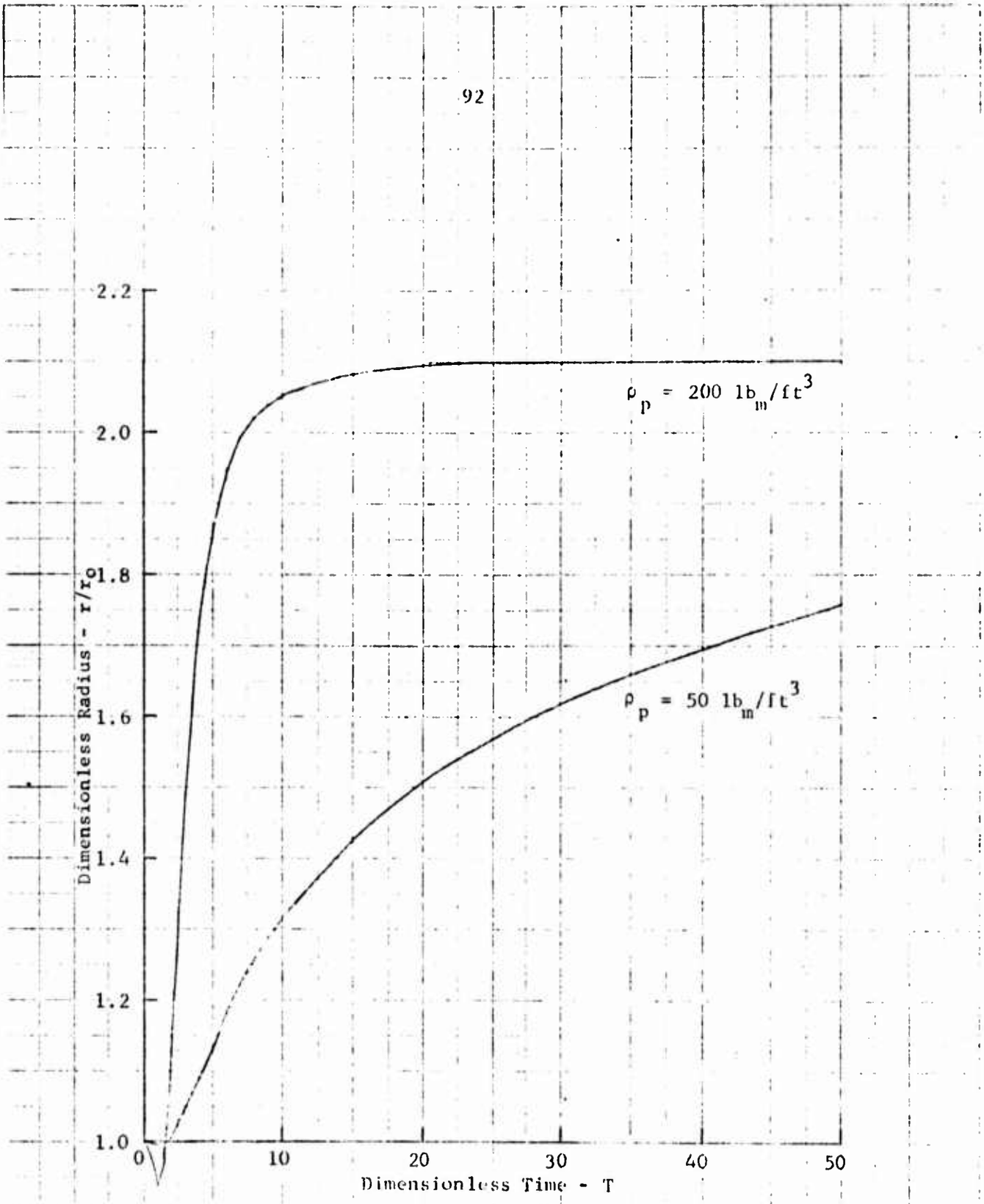

FIGURE 29. Radial Particle Migration as a Function of Particle Density - Case III A

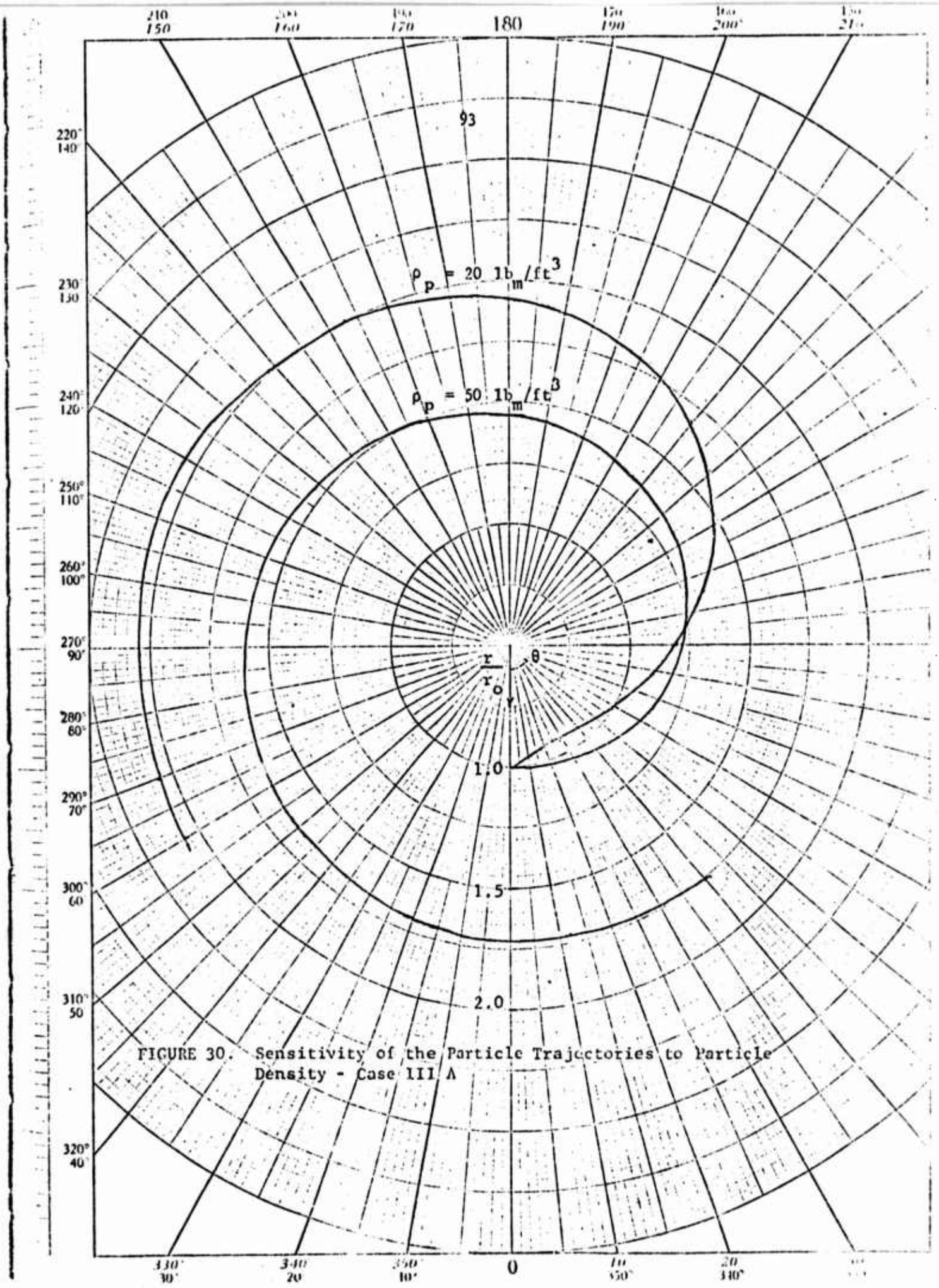

FIGURE 30. Sensitivity of the Particle Trajectories to Particle Density - Case III A

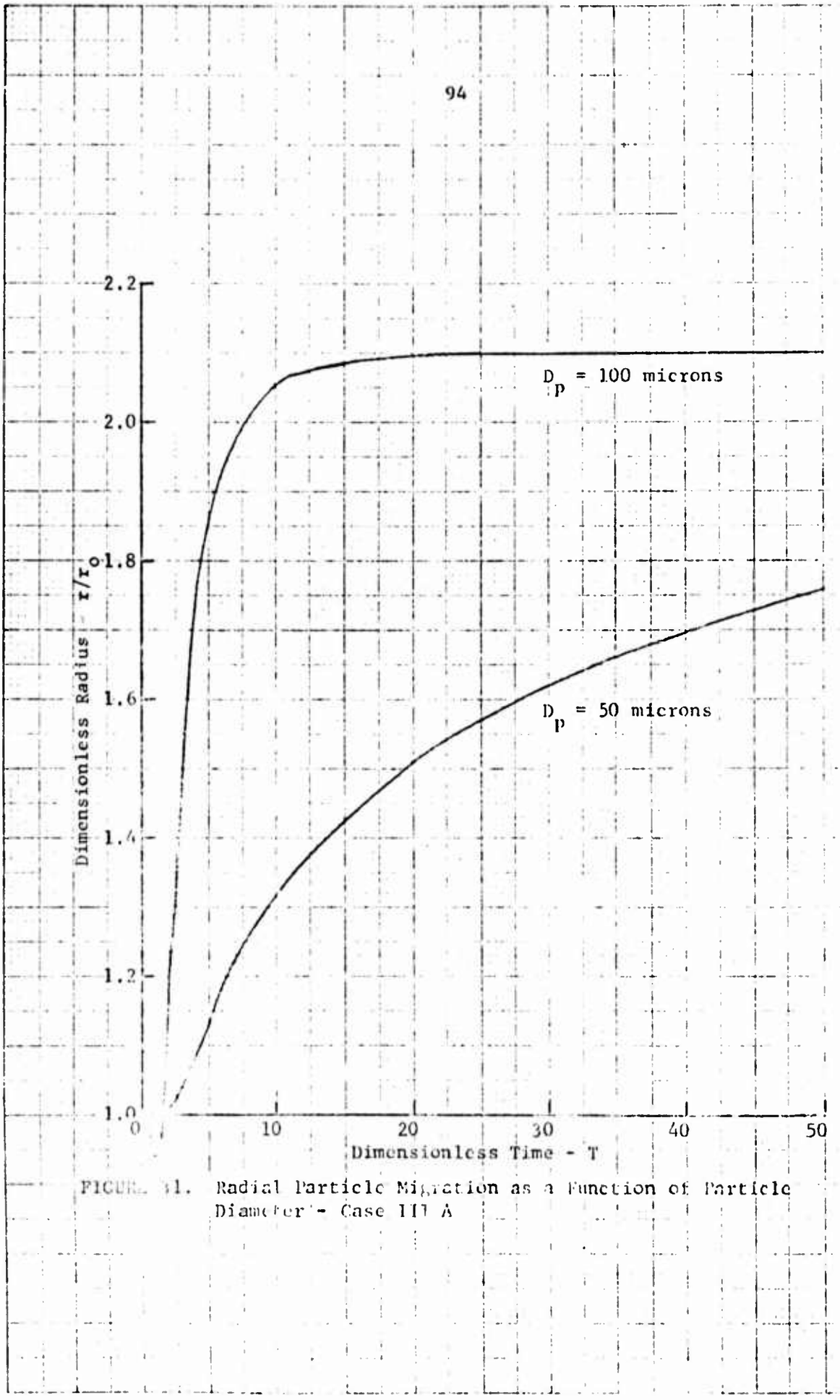

FIGURE 31. Radial Particle Migration as a Function of Particle Diameter - Case III A

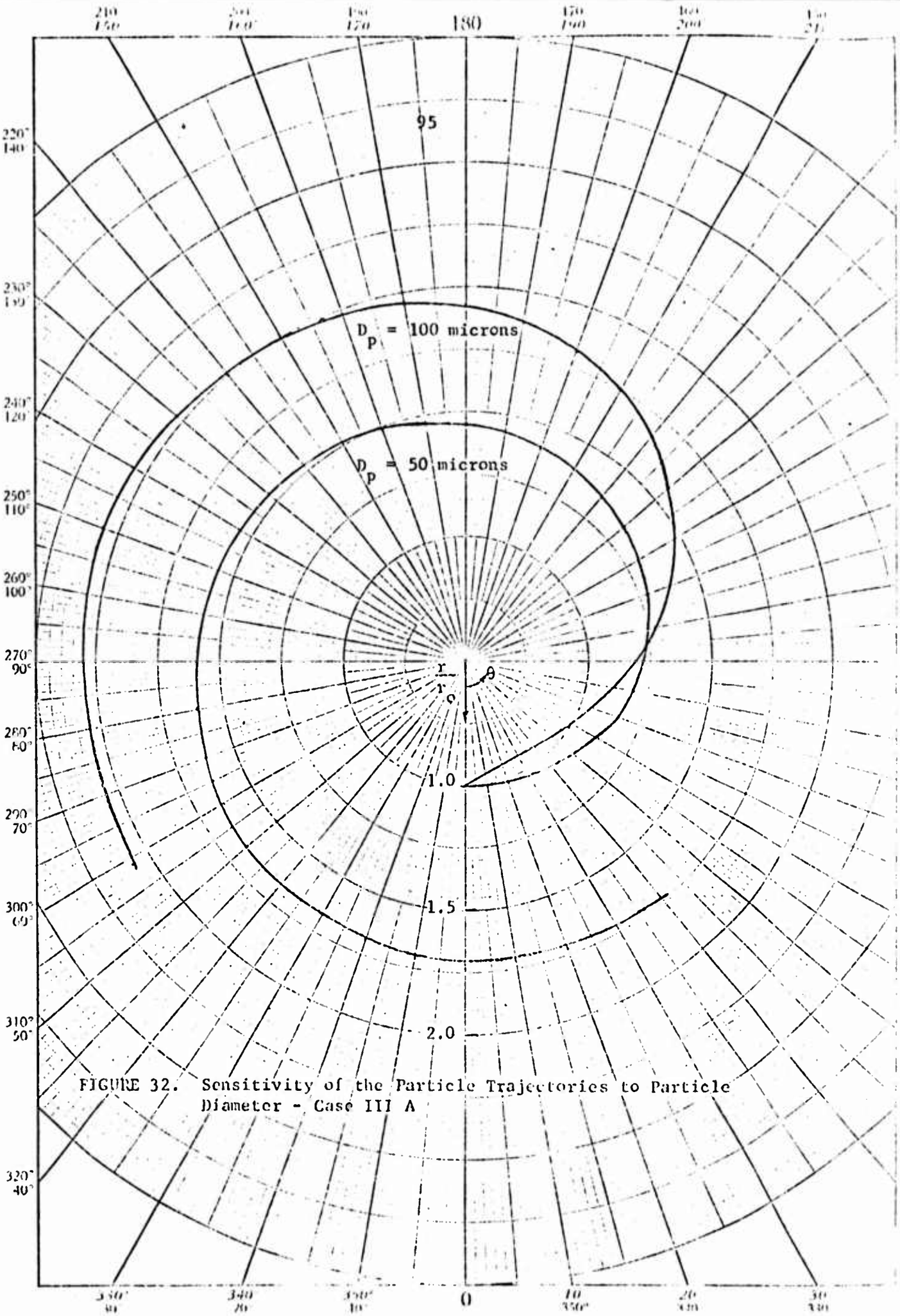

FIGURE 32. Sensitivity of the Particle Trajectories to Particle Diameter - Case III A

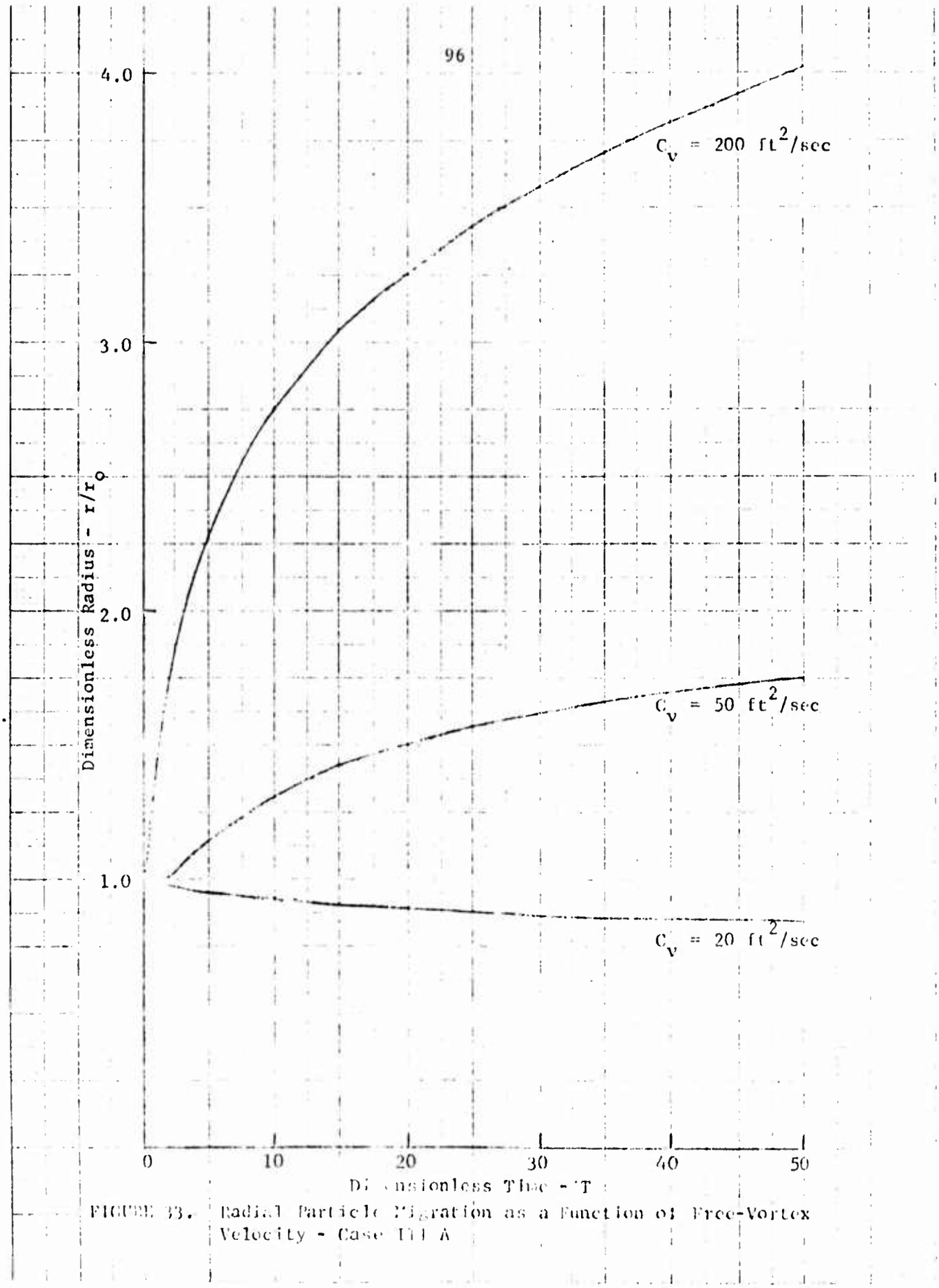

FIGURE 33. Radial Particle Migration as a Function of Free-Vortex Velocity - Case III A

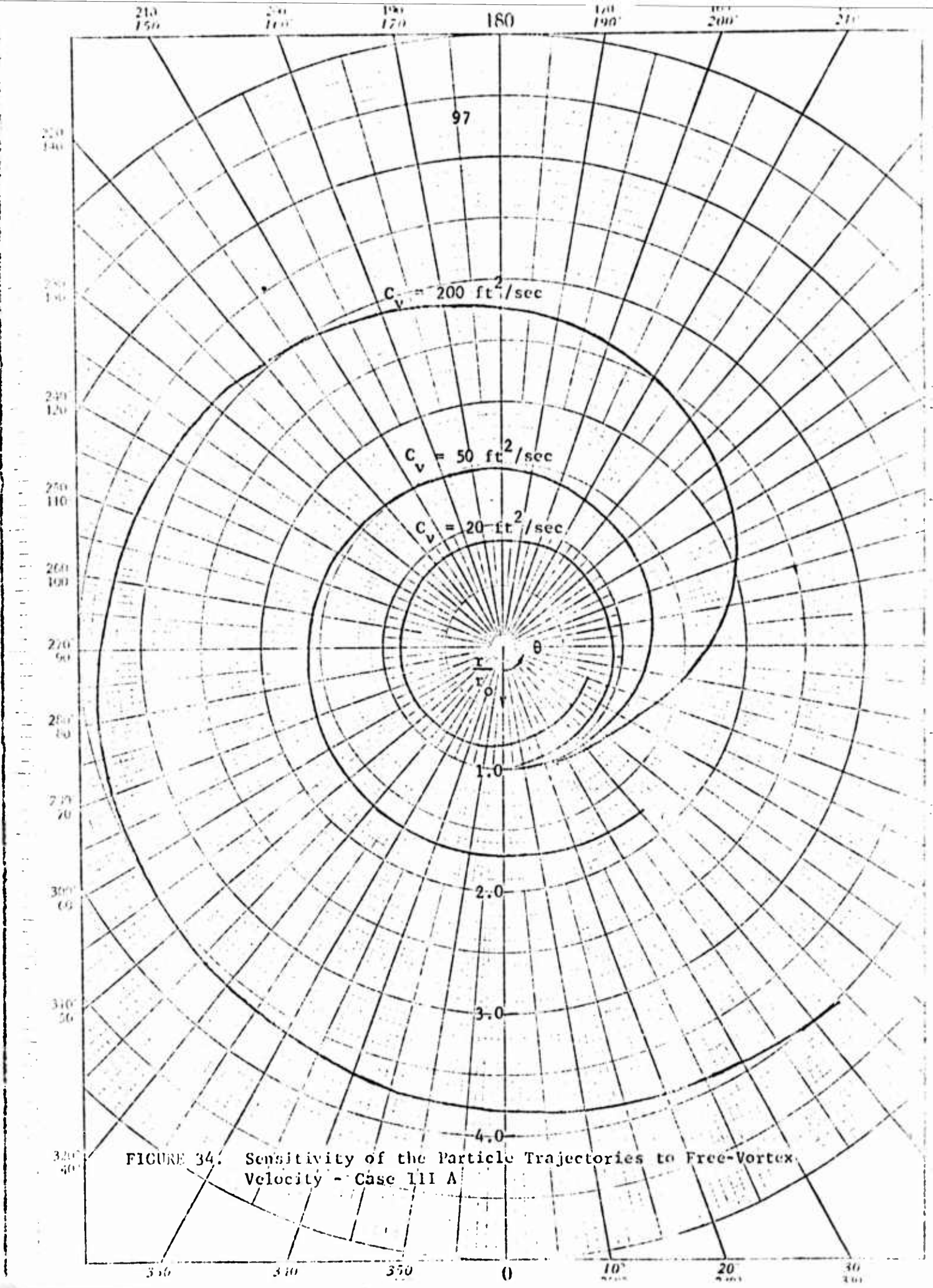

FIGURE 34. Sensitivity of the Particle Trajectories to Free-Vortex Velocity - Case III A

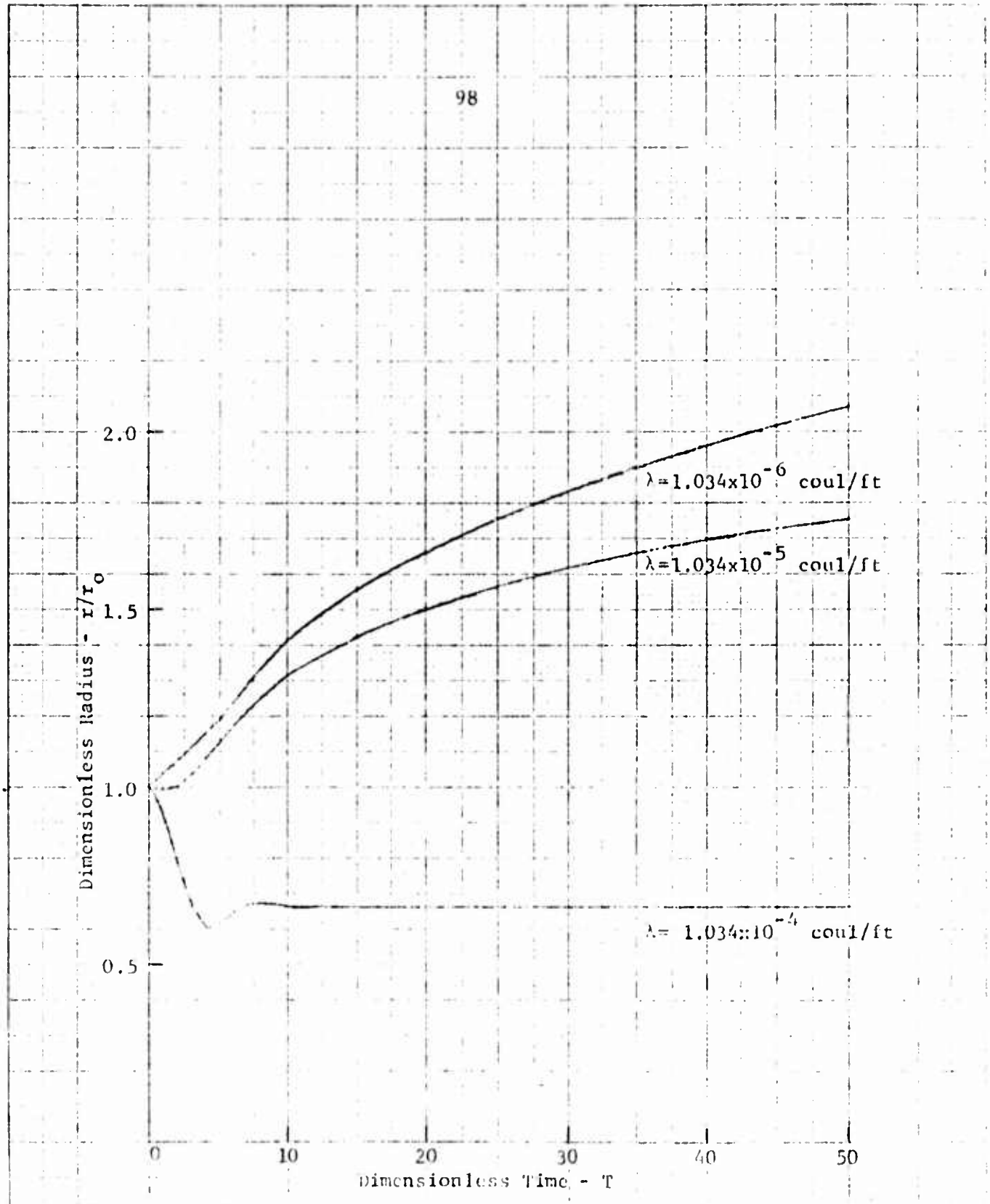

FIGURE 15. Radial Particle Migration as a Function of Line Source Strength - Case III A

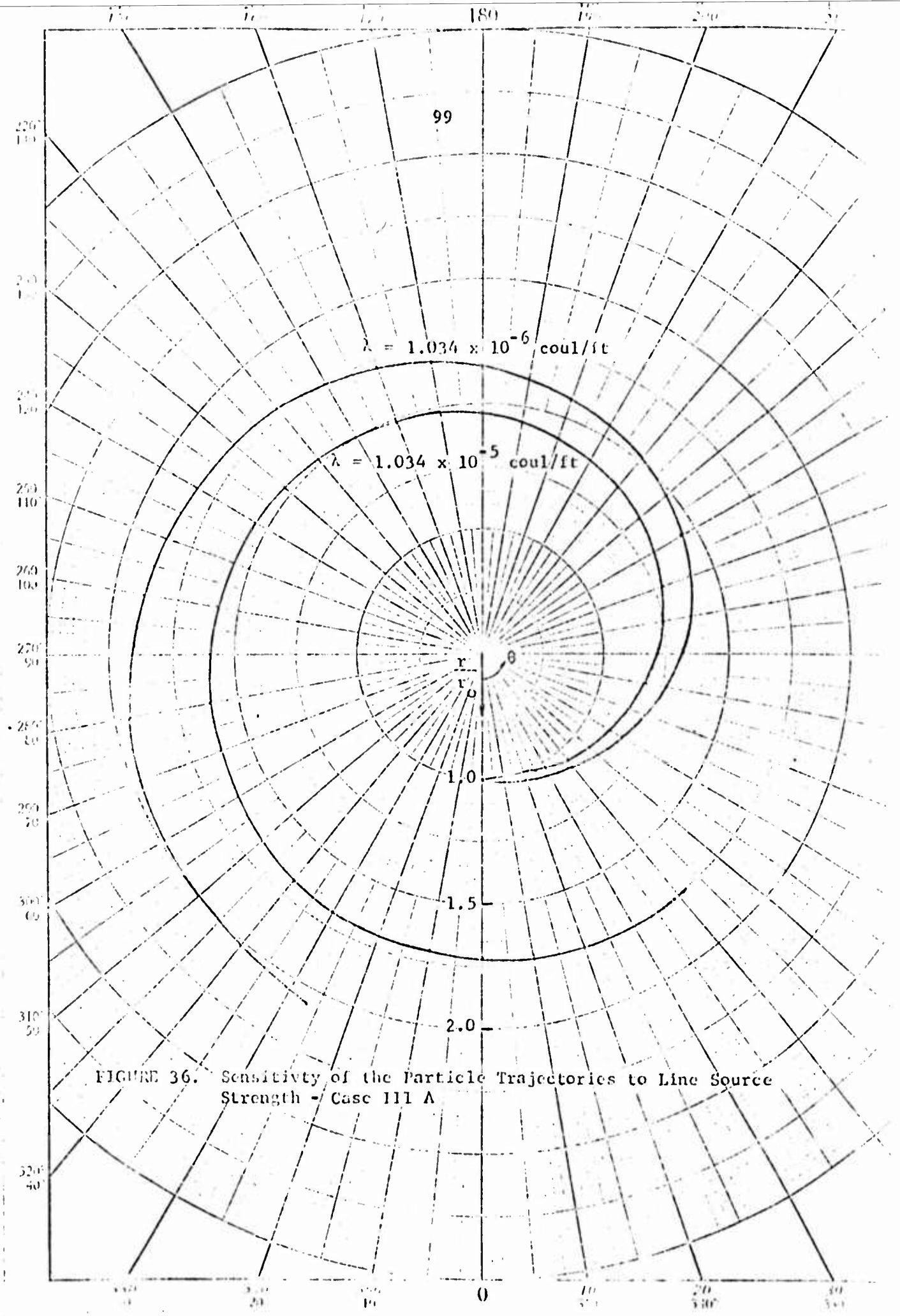

FIGURE 36. Sensitivity of the Particle Trajectories to Line Source Strength - Case III A

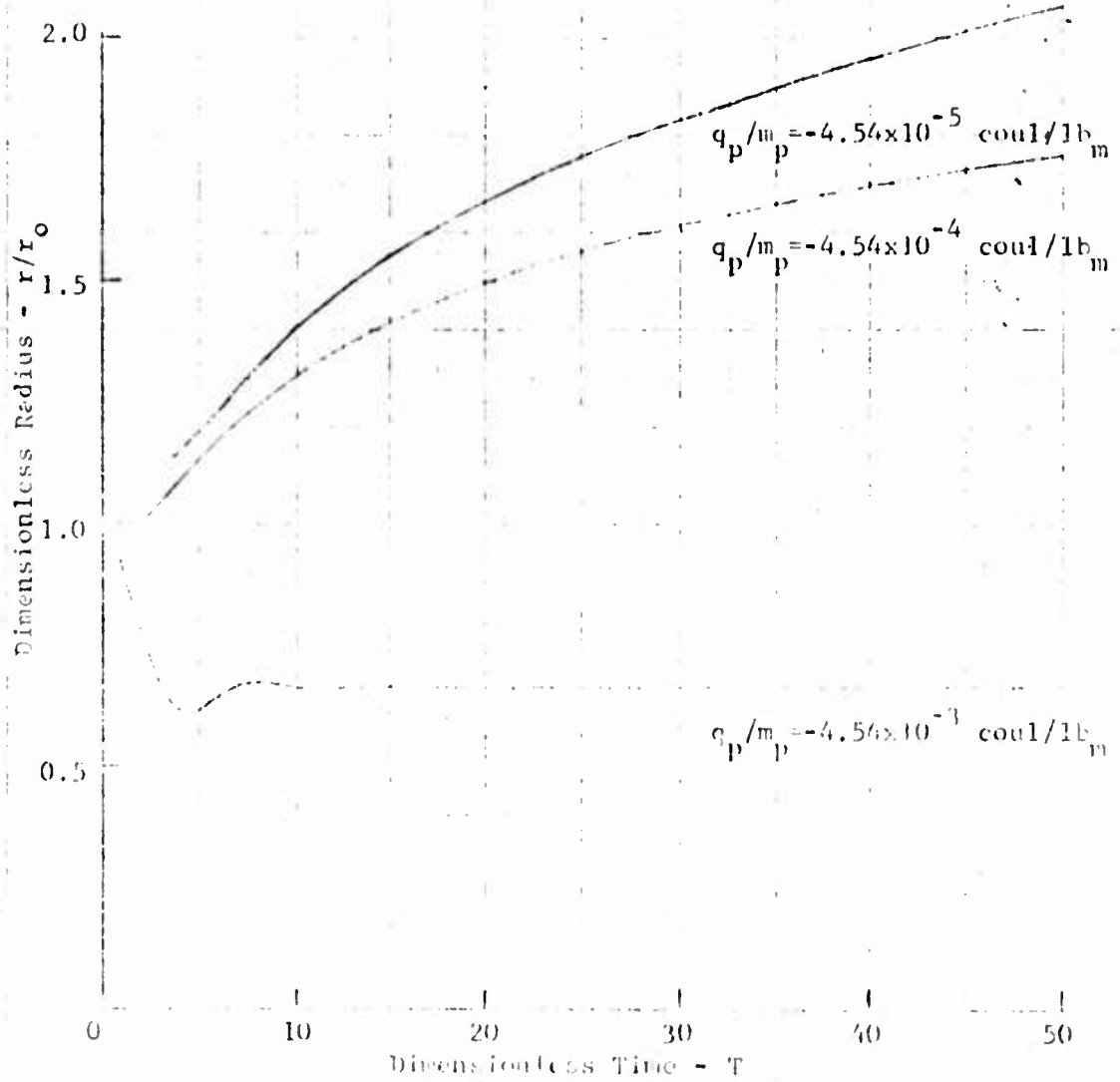

FIGURE 17. Radial Particle Migration as a Function of Particle Charge-to-Mass Ratio - Case III A

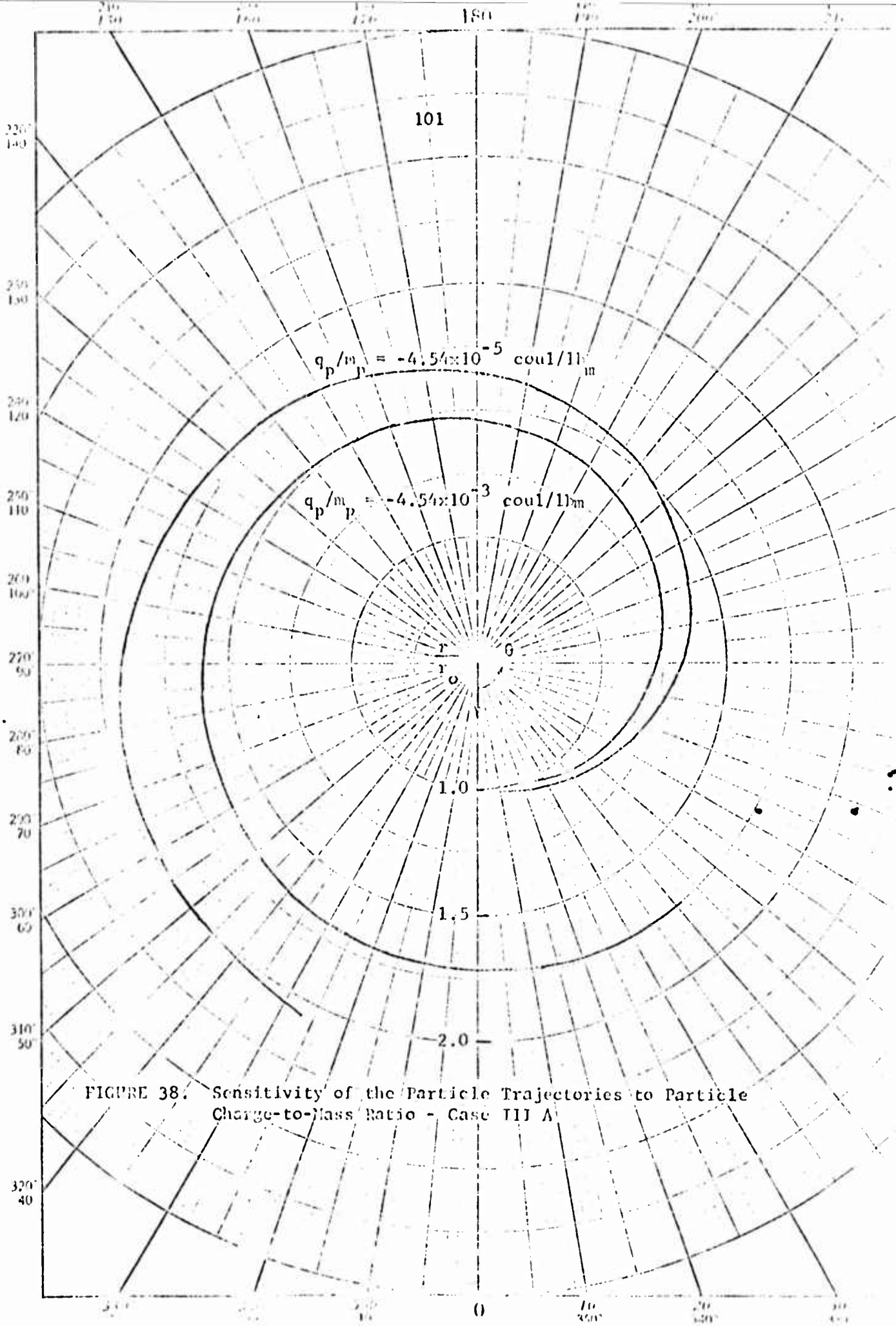

FIGURE 38. Sensitivity of the Particle Trajectories to Particle Charge-to-Mass Ratio - Case III A

In order to assess the relative effects of the forces considered to act on a particle released in a free-vortex, comparisons between the three cases just discussed were made and the results presented in Figures 39 through 44. Figures 39 and 40 compare the radial particle migration and particle trajectories for Case I, an uncharged particle entrained in a free-vortex, and Case II, a charged particle moving in a viscous medium under the influence of an applied electric field. It is evident that the repulsive electrostatic force has a greater effect on radial migration than the centrifugal or inertial force. This is due to the fact that the electrostatic force is proportional to $1/r$), whereas the centrifugal force is proportional to $(1/r^3)$. Thus greater radial migration is obtained from a particle moving under the influence of the applied electric field. In Figure 40, the particle trajectories for these two cases are compared. As expected, the particle trajectory for Case II is a straight line, since in this case the particle has no initial tangential component and the only forces acting on it, electrostatic and drag, have radial components only.

Figures 41 and 42 provide a comparison of the results from Cases II and III. It is seen that inclusion of the centrifugal force due to the presence of the free-vortex results in an increase in radial migration in Case III over that predicted for Case II. The centrifugal force augments the radial electrostatic force, increasing radial particle migration.

Figures 43 and 44 compare the results from Case I, Case III, and Case III A. When the line source and the particle are both positively charged, as in Case III, the electrostatic force, which is repulsive in nature, augments the centrifugal force and causes the radial particle migration to increase. When the line source and the particle are assumed to be oppositely charged, as in Case III A, the results indicate that the electrostatic force, which is now attractive, and the centrifugal force tend to balance each other out, allowing the particle to attain an equilibrium radius. The particle trajectories shown in Figure 44 also exhibit the same behavior noted previously -- as the radial migration increases, the angular distance the particle travels is decreased.

The fourth case considered analyzed the motion of two charged particles in a free-vortex flow field under the influence of the electric field due to the charge on each particle. Calculations were made to determine the effect on particle motion of: particle charge and the sign of the charge, and particle mass. The particle trajectories and radial particle migration are presented in Figures 45 and 46. The results indicate that field effects due to particle charge on particle motion are negligible, if the particle charge is of the same magnitude as that considered in Cases II and III. The results also indicated that changing the sign of the charge on one of the particles, in effect changing the electrostatic force from a repulsive force to an attractive force, had no effect on particle motion. Increasing the mass of the particle assumed to be initially

farther from the center of the free vortex increased its radial migration, since, as expected from the results obtained in Cases I and III, the drag force acting on the particle was reduced. Since the parameters governing the motion of the particle nearer the center of the free vortex were not changed, its motion was unchanged from the previous prediction. An increase in the magnitude of the particle charge by a factor of 2000 did result in a substantial change in the radial particle migration and the particle trajectories. The repulsive electrostatic force between the charged particles caused the particles to separate rapidly before the free-vortex flow field began to affect their motion. Relatively large particle charge-to-mass ratios are required before field effects due to the charge on the particles would be of sufficient strength to affect particle motion. A particle-flow system containing a large number of charged particles may result in electrostatic fields of sufficient strength to affect the particle motion.

Any extension of this analysis should attempt to account for field effects on fluid motion. In the one and two particle systems considered here, field effects on fluid motion are no doubt small due to the highly localized body force acting on the fluid as a result of the electrostatic field. This may not be the case in a particle system composed of a large number of charged particles, in which the electrostatic body force may cause the fluid to be accelerated.

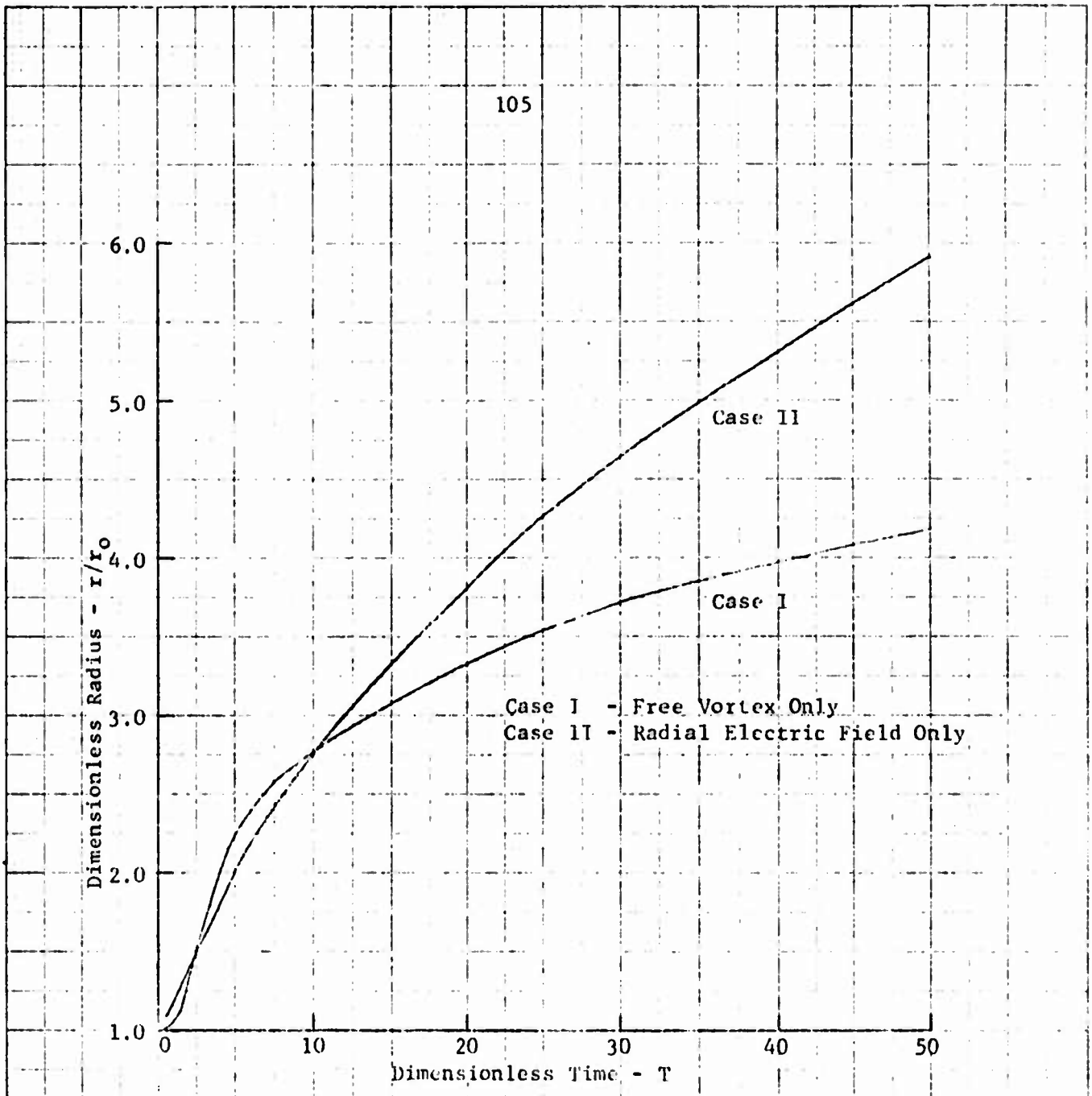

FIGURE 39. Radial Particle Migration Comparison - Cases I and II

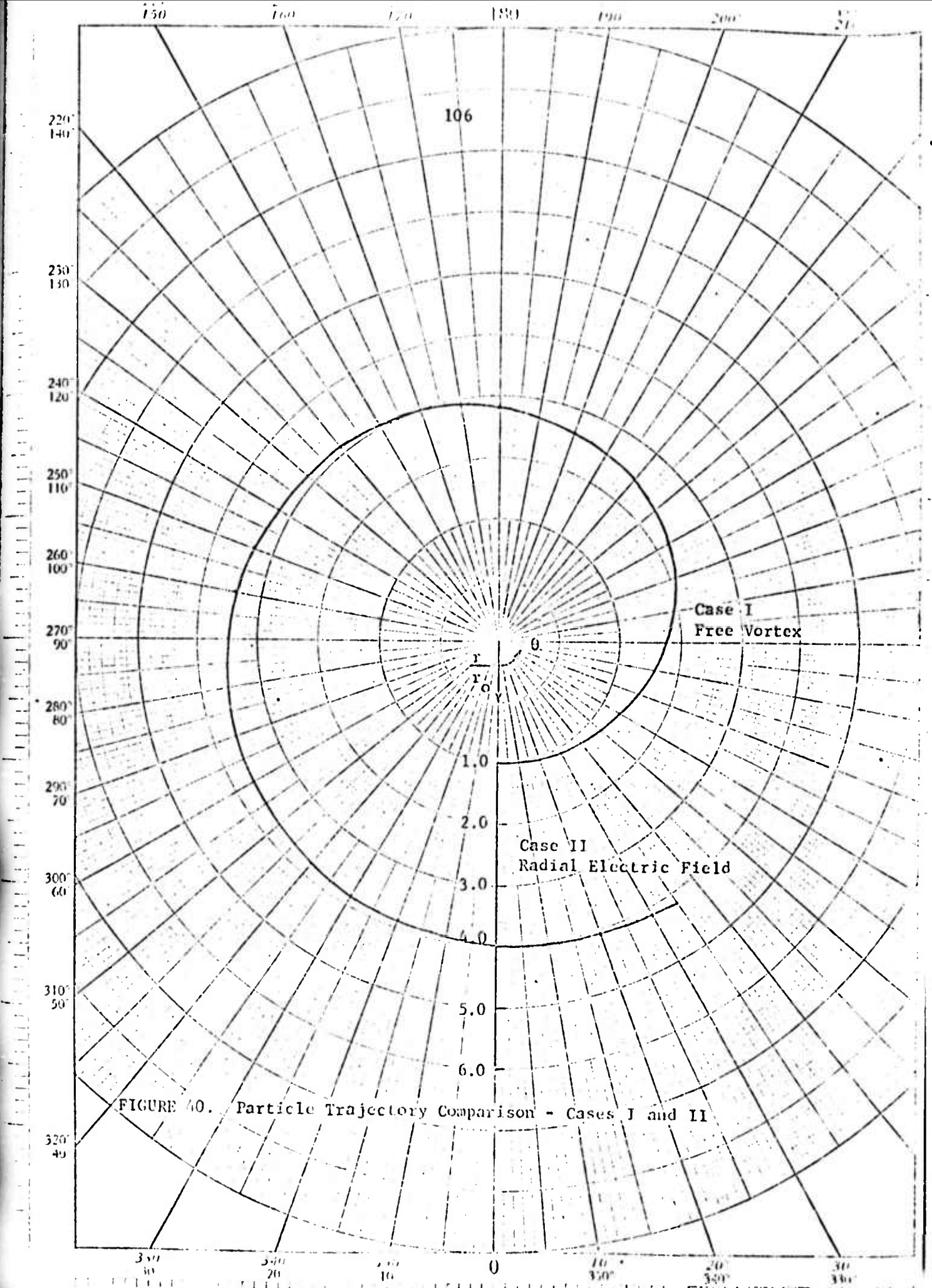

FIGURE 40. Particle Trajectory Comparison - Cases I and II

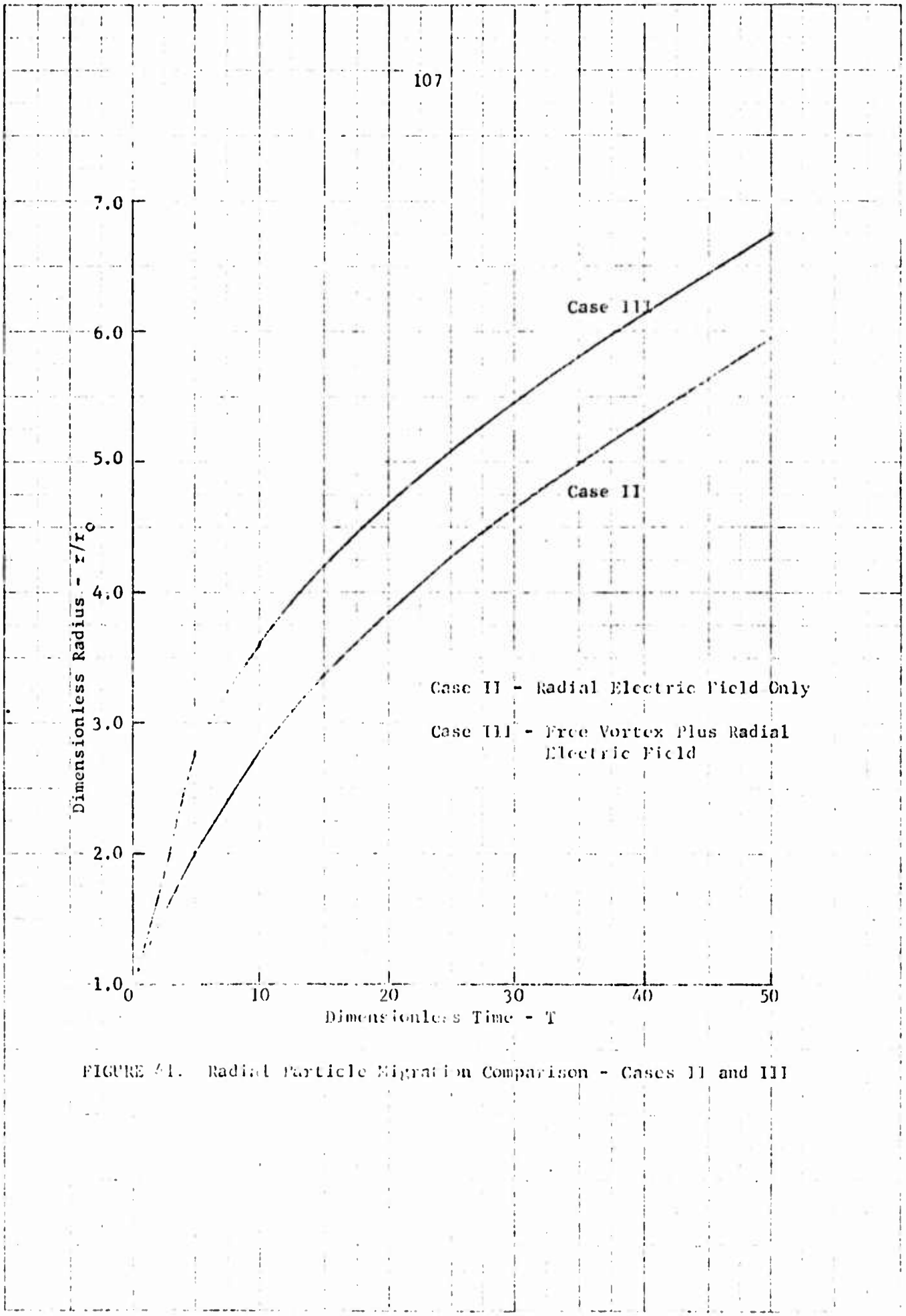

FIGURE 41. Radial Particle Migration Comparison - Cases II and III

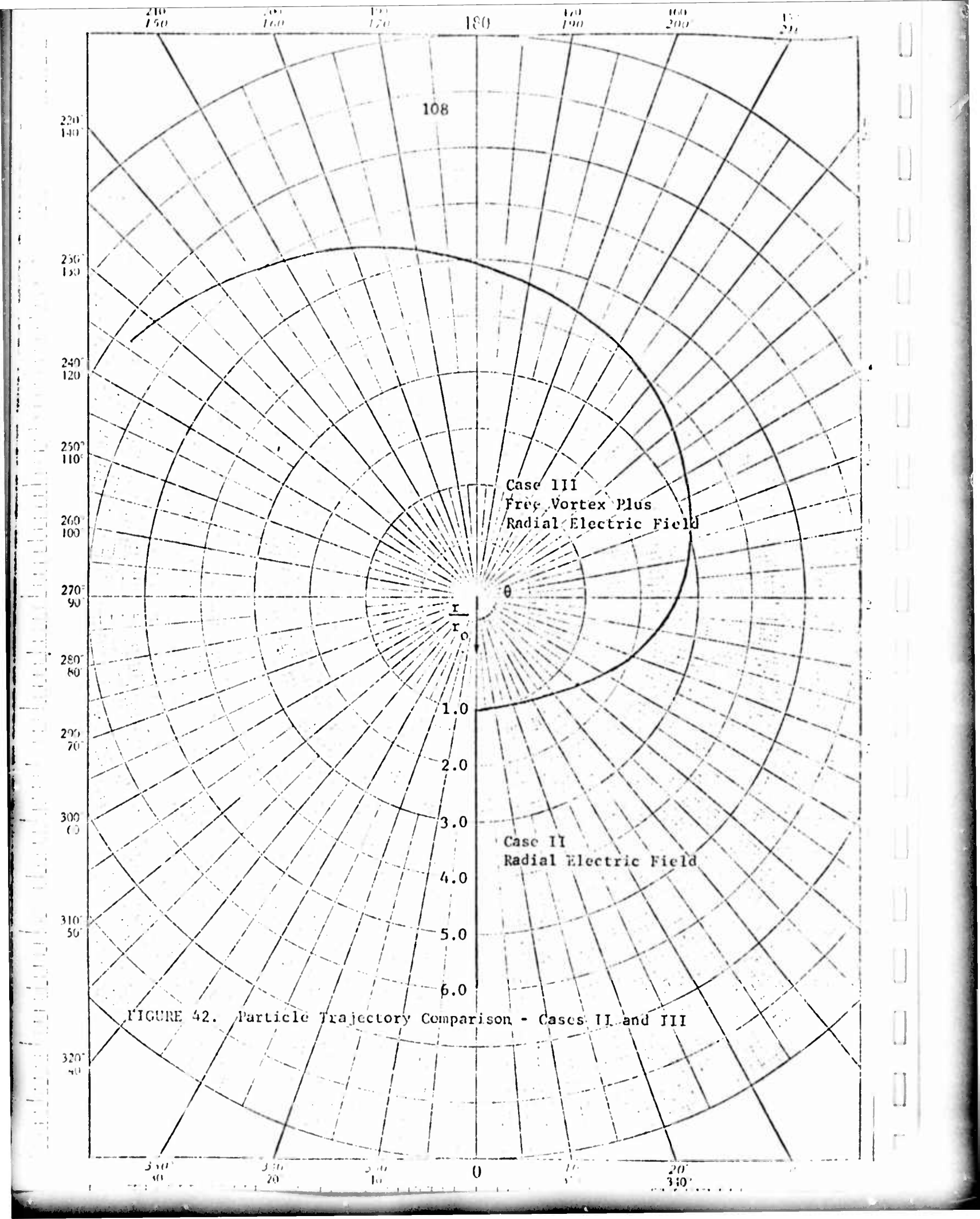

FIGURE 42. Particle Trajectory Comparison - Cases II and III

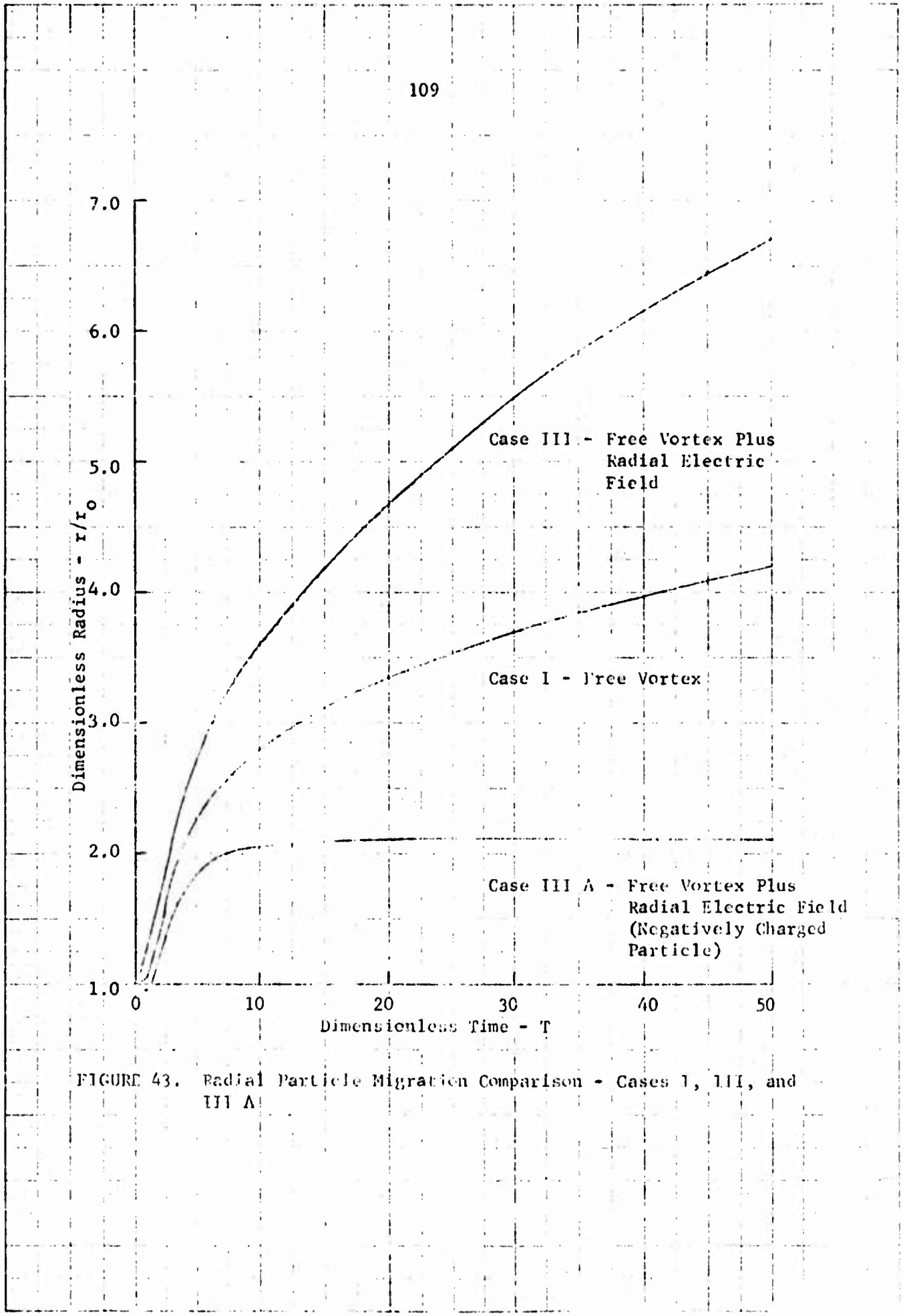

FIGURE 43. Radial Particle Migration Comparison - Cases I, III, and III A

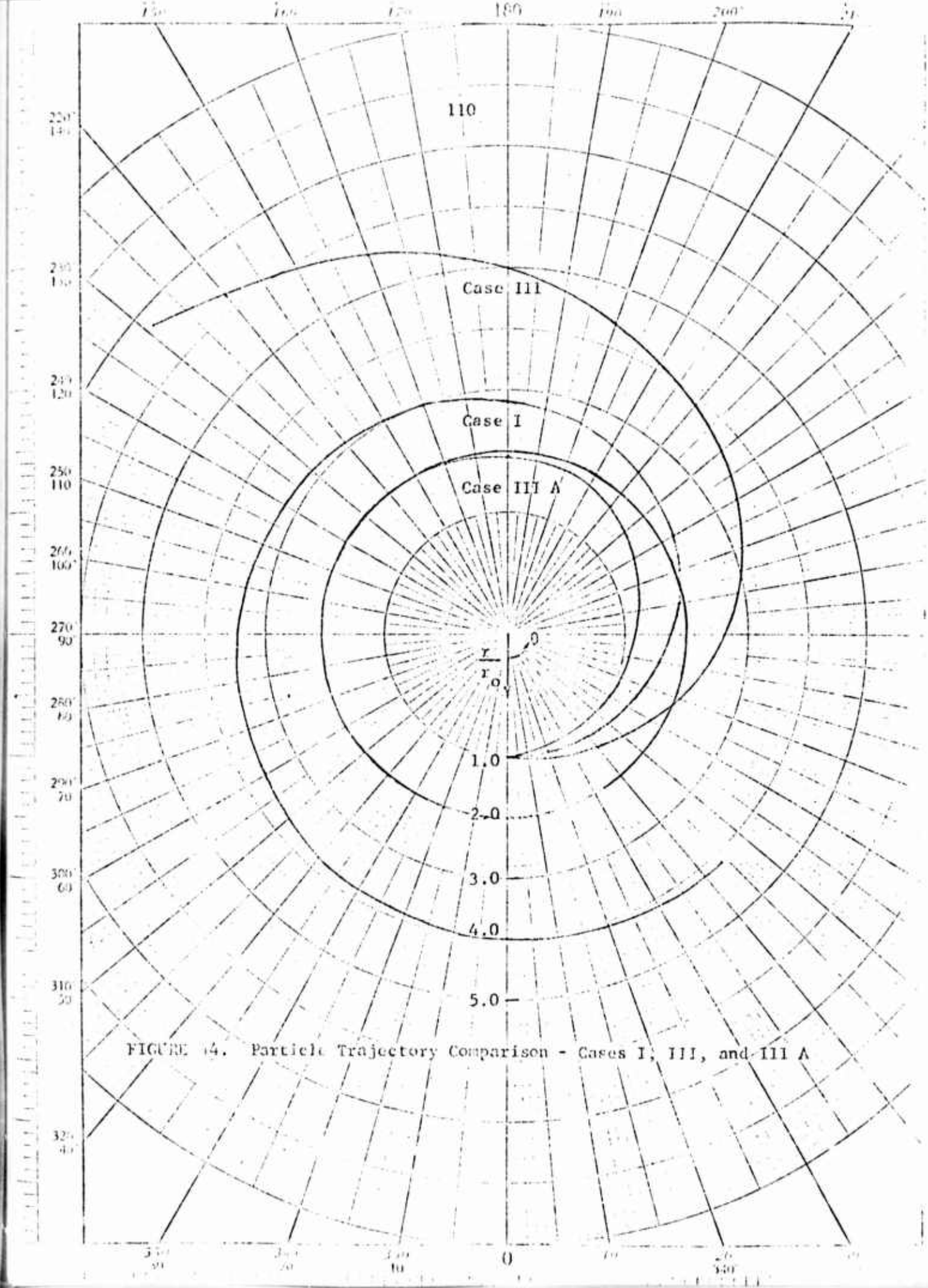

FIGURE 4. Particle Trajectory Comparison - Cases I, III, and III A

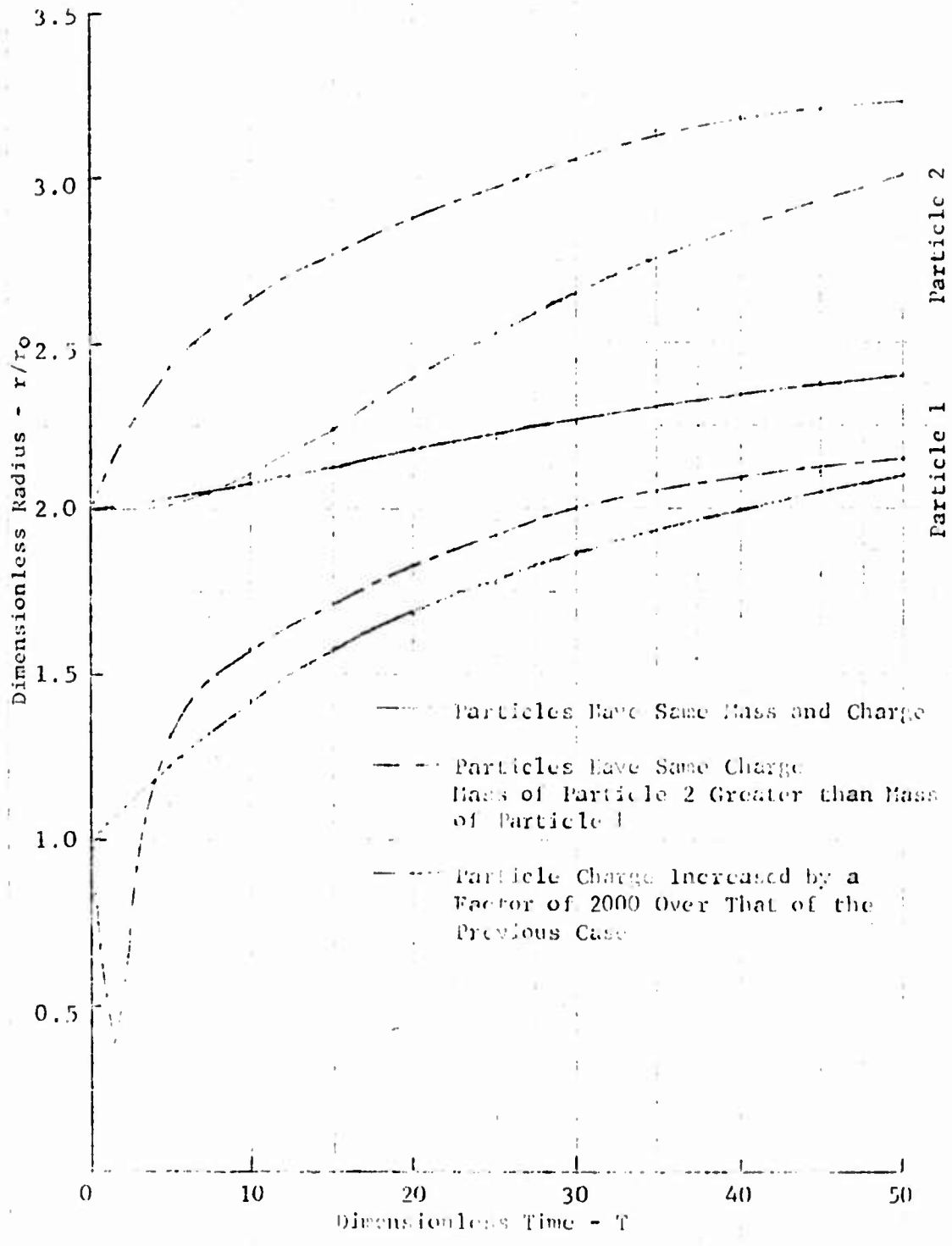

FIGURE 45. Radial Particle Migration For Case IV

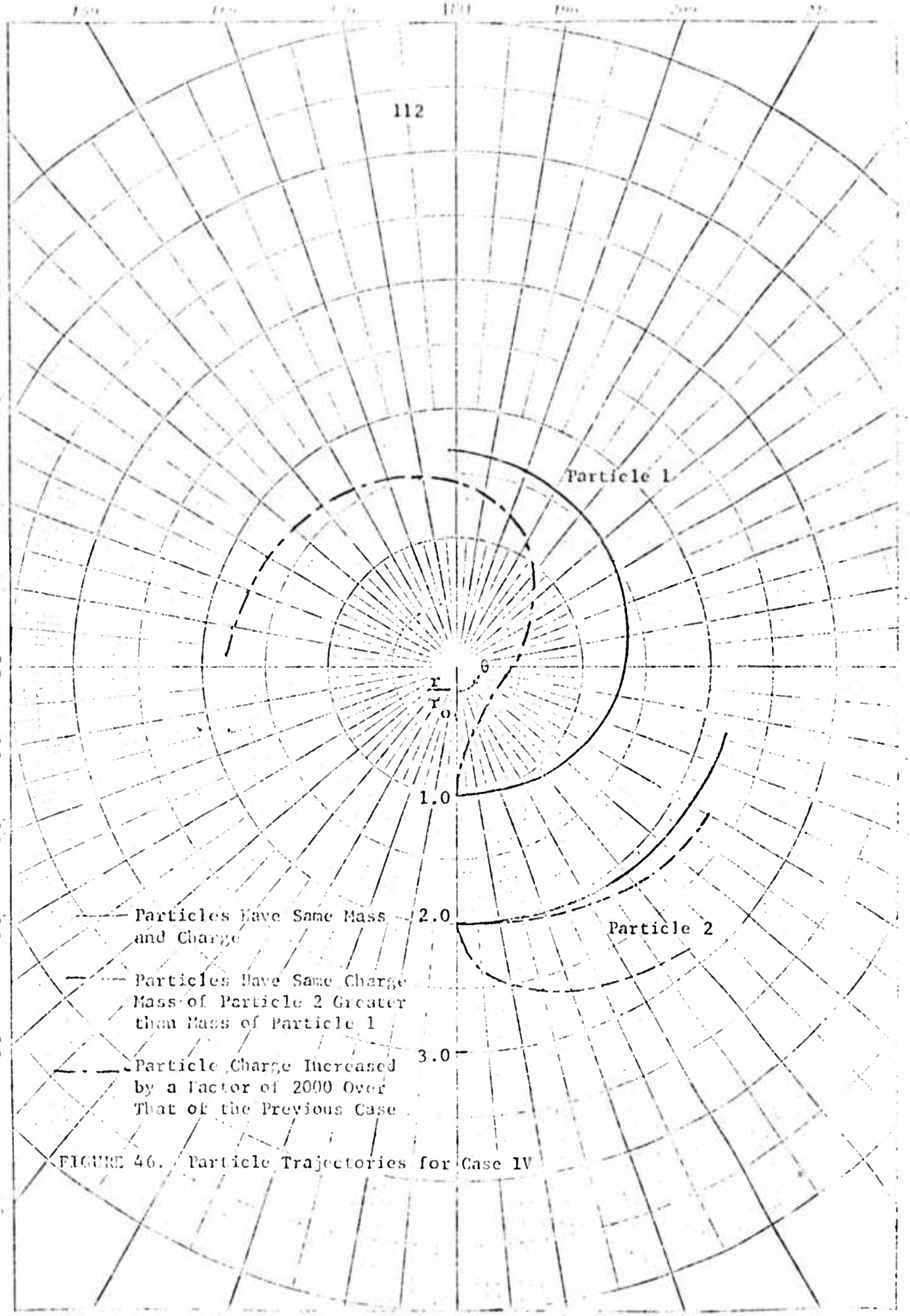

FIGURE 46. Particle Trajectories for Case IV

CONCLUSIONS

For the case of an uncharged particle moving in a free-vortex system, the results indicate that at constant free-vortex velocity, entrainment of a particle is decreased or conversely, the radial particle migration is increased. Radial particle migration also is increased as the free-vortex flow velocity is increased while the particle density and diameter are held constant. As radial particle migration increases, the angular displacement of the particle is decreased. Since the axial flow velocity was assumed to be constant, the equation of motion of the particle in the axial direction is independent of the radial and tangential coordinates of the particle. Thus particle motion in the axial direction is not influenced by what is occurring in the radial and tangential directions.

For the case of a charged particle moving in a viscous medium under the influence of a charged line source, particle motion is strongly influenced by the particle charge-to-mass ratio and the line source strength.

For the case of a positively charged particle moving in a free vortex under the influence of an applied electric field due to a line source of positive charges, the electrostatic force reinforces the centrifugal force, causing an increase in radial migration over the cases in which each force is considered to act individually. If the particle is assumed to be negatively charged, the electrostatic force and the centrifugal force tend to balance each other out, allowing the particle to attain an equilibrium radius. The drag

force alone is not of sufficient magnitude to balance either the electrostatic force or the centrifugal force.

Results from the case of two charged particles moving in a free-vortex indicated that the electric fields due to each of the particles were not strong enough to affect the motion of the particles. If a system with a large number of charged particles were to be analyzed in a similar manner, electric field effects due to the particle charges would influence the particle motion.

RECOMMENDATIONS

The following recommendations are made as a result of this study:

1) The analysis should be repeated using a more complex vortex system with a more realistic axial flow distribution. Some of the more complex vortex systems mentioned in the literature survey could be incorporated in this analysis.

2) The analysis should be extended to a system incorporating a large number of particles, with the particles preferably distributed in size, so that the vortex could be used as a particle separator. A charge distribution should also be imposed on the particles, so that electrostatic effects could be studied.

3) Field effects on fluid motion should be determined to see if this would have a significant effect on particle motion. It is believed that in a one or two particle system, field effects on fluid motion are negligible.

REFERENCES

1. Hirschkron, R., and Ehrich, F. F., "Entrained-Particle Trajectories in a Swirling Flow", ASME Paper No. 64-WA/FE-30.

2. Kriebel, A. R., "Particle Trajectories in a Gas Centrifuge", Transactions of the ASME, Journal of Basic Engineering, September, 1961, pp. 333-340.

3. Lapple, C. E., and Shepherd, C. B., "Calculation of Particle Trajectories", Industrial and Engineering Chemistry, Volume 32, Number 5, May, 1940, pp. 605-617.

4. Uematu, T., Omi, M., and Fuzisawa, T., "Separation Performance of the Hydrocyclone", Bulletin of the JSME, Volume 5, Number 19, 1962, pp. 470-478.

5. Soo, S. L., "Effect of Electrification on the Dynamics of a Particulate System", I & EC Fundamentals, Volume 3, Number 1, February, 1964, pp. 75-80.

6. Soo, S. L., "Gas-Solid Suspensions at High Temperatures", Journal of Applied Physics, Volume 34, Number 6, June, 1963, pp. 1689-1696.

7. Soo, S. L., Trezek, G. J., Dimick, R. C., and Hohnstreiter, G. F., "Concentration and Mass Flow Distributions in a Gas-Solid Suspension", I & EC Fundamentals, Volume 3, Number 2, May, 1964, pp. 98-106.

8. Soo, S. L., and Trezek, G. J., "Turbulent Pipe Flow of Magnesia Particles in Air", I & EC Fundamentals, Volume 5, Number 3, August, 1966, pp. 389-392.

9. Vonnegut, B., "Electrical Theory of Tornadoes", Journal of Geophysical Research, Volume 65, Number 1, January, 1960, pp. 203-212.

10. Freier, G. D., "The Earth's Electric Field During A Tornado", Journal of Meteorology, Volume 16, 1959, pp. 333-334.

11. Vonnegut, B., and Weyer, J. R., "Luminous Phenomena in Nocturnal Tornadoes", Science, Volume 153, September, 1966, pp. 1213-1220.

12. Brook, M., "Electric Currents Accompanying Tornado Activity", Science, Volume 157, September, 1967, pp. 1434-1436.

13. Vonnegut, B., and Moore, C. B., "Electrical Activity Associated with the Blackwell-Udall Tornado", Journal of Meteorology, Volume 14, 1957, pp. 284-286.

14. Gunn, R., "Electric Field Intensity at the Ground Under Active Thunderstorms and Tornadoes", Journal of Meteorology, Volume 13, June, 1956, pp. 269-273.

15. Silberg, P. A., "Dehydration and Burning Produced by the Tornado", Journal of the Atmospheric Sciences, Volume 23, March, 1966, pp. 202-205.

16. Silberg, P. A., "Passive Electrical Measurements from Three Oklahoma Tornadoes", Proceedings of the IEEE, Volume 53, Number 9, September, 1965, pp. 1197-1204.

17. Freier, G. D., "The Electric Field of a Large Dust Devil", Journal of Geophysical Research, Volume 65, Number 10, October, 1960, p. 3504.

18. Crozier, W. D., "The Electric Field of a New Mexico Dust Devil", Journal of Geophysical Research, Volume 69, Number 24, December, 1964, pp. 5427-5429.

19. Bradley, W. E., and Semonin, R. G., "Airborne Electrical Measurements in Dust Whirls", Journal of the Atmospheric Sciences, Volume 20, November, 1963, pp. 622-623.

20. Silberg, P. A., and Goshgarian, G., "Electrostatically Induced Rotary and Vortical Motion", Proceedings of the IEEE, Volume 52, June, 1964, pp. 732-733.

21. Silberg, P. A., Goshgarian, G., and Johnson, J. C., "Measurements of Electrostatically Produced Vortical Motion", Proceedings of the IEEE, Volume 52, December, 1964, pp. 1754-1755.

22. Lavan, Z., and Fejer, A. A., "Luminescence in Supersonic Swirling Flows", Journal of Fluid Mechanics, Volume 23, Part 1, 1965, pp. 173-183.

23. Wilkins, E. M., "The Role of Electrical Phenomena Associated with Tornadoes", Journal of Geophysical Research, Volume 69, 1964, pp. 2435-2448.

24. Colgate, S., "Tornadoes: Mechanism and Control", Science, Volume 157, September, 1967, pp. 1431-1434.

25. Rathbun, E. R., "An Electromagnetic Basis for the Initiation of a Tornado", Journal of Meteorology, Volume 17, June, 1960, pp. 371-373.

26. Lewellen, W. S., "Magnetohydrodynamically Driven Vortices", Proceedings of the 1960 Heat Transfer and Fluid Mechanics Institute, Mason, Reynolds and Vincenti, Editors, Stanford University Press.

27. Loeb, L. B., "Tornadoes: Puzzling Phenomena and Photographs", Science, Volume 155, February, 1967, p. 1037.

28. Turner, J. S., and Lilly, D. K., "The Carbonated-water Tornado Vortex", Journal of the Atmospheric Sciences, Volume 20, September, 1963, pp. 468-471.

29. Turner, J. S., "The Constraints Imposed on Tornado-like Vortices by the Top and Bottom Boundary Conditions", Journal of Fluid Mechanics, Volume 25, Part 2, 1966, pp. 377-400.

30. Logan, S. E., "A Simple Analytical Model for a Dust Devil", UCRL-50667, May, 1969.

31. Barcilon, A., "A Theoretical and Experimental Model for a Dust Devil", Journal of the Atmospheric Sciences, Volume 24, September, 1967, pp. 453-465.

32. Battan, L. J., "Energy of a Dust Devil", Journal of Meteorology, Volume 15, April, 1958, pp. 235-237.

33. Dergarabedian, P., and Fendell, F., "Parameters Governing the Generation of Free Vortices", Physics of Fluids, Volume 10, Number 11, November, 1967, pp. 2293-2299.

34. Donaldson, C. duP., and Sullivan, R. D., "Behavior of Solutions of the Navier-Stokes Equations for a Complete Class of Three-Dimensional Viscous Vortices", Proceedings of the 1960 Heat Transfer and Fluid Mechanics Institute, Mason, Reynolds, and Vincenti, Editors, Stanford University Press.

35. Burgers, J. M., "Application of a Model System to Illustrate Some Points of the Statistical Theory of Free Turbulence", Proc. Acad. Sci. Amsterdam, Volume 43, 1940, pp. 2-13.

36. Sullivan, R. D., "A Two-Cell Vortex Solution of the Navier-Stokes Equations", Journal of the Aero/Space Sciences, Volume 26, November, 1959, pp. 767-768.

37. Vonnegut, B., Moore, C. B., and Harris, C. K., "Stabilization of a High-Voltage Discharge by a Vortex", Journal of Meteorology, Volume 17, August, 1960, pp. 468-471.

38. Wilkins, E. M., and McConnell, L. T., "Threshold Conditions for Vortex-Stabilized Electrical Discharges in the Atmosphere", Journal of Geophysical Research, Volume 73, Number 8, April, 1968, pp. 2559-2568.

39. Dunham, S. E., "Electrostatic Charging by Solid Precipitation", Journal of the Atmospheric Sciences, Volume 23, July, 1966, pp. 412-415.

40. Latham, J., "The Electrification of Snowstorms and Sandstorms", Quarterly Journal of the Royal Meteorological Society, Volume 90, 1964, pp. 91-95.

41. Kunkel, W. B., "The Static Electrification of Dust Particles on Dispersion into a Cloud", Journal of Applied Physics, Volume 21, August, 1950, pp. 820-832.

42. Gunn, R., "The Hyperelectrification of Raindrops by Atmospheric Electric Fields", Journal of Meteorology, Volume 13, 1956, pp. 283-288.

43. Gunn, R., "Raindrop Electrification by the Association of Randomly Charged Cloud Droplets", Journal of Meteorology, Volume 12, December, 1955, pp. 562-568.

44. Gunn, R., and Devin, C., "Raindrop Charge and Electric Field in Active Thunderstorms", Journal of Meteorology, Volume 10, August, 1953, pp. 279-284.

45. Gunn, R., "Droplet-Electrification Processes and Coagulation in Stable and Unstable Clouds", Journal of Meteorology, Volume 12, Number 6, December, 1955, pp. 511-518.

46. Gunn, R., "Initial Electrification Processes in Thunderstorms", Journal of Meteorology, Volume 13, February, 1956, pp. 21-29.

47. Soo, S. L., "Dynamics of Multiphase Flow Systems", I & EC Fundamentals, Volume 4, Number 4, November, 1965, pp. 426-433.

48. Reitz, J. R., and Milford, F. J., Foundations of Electromagnetic Theory, Addison-Wesley Publishing Co., Inc., Reading, Mass., 1960, p. 35.

49. Kuo, Shan S., Numerical Methods and Computers, Addison-Wesley Publishing Co., Inc., Reading, Mass., 1965.

Appendix A

NOMENCLATURE

Symbol	Description	Units
$\bar{B}$	Body force acting on the particle	lb_f
C	Particle drag parameter	sec^{-1}
C_D	Particle drag coefficient	-
C_V	Free-vortex constant	ft^2/sec
D_p	Particle diameter	ft
$\bar{E}$	Electrostatic field	$lb_f/coul$
$\bar{F}$	Total force acting on the particle	lb_f
g	Acceleration due to gravity	$32.2\ ft/sec^2$
g_c	Gravitational constant	$32.2\ ft\text{-}lb_m/lb_f\text{-}sec^2$
$\hat{i}$	Unit vector in the x-direction	-
$\hat{j}$	Unit vector in the y-direction	-
m_p	Particle mass	lb_m
q_p	Particle charge	coul
r	Radial coordinate	ft
R	Dimensionless radial coordinate, $R=r/r_o$	-
t	Time	sec
T	Dimensionless time, $T=Ct$	-
$\bar{u}$	Flow field velocity	ft/sec
$\bar{v}_p$	Particle velocity	ft/sec
z	Axial coordinate	ft
Z	Dimensionless axial coordinate, $Z=z/z_o$	-
ρ	Fluid density	lb_m/ft^3

Symbol	Description	Units
ρ_p	Particle density	lb_m/ft^3
μ	Fluid viscosity	$lb_m/ft\text{-}sec$
θ	Tangential coordinate	-
λ	Line source strength	coul/ft
ϵ_o	Permittivity constant	$3.66 \times 10^{-12} \frac{coul}{lb_f\text{-}ft^2}$

Subscripts	Description
D	Drag
P	Particle
r	Radial component
θ	Tangential component
z	Axial component

Appendix B

DATA

The data used in the analysis of each of the four cases which have been discussed will be presented here. To determine the effects on particle motion of variations in particle density and diameter, and free-vortex flow velocity, these parameters were varied through the following range of values:

Particle diameter, D_p, 50, 100, 200 microns

Particle density, ρ_p, 50, 200 lb_m/ft^3

Free-vortex flow parameter, C_v, 20, 50, 200 ft^2/sec

To determine the effects on particle motion of charged line source strength and particle charge-to-mass ratio, these parameters were varied in this analysis through the following range of values:

Line source strength, λ, 1.03×10^{-6}, 1.03×10^{-5}, 1.03×10^{-4} coul/ft

Particle charge-to-mass ratio (q/m) 4.54×10^{-7}, 4.54×10^{-5}, 4.54×10^{-3} coul/lb_m